POLITECNICO di TORINO

Laurea Magistrale in Ingegneria Civile

STABILITY OF TANK-LEVEL CONTROL SYSTEMS IN HYDROPOWER PLANTS

ADVISORS

Prof. Luca Ridolfi
Eng. Riccardo Vesipa

CANDIDATE

Alejandro Marmolejo Gutiérrez

Turin, Italy
July 2020

CONTENTS

ACKNOWLEDGEMENTS

This document represents the start of a new cycle but the end of a process that started several years ago and that would not have been possible without the support and advice of many people. To this people, I want to be grateful and make a brief dedication.

First, I want to be grateful to my family who have given me not only the opportunity to study abroad but also the emotional support to become today a master's degree in Civil Engineering. They have given me the precise tools to become the person I am today.

Then of course, there is my girlfriend Ana Cristina whose example of a great human being and support during these years have helped me go through this process and finish this life stage.

I want to acknowledge and feel indebted to the many friends that have supported and been with me during this process. They know who they are. However, I feel especially grateful to the people from "Corso Rosselli" and from "Corso Salvemini" who have made of their place a second home for me during these three years.

I want to extend my gratitude to the people that have made this document possible. Chief among them: my thesis advisors, specially Eng. Vesipa, who always adviced me willingly and whose advice has helped me improve as a hydraulic engineer. In addition, I want to thank Mr. Londoño and CELSIA who provided me with the necessary information to develop the study case.

ABSTRACT

In the operation of a run-of-river hydropower plant, flow control to ensure a suitable head in the forebay is a key issue and is often performed by a regulation system combining a level sensor, a controller and a downstream valve. The stability assessment of this system is performed to avoid filling or emptying of the upstream tank. In the past, stability assessment was performed by analytical means but neglecting the transients in the conduits, the uncertainties of the sensor, the delays in the PLC, the finite velocity downstream valve and the backlash in mechanical parts. However, these mechanisms are real-life phenomena and assessing stability considering them has gained attention nowadays. For this purpose, a stability assessment is here performed on a hydropower plant including these mechanisms. The analysis is performed using numerical simulations where the behaviour of the plant is reproduced and then the oscillations of the level in the forebay are studied to determine stability. The obtained results include the analysis of the effect of each mechanism on the stability of the system, the effects of the chosen stability criteria and stability curves showing when a system is stable under certain combinations of variables of the system.

1. INTRODUCTION

Hydropower has been present in human history for a long time, dating from the ancient civilisation to modern times, and today represents one of the most important alternatives facing the climate change and other social issues in the world (international hydropower association [iha], 2019). Hydropower has been developed widely in form of big dams, representing even the largest source of renewable energy in the world, but, though this type of hydropower has been implemented in many countries in the world, its costs of construction and operation along with the environmental and social impact has led to the development of small hydropower in the form of Run-of-river (ROR) hydropower plants (Farris & Helston, 2017; Nunez, 2019). ROR hydropower plants work diverting only some discharge from a flowing river, maintaining a head in a forebay (upstream tank) and then conveying water by head difference at a downstream turbine where electric power is produced (international hydropower association [iha], 2019). The key difference between ROR hydropower plants and big dams is that in the former, the upstream tank is not intended for large water volume storage but only to ensure a suitable head in order to maintain a regular electricity production.

Following this idea, the challenge that arises when designing and operating a ROR hydropower plant is thus that, since water storage is not the main scope of these systems, a level regulation needs to be done in order to maintain a suitable head in the forebay. Fluctuations of the level in the forebay may occur randomly due to river discharge variations, instrumental errors and other effects, therefore, due to these fluctuations, the level in the forebay is controlled to avoid emptying or filling because in the former case, air entering could occur, causing cavitation phenomena and problems in the restarting of the plant and in the latter, water could be wasted (Vesipa & Fellini, 2019). This control is done by varying the opening of the turbine, but, as fluctuations in the forebay level may occur randomly and continuously throughout time, an automatic control system of the level in the forebay and the turbine opening is used.

A usual automatic control system of a hydropower plant integrates a tank level sensor in the forebay, a PLC or computer that performs the desired algorithms and a downstream valve (Vesipa & Fellini, 2019). The PLC may have different configurations but one that has been used in this field is the PI Controller where the level in the forebay is continuously monitored, compared with the reference or target value and then adjusted via the modification in the downstream valve. The PI Controller parameters need to be tuned up to fit the hydropower geometry and hydraulic requirements of the plant to maintain the suitable head and to avoid large deviations (Jiménez & Chaudhry, 1992). A controller that can restore or keep the reference value head against the possible disturbances is called a "stable" system whereas a control system where equilibrium is never restored is called "unstable". The stability assessment is thus the core task in the tuning of the controller and the fate of the disturbances need to be determined to fine the optimum controller parameters (Vesipa & Fellini, 2019). The stability assessment may be performed through adequate modelling of the plant where a set of equations is stated, and a stability criterion is then applied to determine stability.

In the past, a stability assessment approach that was used included a set of dimensionless governing equations as a function of time and stability based on the Routh-Hurwitz criterion (Jiménez & Chaudhry, 1992). However, when this approach has been used, a number of

mechanisms have been neglected such as the hydraulic transients, the uncertainties in the measure, delays between the sensor, the PLC and the valve, the finite valve velocity and the backlash between mechanical parts of the valve. Thus, the purpose of this paper is to propose a stability assessment including all these mechanisms, discussing the effects of each of them and the stability criteria.

In this framework, this paper is organized as follows, first a detailed description of the problem and the variables involved is presented, then the equations and methods through which the behaviour of the system is modelled is presented followed by the numerical methods to solve this equations. Finally, the results and a discussion are exposed along with a study case that helped to prove the effectiveness of the methods that were proposed.

2. PROBLEM STATEMENT

2.1. Typical Run-of-River Hydropower Plant

A typical ROR hydropower plant provided with a surge tank as the one shown in Figure 2.1 is considered. From the hydraulic point of view this plant is divided in two major group of components: hydraulic components and regulation system. It is important to study both in detail.

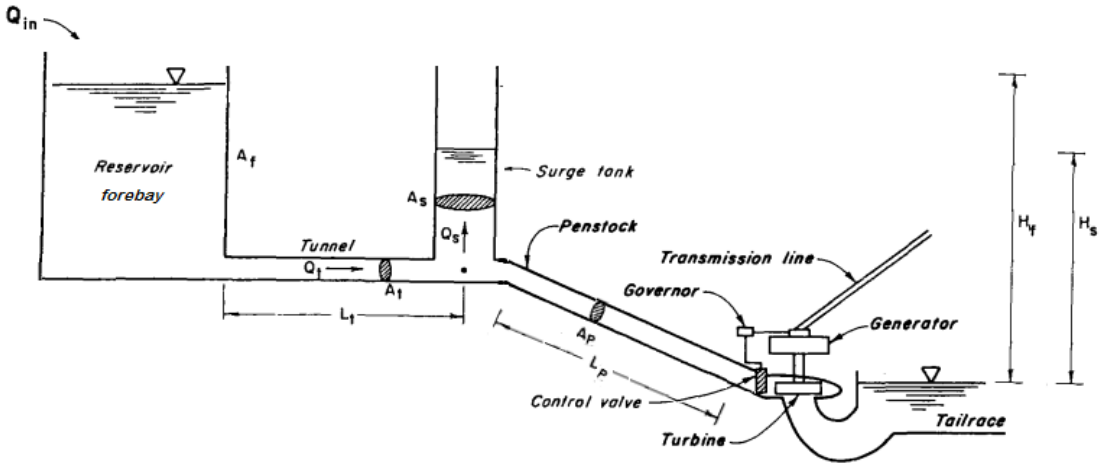

Figure 2.1 - Typical ROR Hydropower plant (with surge tank) adapted from Chaudhry (1979)

2.1.1. Hydraulic Components and working scheme

The hydraulic components in this document are defined as the components that are necessary to run the plant from the hydraulically, this means that the electric components or other structural components that make up the plant are not taken into account. As shown in Figure 2.1 it is considered

- The forebay or upstream reservoir
- The head-race tunnel
- The penstock
- The surge tank
- The turbine

The forebay or upstream reservoir is the component of the system that guarantees a low storage of water and a suitable head on the system. It is characterized by A_f = Surface area of the forebay, H_f (t)= Theorical head in the forebay, H_{fm} (t)= Head in the forebay considering uncertainties in the measure, $H_{f,measure}$ = measured head in the forebay, taken every t_m seconds, H_{target} = reference or optimum forebay head and Q_{in} (t)= Flowrate entering the forebay coming from the river.
Water is conveyed from the forebay to the turbine through a long tunnel which carries the water with a small slope and low pressure to a point in which a greater slope is going to be found and a penstock will carry the water at high pressure to the turbine. The tunnel is characterized by hydraulic diameter $D_{h,t}$, cross-section area A_t, length L_t, equivalent roughness ε_t, lining Ypung Modulus E and surrounding rock rigidity modulus E_R. The hydraulic diameter is defined by (White, 2011)

$$D_{h,t} = \frac{4A_t}{P_t}$$

where P_t = wetted perimeter. If the tunnel is circular the hydraulic diameter coincides with the diameter of the circular tunnel. The penstock is a steel pipe characterized by diameter D_p, Length L_p, equivalent roughness ε_p, wall thickness e, wall's Young Modulus E and wall's Poisson's ratio μ.
From the hydraulic point of view, the turbine works as a control valve that is opened or closed when the level in the forebay H_f increases or decreases to control the discharge that comes in. In this sense, the characteristics of interest of the turbine are the valve discharge Q_v, the valve area A_v, coefficient of discharge c_v, and maximum closing/opening velocity $v_{v,max}$.
The surge tank is a component of the ROR hydropower plant whose task is to reduce or mitigate the overpressures developing in the tunnel following a flow change and is characterized by surface area A_s and head H_s(t).

2.1.2. Regulation System

The regulation system of the hydropower plant is the component that links the discharge coming from the forebay and the discharge in the valve to keep the level in the forebay at H_{target}. The regulation system integrates:

- a level sensor in the forebay
- a PLC or computer
- the opening/closure mechanism of the turbine

The regulation system is an automatic control system that works continuously in time following these operations:

1. A level sensor measures the level $H_{f,measure}$ in the forebay
2. The sensor sends the measured value $H_{f,measure}$ to the computer and is compared with the desired level H_{target}
3. Through an algorithm, the computer decides the next position of the actuator in order to change the opening of the turbine

4. The desired position is then sent to the actuator
5. The actuator performs the mechanical operation to adjust the turbine opening

Different algorithms may be used to transform H_f (input signal) to the next turbine opening A_v (output signal). In this document the PI Controller is used (Jiménez & Chaudhry, 1992)

Opening/closure mechanism

The opening/closure turbine system depends on the type of turbine, for Pelton and Francis turbines, for example, the opening systems are a needle nozzle valves and guide vanes, respectively. Since the opening/closure mechanism of the turbine works as a valve, in this document, unless specified, this mechanism is called Downstream Valve (DS Valve)

In this document it is going to be referred as *flow control system* to the whole regulation system of the plant.

2.2. Assessment of the Flow Control System Stability

The aim of flow control system is to keep a constant level H_{target} in the forebay by adjusting the DS valve (opening/closure of the turbine). If the flow that supplies the forebay Q_{in} is constant and the valve opening, A_v, is such that $Q_v(A_v)=Q_{in}$, the level of the forebay H_f is kept constant and no valve adjustment is required, however, this ideal configuration of equilibrium is very uncommon in real systems due to variations in the river discharge and other mechanisms. The result of these processes is that the flow discharged by the DS valve is different from the flow entering the forebay, thus, since $Q_v \neq Q_{in}$, the level of the forebay deviates from is target value H_{target} and adjustments of the valve opening must be performed.
The deviations of the valve opening from its equilibrium configuration are called “disturbances” and the assessment of the fate of these disturbances (i.e., the stability of the dynamical system) is a key point. If the characteristics of the control system are such that the disturbances are damped (i.e., after a transient time the equilibrium configuration is restored), the dynamical system is defined as “stable”. On the other hand, if the disturbances amplify (e.g. flow or level oscillations arise), the dynamical system is defined as unstable (Vesipa & Fellini, 2019).

To determine the stability of a dynamical system there is no exclusive way and there may be different approaches. The approach to be used depends on the set of governing equations, that is, on the level of detail extracted from the plant and ultimately, on the number of variables involved. When adequate simplifications are considered, namely, if some variables are neglected in the analysis, the approach to determine stability may be simpler.

Jiménez & Chaudhry (1992) proposed a *flow control system* that uses a PI Controller and works neglecting some phenomena that take place in this kind of plants:

- No transients in the conduits
- No measuring instrument issues
    - No instrumental uncertainties
    - Instantaneous measure

- No delays
- Instantaneous valve
- No backlash

This *flow control system* has been widely used in the past and its key characteristic is that stability may be assessed linearizing the set of governing equations and using the Routh-Hurwitz criterion, thus, leading to determination of the dynamic stability by analytical means. Although this approach has given reasonable results and has been tested by numerical simulations, since the exposed phenomena are real-life issues in hydropower plants, the question whether the assumption to neglect them is relevant or not arises, and if considering these variables affect the stability of the control system. Thus, in this document the assessment of flow control system stability was performed considering the presence of these phenomena, for this reason they are exposed in more detail.

2.2.1. New Mechanisms included in the present study

Hydraulic transients

Hydraulic transient is the term referred to the unsteady flow caused by flow changes such as opening/closing of the valve, starting of a pump, among others. Following a flow change there is a pressure wave that travels with finite velocity along the conduits, therefore flow rate variations do not take place immediately but require finite times to be effective (Chaudhry, 1979). Mathematically speaking, the consideration of hydraulic transients in the conduits means that flowrate and head variations are considered as functions of both time and distance. In the present study, hydraulic transients in both the penstock and the head-race tunnel are considered

Uncertainties

In the field of metrology, it is stated that when a variable x is measured, its true value x_{true} is never known, instead, depending on the measuring instrument, it is only possible to determine a measured value $x_{measured}$ with an interval Δx in which x_{true} lies with a given probability (Freedman & Young, 2012). The control of ROR hydropower requires continuous measure of the water level in the forebay, thus, following the ideas stated by metrology, it is always associated to a degree of uncertainty.

Instantaneous measure

Instantaneous measure means that it was considered that the instrument did the measure in continuous time. However, no measuring instrument can do this, and it always take finite times to take a measure.

Delays

Delays in this context are understood as the interval of time taken by the control system from the measure of the water level in the forebay to the activation of the actuator, or in other words, the

time to perform the steps 1-4 described in the automation of the control. This time interval is referred as delay by the fact that the control operations are not performed immediately.

Non-instantaneous valve

An instantaneous valve means that any opening A_v set by the computer may be achieved
This is not always true because the valve has a finite velocity and the A_v is requested during a finite time interval. If the A_v is big enough it may never be achieved by the valve.

Backlash

Backlash (Figure 2.2.) is a clearance or loss of motion in a mechanism due to gaps between the parts or insufficient torque (friction) (Wang et al., 2019). Considering backlash in control systems is an important issue because if it occurs, it is not certain that an operation requested by the controller will be actually achieved.

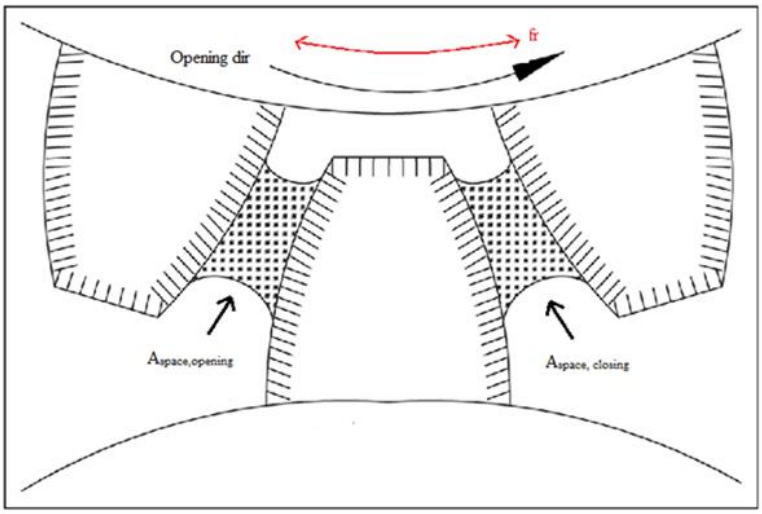

Figure 2.2 - Backlash in mechanical parts adapted from Liu et al. (2017*)*

Numerical Simulations

The consequence of considering flow transients in the conduits is that no analytical approach has been developed to assess stability, however, in fluid mechanics and hydraulic engineering, the stability properties of a dynamical system can be assessed by *numerical simulations.* To perform these *numerical simulations* the characteristics and the governing equations are modelled and implemented in a computer, then the equations are solved, the behaviour of a hydropower plant is reproduced and time series of the forebay level and the valve opening are obtained to assess the stability of the control system.

Numerical simulations were thus adopted in this study to assess the stability of the water-level PI controller considering the new phenomena exposed. In detail, the Palomo Hydroelectric Project in Costa Rica was considered (Jiménez & Chaudhry, 1992). The system was set to be at equilibrium position at the beginning working at the steady-state condition and then subjected to disturbances caused by the *instrumental uncertainties, delays, non-instant valve effects and*

backlashes, and analysed considering the *hydraulic transients* in the conduits. Moreover, different parameters of the PI controller were varied to study its stability.

Time-series of the forebay level and the DS valve opening were analysed to determine whether the PI-controller was stable or not. The stability of the system was determined after the simulation evaluating if the oscillations in $H_f(t)$ tended to damp to H_{target} in respect to time. Since for every numerical simulation stability depends on the disturbances considered and the parameters of the PI controller, stability limit curves were produced and analysed considering combinations of different instrumental uncertainties, measuring times, delay times, non-instant valve effects, backlash effects and parameters of the PI controller. The stability limit curves show for given values of instrument uncertainty, measuring times, delays, non-instant valve parameters, backlash parameters and PI Controller parameters, the limit values of the PI controller parameters for which any point inside the curve will represent a stable case and any point outside it an unstable one. An additional analysis on the mean and the standard deviation of the time-series was done to control the centre and the amplitude of the oscillations.

3. METHODS

To perform a stability assessment of the flow control system the following two tasks need to be done, first, it is necessary to state the governing equations that describe the operation of the dynamic system in a mathematical way. To this scope, control variables that describe this operation are defined relating them to the plant characteristics in form of equations based on physical laws. This process is called the construction of the mathematical model of the flow control system. Then, the second task is to define the mathematical method that determines whether the dynamic system is stable or not.

3.1. Mathematical Model of the dynamic system

To state the set of equations that describe the system let us first consider the general scheme of the ROR hydropower plant presented in Figure 2.1. The following notation is used: t is the time, x is the longitudinal coordinate and Q(x,t) and H(x,t) are the space-time dependent discharge and piezometric head, respectively. The longitudinal coordinate is taken locally for each conduit, therefore x_t and x_p are the local longitudinal coordinates of the tunnel and the penstock, respectively. Using this notation, $x_t=0$ represents the entrance in the tunnel, $x_t=L_t$ and $x_p=0$ represent the node at which the tunnel, the penstock and the surge tank converge and, $x_p=L_p$ represent the linking node between the penstock and the turbine.

-

Control Variables

The dynamics of a ROR hydropower plan are controlled by the level in the forebay $H_f(t)$, the level in the surge tank $H_s(t)$ and the valve opening $A_v(t)$. The water level in the forebay varies over the time according to the mass balance equation

$$\frac{dH_f(t)}{dt} = \frac{Q_{in}(t) - Q_t(t, x_t = 0)}{A_f} \quad (3.1)$$

where H_f = head in the forebay, $Q_t(t,x_t=0)$ = the discharge at the entrance of the tunnel, Q_{in} = the discharge entering from the river and A_f = Surface area of the forebay. The level in the surge tank is described by

$$\frac{dH_s(t)}{dt} = \frac{1}{A_s} Q_s(t) \tag{3.2}$$

in which H_s = water level in the surge tank and Q_s = flowrate in the surge tank, taken positive if flow is entering the surge tank, and given by

$$Q_s(t) = Q_t(t, x_t = L_t) - Q_p(t, x_p = 0) \tag{3.3}$$

The turbine opening A_v is regulated by the PI controller. In this type of control, the level in the forebay is measured and compared with a reference value, then, if the measured level is different to the reference value valve opening is modified using the equations (Jiménez & Chaudhry, 1992)

$$\frac{d\tau(t)}{dt} = \frac{H_{fm}(t) - H_{ref}}{T_i} + k\frac{d(H_{fm}(t) - H_{ref})}{dt} \tag{3.4}$$

$$\tau(t) = \frac{A_v(t)}{A_{ref}} \tag{3.5}$$

where τ= the ratio between the current valve opening and the steady-state valve opening and Href = the reference water level in the forebay which is considered as the steady-state level, namely

$$H_{ref} = H_{target} = H_{fo} \tag{3.6}$$

T_i, k are the integral and proportional constants of the PI given by

$$T_i = \frac{L_t\, Q_o H_{target}\, \tau_o}{K_1\, g\, H_{so}\, A_t} \tag{3.7}$$

$$k = \frac{\alpha\, \tau_0}{H_{target}} \tag{3.8}$$

in which α and K_1 are parameters of the PI controller, g is the gravity acceleration and the subscript *o* means the initial state of the variable

Dynamic and Continuity Equations

The dynamic and the continuity equations are the equations that couple the discharge and the piezometric head in the conduits. The dynamic equation is obtained by applying Newton's Second Law of motion to an element of fluid and the continuity equation is obtained by

considering mass conservation and deformation in a control volume of a conduit (Chaudhry, 1979), i.e.,

$$\frac{\partial Q}{\partial t} + gA\frac{\partial H}{\partial x} + \frac{f}{2DA}Q|Q| = 0 \tag{3.9}$$

$$\frac{a^2}{gA}\frac{\partial Q}{\partial x} + \frac{\partial H}{\partial t} = 0 \tag{3.10}$$

In both equations g = gravity acceleration, D = diameter of the conduit, A = cross-sectional area of the conduit, f = friction factor according to Darcy-Weisbach formula and a = wave speed in the conduit. The wave speed a is not unique for all conduits and depends on the fluid and the conduit deformation properties and constraints (Chaudhry, 1979). The wave speed formulas of the type of conduits considered in this document are (Streeter & Wylie, 1978)

If the conduit is a circular tunnel excavated in rock

$$a^2 = \frac{K}{\rho\left[1 + \left(2\frac{K}{E_R} + (1+\mu)\right)\right]} \tag{3.11}$$

where ρ = density of the fluid, K = bulk modulus of elasticity of the fluid, E_R = Modulus of rigidity of the tunnel material, μ = Poisson's ration of the tunnel material.

If the conduit is a steel pipe

$$a^2 = \frac{K}{\rho\left[1 + \left(\frac{KD}{eE}\right)c_1\right]} \tag{3.12}$$

where ρ = density of the fluid, D = diameter of the pipe, K = bulk modulus of elasticity of the fluid, E = Young modulus of elasticity of the conduit material, e = conduit wall thickness and c_1 is a coefficient that depends on the support conditions of the conduit. In the cases considered c_1=1 if pipe anchored with expansion joints throughout and c_1=2Ee/(E_RD+2Ee) for steel lined circular tunnels.

Boundary Conditions

Since the equations involve both time and space dependence, boundary and initial conditions must be stated. The boundary conditions depend on the physical constrictions found in the hydropower plant. Boundary conditions for forebay, surge tank and downstream valve are here presented (Chaudhry, 1979):

Forebay

As a result of the flow entering from the forebay, the discharge $Q_t(t=0, x_t=0)$ and the head $Q_t(t=0, x_t=0)$ at the entrance of the tunnel may be computed coupling equation (3.1) with the following equation

$$H_t(t, x_t = 0) = H_f(t) - (1 + k_e)\frac{(Q_t(t, x_t = 0))^2}{2g{A_t}^2} \quad (3.13)$$

k_e = coefficient of entrance loss

Surge tank

The losses at the junction are neglected, so the head in the node in which the tunnel, the penstock and the surge tank converge is

$$H_t(t, x_t = L_t) = H_p\big(t, x_p = 0\big) = H_s(t) \quad (3.14)$$

Downstream valve

Considering the datum at the free surface of the tailrace (approximately the level of the turbine), the discharge flowing through the needle valve is described by the equation

$$Q_v(t) = A_v(t)c_v\sqrt{2gH_v(t)} \quad (3.15)$$

In which the head at the end of the penstock is taken as the head at the valve that is $H_v(t) = H_p(t, x_p = L_p)$

Initial Conditions

The initial conditions are set as the steady-state flow when the level in the forebay is H_{target}. The initial condition is thus obtained solving the following system of equations

$$H_{target} - H_t(t = 0, x = 0) = -(1 + k_e)\frac{(Q_o)^2}{2g{A_t}^2} \quad (3.16)$$

$$H_t(t = 0, x = 0) - H_t(t = 0, x = L_t) = f_t\frac{l_t}{D_{h,t}}\frac{Q_o|Q_o|}{2g{A_t}^2} \quad (3.17)$$

$$H_t(t = 0, x = L_t) = H_p(t = 0, x = 0) \quad (3.18)$$

$$H_p(t = 0, x = 0) - H_v(0) = f_p\frac{l_p}{D_p}\frac{Q_o|Q_o|}{2g{A_p}^2} \quad (3.19)$$

$$Q_o = A_v(t = 0)c_v\sqrt{2gH_v(0)} \quad (3.20)$$

Where the subscript *o* represents a steady-state condition. The system is solved for $H_t(t=0, x_t=0)$, $H_t(t=0,x_t=L_t)$, $H_s(t=0,x=0)$, $A_v(t=0)$ and $H_v(t=0)$

3.1.1. New Mechanisms

Uncertainty of the measure

The uncertainty in a measure may be accounted in the mathematical model by considering the measured value as a random variable $X=H_{measure}$ described by a certain probability distribution function. In the present study, the Standard Normal Distribution is used described by the probability density function (Devore, 2012)

$$\varphi(Z) = \frac{e^{-\frac{Z^2}{2}}}{\sqrt{2\pi}} \tag{3.21}$$

with standardized normal random variable

$$Z = \frac{H_{f,measure} - H_f}{\sigma_1} \tag{3.22}$$

where σ_1= standard deviation of the distribution.

Non-instantaneous measure

The finite time that a measuring instrument takes to perform a measure is considered setting a measuring time $t_{measure}$, i.e., the level in the forebay is supposed to be measured every $t_{measure}$ seconds.

Delays

The delay in the system is considered by setting a delay time t_{delay}, therefore, the operation performed by the actuator is supposed to be carried out t_{delay} seconds after the measure in the forebay.

Non-instant valve

To acknowledge the presence of a non-instant valve it is considered that the valve has a finite maximum velocity $v_{v,max.}$ In consequence, the maximum operation that the valve can perform for a given time t is

$$\left(\frac{d\tau(t)}{dt}\right)_{max} = v_{valve,max} \tag{3.23}$$

The $d\tau$ that can be arranged due to the non-instant-valve effects, denoted by $d\tau_{eff}$ is

$$\frac{d\tau_{eff}(t)}{dt} = \begin{cases} \frac{d\tau(t)}{dt}; & if\ \frac{d\tau(t)}{dt} < \left(\frac{d\tau(t)}{dt}\right)_{max} \\ \left(\frac{d\tau(t)}{dt}\right)_{max}; & if\ \frac{d\tau(t)}{dt} \geq \left(\frac{d\tau(t)}{dt}\right)_{max} \end{cases} \quad (3.24)$$

Due to insufficient velocity of the valve, the quantity of $d\tau$ that could not be arranged, denoted by $d\tau_{miss}$ is

$$d\tau_{miss}(t) = \begin{cases} 0; & if\ \frac{d\tau(t)}{dt} \leq \left(\frac{d\tau(t)}{dt}\right)_{max} \\ d\tau(t) - d\tau_{eff}(t); & ;\ if\ \frac{d\tau(t)}{dt} > \left(\frac{d\tau(t)}{dt}\right)_{max} \end{cases} \quad (3.25)$$

Backlash

The gaps are modelled as a percentage of the steady-state area (Norconsult SA, 2016), referring to Figure 2.2 this means that

$$gap_{pos}(t) = \frac{A_{space\ ,opening}(t)}{A_{vo}} \quad (3.26)$$

$$gap_{neg}(t) = -\frac{A_{space,\ closing}(t)}{A_{vo}} \quad (3.27)$$

where $A_{space,opening}$(t)= area of space between mechanical parts in the opening direction, $gap_{pos}(t)$ = ratio between the area of space between mechanical parts in the opening direction and the steady-state area of the valve, $A_{space,closing}(t)$= area of space between mechanical parts in the closing direction and $gap_{neg}(t)$ = ratio between the area of space between mechanical parts in the closing direction and the steady-state area of the valve, considered always as a negative quantity. The total amount of gap is always given by

$$gap_{total} = gap_{pos}(t) + |gap_{neg}(t)| \quad (3.28)$$

The friction is considered setting a parameter b defined as

$$b = (1 - fr) \quad (3.29)$$

in which b = is a parameter that expresses for each operation what percentage of movement between mechanical parts can be effectively performed due to frictional losses and fr = friction coefficient between mechanical parts expressed as a percentage of area that cannot be opened or closed due to frictional losses. The friction forces are always opposite to the direction of the movement. The dτ that can be arranged due to backlash effects, denoted by $d\tau_{real}$ is

For opening operations, i.e. dτ is positive

$$d\tau_{real}(t) = \begin{cases} 0; & d\tau(t) \leq gap_{pos}(t) \\ b \cdot \left(d\tau(t) - gap_{pos}(t)\right); & d\tau(t) > gap_{pos}(t) \end{cases} \quad (3.30)$$

For closing operations, i.e. dτ is negative

$$d\tau_{real}(t) = \begin{cases} 0; & d\tau(t) \geq gap_{neg}(t) \\ b \cdot \left(d\tau(t) - gap_{neg}(t)\right); & d\tau(t) < gap_{neg}(t) \end{cases} \quad (3.31)$$

For a given time t, the $d\tau_{real}$ con be obtained from the graph shown in Figure 3.1

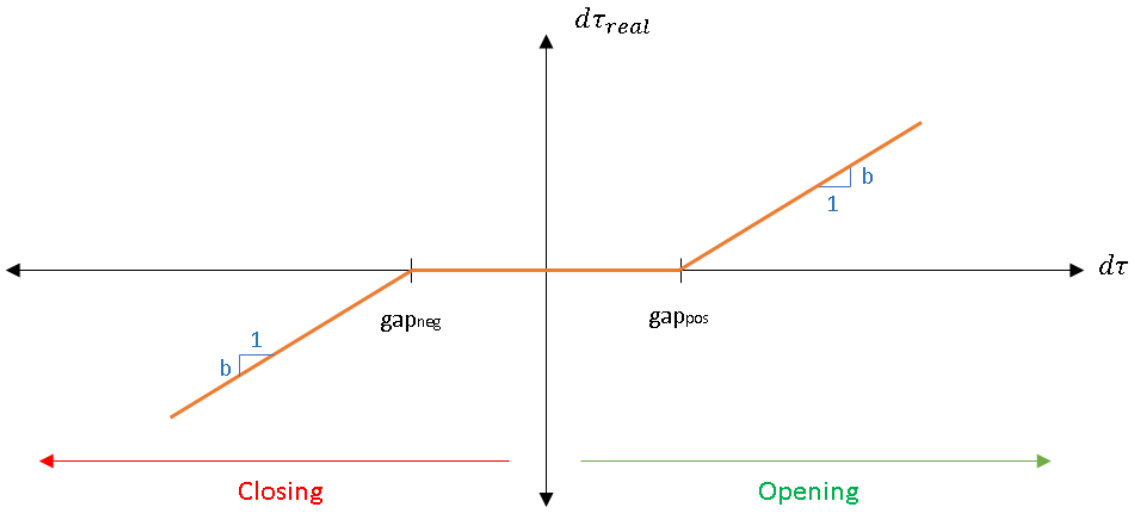

Figure 3.1 - $d\tau_{real}$ obtained at a given time t as a function of dτ, the gaps and b

If the non-instant-valve effects are taken into account, the τ in equations (3.30) and (3.31) must be taken as τ_{eff}.

3.2. Mathematical model of the stability assessment

3.2.1. The Stability Function, the Stability Criterion, and the Stability Limit

A dynamic system is defined as "stable" if the disturbances tend to damp in time and "unstable" if the disturbances amplified or did not converge to a certain value. This definition is rather qualitative and the necessity of defining stability in a more mathematical way arises to systematically determine it. For this reason, the *stability function* and the *stability criterion* are here defined.

Let us define mathematically the *stability* as a Boolean function of the form

$$Stability = \begin{cases} 1, & if\ the\ dynamic\ system = "stable" \\ 0, & if\ the\ dynamic\ system = "unstable" \end{cases} \quad (3.32)$$

To determine the stability of the flow control system by numerical simulations time-series of $H_f(t)$ as shown in Figure 3.2 (a) are obtained. The stability requires the oscillations of $H_f(t)$ to damp after a certain transient time t_t, in this sense let us define H as

$$H = \lim_{t \to t_t} (H_f - H_{target}) \quad (3.33)$$

The dynamic system will be stable if

$$H = \lim_{t \to t_t} (H_f - H_{target}) = 0 \quad (3.34)$$

To determine whether this condition is satisfied or not, after the time-series of $H_f(t)$ has been obtained, the peaks of the oscillations of $H_f(t)$ around H_{target} are identified (Figure 3.2 (b)) and subjected to an exponential fit (Figure 3.2 (c)) of the form

$$expfit = ef = a \cdot e^{St} \quad (3.35)$$

If S<0 then H tends to 0 and the system is stable because

$$\lim_{t \to \infty} a \cdot e^{St} = 0 \quad (3.36)$$

only if

$$S < 0$$

This behaviour is known as asymptotic stability so *stability* may be redefined as

$$Stability = a_{stability} = as = \begin{cases} 1; S < 0 \\ 0; S \geq 0 \end{cases} \quad (3.37)$$

or

$$Stability = a_{stability} = as = \begin{cases} 1; H = 0 \\ 0; H \neq 0 \end{cases} \quad (3.38)$$

It is important to emphasize that S=0 does not represent asymptotic stability because in this case, although the oscillations do not amplify, H does not tend to 0. The condition of S<0 in the exponential fit is defined as the *stability criterion* and is used to determine whether the system is stable or not.

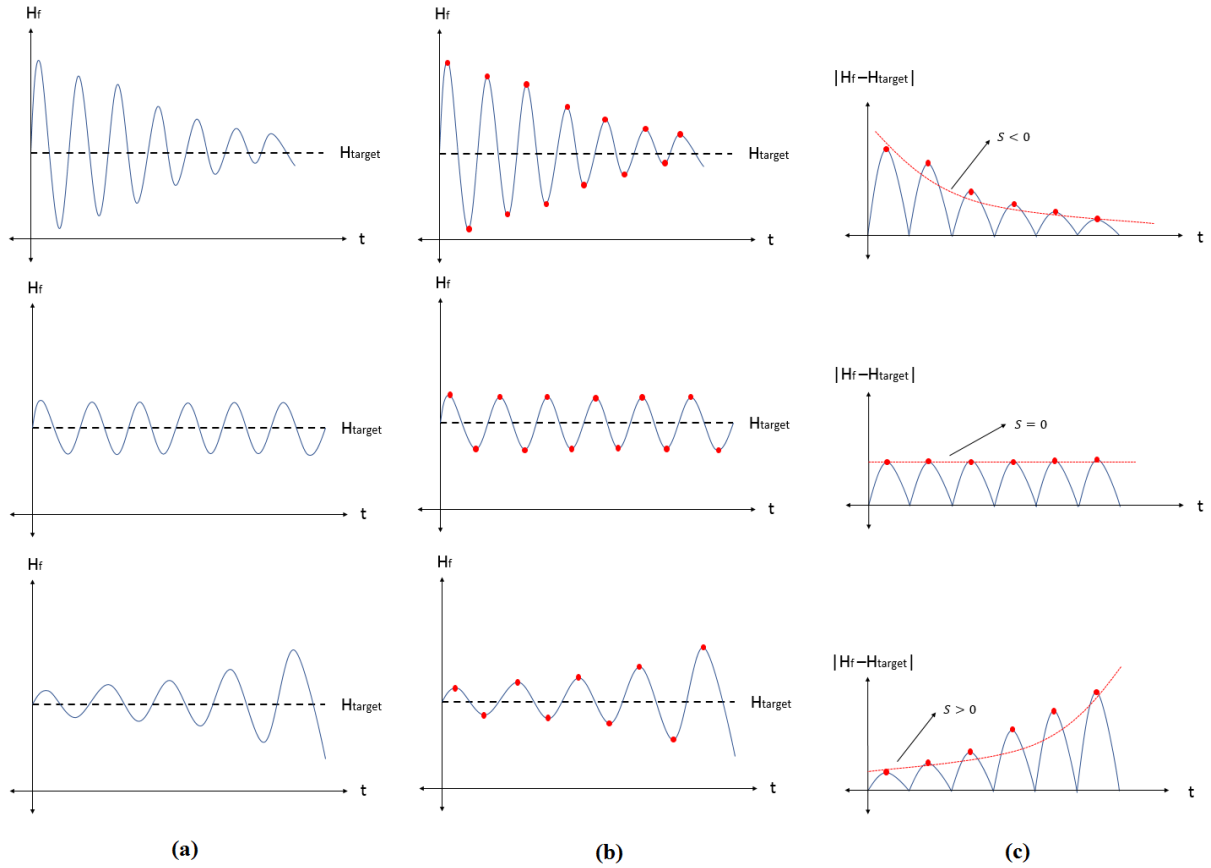

Figure 3.2 – (a) Evolution of $H_f(t)$ throughout time – (b) Individuation of the peaks of $H_f(t)$ around H_{target} – (c) Peaks of $H_f(t)$ around H_{target} subjected to an exponential fit

Now, to compute S, the time-series of $H_f(t)$ must first be obtained. This time-series are obtained after defining a certain number of variables Y_i, so S is a function of Y_i, that is

$$S = f(Y_1, Y_2, \dots, Y_n) \tag{3.39}$$

Where n is the number of variables involved

If the set of variables that need to be defined to find S is called Y these variables may be classified into three major subsets (Figure 3.3)

- Set of variables related to the hydraulic components of the plant Y_P, e.g., the surface area of the forebay A_f or the length of tunnel L_t
- Set of variables related to the effects of the mechanisms of the flow control system Y_{FE}, e.g., the uncertainties effects or the backlash effects
- Set of variables related to the PI Controller Y_C.

So

$$S = f\left(Y_{P1}, Y_{P2}, \dots, Y_{Pn_p}, Y_{FE1}, Y_{FE2}, \dots, Y_{FEn_{fe}}, Y_{C1}, Y_{C2}, \dots, Y_{Cn_c}\right) \tag{3.40}$$

Where n_p = number of variables contained in Y_P, n_{fe} = number of variables contained in Y_{FE} and n_c = number of variables contained in Y_C.

Each of the variables contained in the set of Y_{FE} may be also a function of two subsets of variables

- The set Boolean variables which represent the on or off variables of the mechanisms that are taken into consideration $y_{B,M}$
- The set of parameters that describe the effects of that mechanism $y_{FE,M}$

where the subscript *M* represents the *M-th* mechanism so that

$$Y_{FE,M} = f_1\left(Y_{B,M}, Y_{FE,M,1}, Y_{FE,M,2}, \dots, Y_{FE,M,n_m}\right) \tag{3.41}$$

in which n_m = number of variables contained in $Y_{FE,M}$.

Combining equations (3.40) and (3.41) it is obtained

$$S = f\begin{pmatrix} Y_{P1}, Y_{P2}, \dots, Y_{Pn_p}, Y_{FE,1}\left(Y_{B,1}, Y_{FE,1,1}, Y_{FE,1,2}, \dots, Y_{FE,1,n_{m,1}}\right), Y_{FE2}\left(Y_{B,2}, Y_{FE,2,1}, Y_{FE,2,2}, \dots, Y_{FE,2,n_{m,2}}\right), \dots \\ \dots, Y_{FEn_{fe}}\left(Y_{B,n_{fe}}, Y_{FE,n_{fe},1}, Y_{FE,n_{fe},2}, \dots, Y_{FE,n_{fe},n_m}\right), Y_{C1}, Y_{C2}, \dots, Y_{Cn_c} \end{pmatrix} \tag{3.42}$$

In which *S* is defined as the *stability function* and its form depends on the fitting technique.

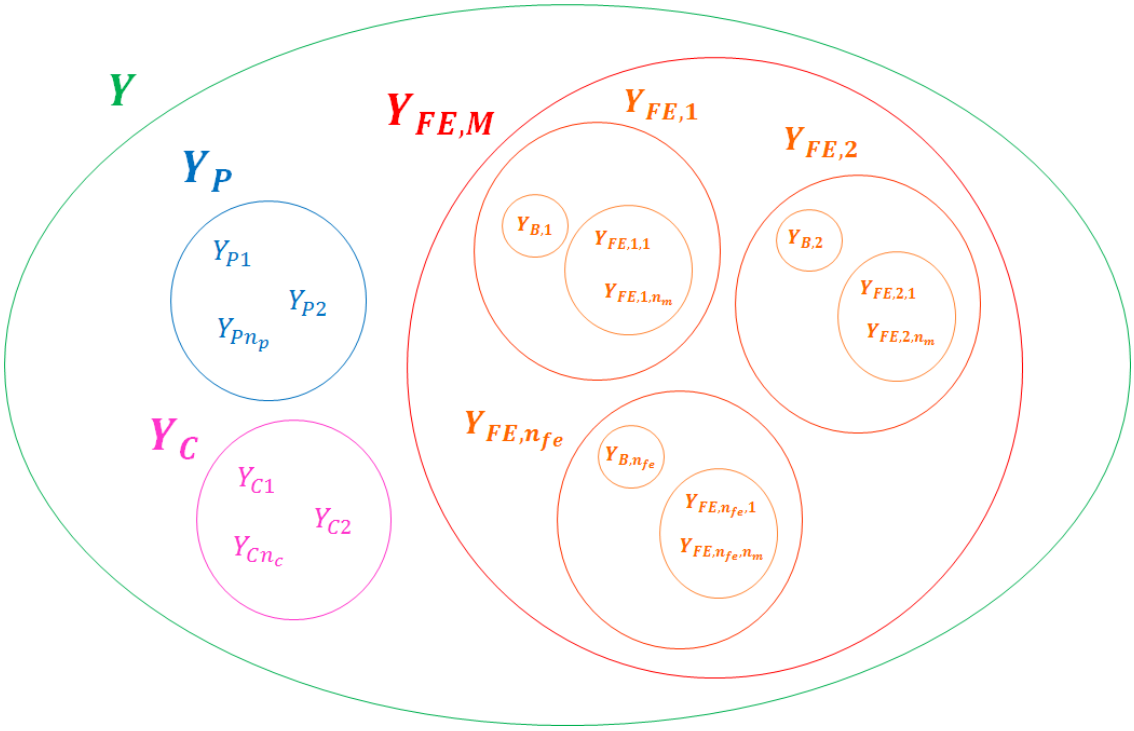

Figure 3.3 – Set of variables necessary to define the stability function

Let us now define as *global case* any combination of the variables $Y_{P,i}$ and Y_{FE} (without considering Y_C) and a *particular case* of a *global case* as any combination of all the variables Y_C after already defined the variables $Y_{P,i}$ and Y_{FE}. to determine the stability of a *stability function,* a *particular case* must be defined, i.e. all the variables Y_i may be defined, then time-series must be obtained and at last the *stability criterion* is applied.

Now, it is defined as *stability limit* for a *global case* the *surface* of the stability function where

$$S\left(Y_{C1}, Y_{C2}, \dots, Y_{Cn_c}\right) = 0 \tag{3.43}$$

This *surface* represents the border between the "stable" and the "unstable" *particular cases* of a *global case*.

3.2.2. Statistical stability assessment

In addition to the exponential fit of the oscillations of $H_f(t)$ around H_{target} it is of interest to determine the mean value and the standard deviation of the time-series of $H_f(t)$ and $\tau(t)$. This is done fundamentally to study the centre and the amplitude of the oscillations.

The mean values $\overline{H_f}$ and $\bar{\tau}$ and the standard deviations sd_H_f and sd_τ of a particular case are computed with (Devore, 2012)

$$\overline{H_f} = \frac{1}{t_t}\int_0^{t_t} H_f(t)\, dt \tag{3.44}$$

$$\bar{\tau} = \frac{1}{t_t}\int_0^{t_t} \tau(t)\, dt \tag{3.45}$$

$$sd\_H_f{}^2 = \frac{1}{t_t}\int_0^{t_t} (H_f(t) - \overline{H_f})^2\, dt \tag{3.46}$$

$$sd\_\tau^2 = \frac{1}{t_t}\int_0^{t_t} (\tau(t) - \bar{\tau})^2\, dt \tag{3.47}$$

4. NUMERICAL METHODS

The dynamic and continuity equations have been adopted to describe transient flow in the conduits

$$\frac{\partial Q}{\partial t} + gA\frac{\partial H}{\partial x} + \frac{f}{2DA}Q|Q| = 0 \quad (4.1)$$

$$\frac{a^2}{gA}\frac{\partial Q}{\partial x} + \frac{\partial H}{\partial t} = 0 \quad (4.2)$$

are hyperbolic, partial differential equations (PDE). The functions Q(x,t) and H(x,t) that satisfy the equations are the solution of the system. Due to the nature of this problem, analytical solutions of these equations are impossible to find. Instead, some numerical methods have been developed to solve them. The method of the characteristics is here used (Chaudhry, 1979)

4.1. Method of the Characteristics

To apply the method of the characteristics to these equations the following procedure is followed

- The equations (a) and (b) are reduced to ordinary differential equations, valid along the characteristic lines, and solved by the finite-difference technique.
- A suitable time step Δt and the total simulation time t_{total} are chosen. The solutions at each time step are indexed with the subscript *i*.
- The conduits are numbered and are indexed with *m*. For the plant considered, m=1 represents the tunnel and m=2 represents the penstock.
- The wave speed a_m is computed for every conduit
- To guarantee a numerically stable solution a space discretization of $\Delta x_m = \Delta t \cdot a_m$ is computed for each conduit.
- Each conduit is divided in *n* reaches of length Δx_m. where *n=0* and *n=N* refer to the first and last nodes, respectively.
- The following notation is used

$$Y_{m,n}^{i}$$

where *Y*=the generic variable that is being computed, *i* = *i-th* time step, *m* = *m-th* conduit and *n* = *n-th* node

4.1.1. Governing Equations

Following the finite difference scheme, the flowrate and the piezometric head at the *m-th* conduit, at the *n-th* node at time step *i* can be calculated as a function of Q and H, at previous time step *i-1* and at the neighbouring nodes *n±1* as

$$Q_{m,n}^{i} = 0.5\left(C_{pos} + C_{neg}\right) \tag{4.3}$$

$$H_{m,n}^{i} = \frac{0.5\left(C_{pos} - C_{neg}\right)}{C_{a,m}} \tag{4.4}$$

where C_{pos} and C_{neg} are the positive and negative characteristics defined as

$$C_{pos} = Q_{m,n-1}^{i-1} + \frac{gA_m}{a_m} Q_{m,n-1}^{i-1} - \frac{f_m \Delta t}{2D_m A_m} Q_{m,n-1}^{i-1} \left|Q_{m,n-1}^{i-1}\right| \tag{4.5}$$

$$C_{neg} = Q_{m,n+1}^{i-1} + \frac{gA_m}{a_m} Q_{m,n+1}^{i-1} - \frac{f_m \Delta t}{2D_m A_m} Q_{m,n+1}^{i-1} \left|Q_{m,n+1}^{i-1}\right| \tag{4.6}$$

and

$$C_{a,m} = \frac{gA_m}{a_m} \tag{4.7}$$

The equations shown above may be used to compute the discharge and head for any internal point of the *m-th* pipe, however, special boundary conditions are required to determine the discharge and the head at the nodes *n=0* and *n=N* of each *m-th* conduit.

4.1.2. Boundary Conditions

Boundary condition for upstream tank (forebay)

The time evolution of the water level in the US tank from the *i-th* to the *(i+1)-th* time step is given by the finite-difference expression of equation (3.1)

$$H_f^i = H_f^{i-1} + (Q_{in}^{i-1} - Q_{m=1,n=0}^{i-1}) \frac{\Delta t}{A_f} \tag{4.8}$$

in which Q_{in}^{i+1} and $Q_{m=1,n=0}^{i+1}$ = flows into and out from the forebay at time step i+1, H_f^i is assumed to remain constant during each *i-th* time step and is used to evaluate the head $H_{m=1,n=0}^{i+1}$ and the discharge $Q_{m=1,n=0}^{i+1}$ at the initial section of the conduit according to the relation in equation (3.13).

Using the finite-difference scheme, this equation is solved together with the negative characteristic [Equation (4.6)] and gives the upstream boundary conditions

$$Q^i_{m=1,n=0} = \frac{-1 + \sqrt{1 + 4k(C_{neg} + C_{a,m=1}H^i_f)}}{2k_1} \quad (4.9)$$

$$H^i_{m=1,n=0} = \frac{Q^i_{m=0,n=0} - C_{neg}}{C_{a,m=1}} \quad (4.10)$$

where

$$k_1 = \frac{C_{a,m}(1+k)}{(2gA_{m=1}{}^2)} \quad (4.11)$$

k=coefficient of entrance loss

Boundary condition for surge tank

In the case of the surge tank, the boundary conditions are given combining the time variations of the level in the surge tank and the characteristic equations of the adjacent pipes. To start, the losses at the junction are neglected, therefore at any time

$$H^i_{m=1,n=N} = H^i_{m=2,n=0} = H^i_s \quad (4.12)$$

The flowrates at the final and initial section of the adjacent pipes are given by their characteristic equations

$$Q^i_{m=1,n=N} = C_{pos} - C_{a,m=1}\, H^i_{m=1,n=N} \quad (4.13)$$

$$Q^i_{m=2,n=0} = C_{neg} - C_{a,m=2}\, H^i_{m=2,n=0} \quad (4.14)$$

The flowrate in the surge tank at the end of the time step is given by

$$Q^i_s = \left(H^i_s - H^{i-1}_s\right)\left(\frac{2A_s}{\Delta t}\right) - Q^{i-1}_s H^i_{m=1,n=N} = H^i_{m=2,n=0} = H^i_s \quad (4.15)$$

Flow control with new mechanism and boundary condition for downstream valve

The boundary condition for the downstream valve depends on the opening set by the PI Controller at each time step *i*, therefore it is first presented how the opening of the valve is computed by the controller and then the boundary condition of the valve. The flow control of the system is carried out varying the opening of the valve using equation (3.4) in a finite-difference form.

$$\Delta\tau^i = \left(\left(\frac{H_{fm}^i - H_{target}}{T_i} \right) + \left(k((H_{fm}^i - H_{target}) - (H_{fm}^{i-1} - H_{target})) \right) \right) * \Delta t \quad (4.16)$$

However, to account for uncertainties, delays, non-instant-valve and backlashes this equation may take several forms. In the first place, the measured forebay water level $H_{fm}(t)$ in the finite-difference scheme takes the form of H_{fm}^i. As shown in Figure 4.1 (a) to determine H_{fm}^i a level measure $H_{measure}$ is simulated to be taken every $t_{measure}$ seconds where $t_{measure} > \Delta t$ and the index j is used. The number of time intervals Δt to take a measure is

$$r = \frac{t_{measure}}{\Delta t} \quad (4.17)$$

This means that a measure is taken every time that

$$i = n_m r \qquad with\ n_m = integer \quad (4.18)$$

To model the behaviour of H_{fm}^i between each measure a filter is used with the form of

$$1 - e^{-\left(\frac{t_i - t^*_j}{Tf}\right)} \quad (4.19)$$

where t_i = current time step, t^*_j= elapsed time when the *j-th* measure has been taken and T_f= parameter of the filter. Thus, H_{fm}^i is described by the following equation

$$H_{fm}^i = H_{measure}^{j-1} + \Delta H * \left(1 - f \cdot e^{-\left(\frac{t_i - t^*_j}{T_f}\right)} \right) \ for\ t_j{}^* < t_i < t_{j+1}{}^* \quad (4.20)$$

where

$$\Delta H = H_{measure}^j - H_{measure}^{j-1} \quad (4.21)$$

The variable *f* in equation (4.20) allows to decide whether the signal filtering is used (*f=1*) or not (*f=0*). If the filter is not used, then

$$H_{fm}^i = H_{measure}^j \ for\ t_j{}^* < t_i < t_{j+1}{}^* \quad (4.22)$$

This means that the measured water level is considered constant until the next measure. Every *r* time intervals the measured level $H_{measure}^j$ is computed with the expression

$$H_{measure}^j = H_f^i + (\sigma * rand) \quad (4.23)$$

where $H^{j}_{measure}$ = measured value taken by the sensor at time i, H^{i}_{f} = theoretical value in the forebay at time i, σ = instrumental uncertainty (precision) and *rand* is a casual number extracted from the standard normal distribution (equation (3.21)) . If the delays are considered, the flow control is performed with a delay of t_{delay} seconds or s time intervals after $H_{fm,i}$ has been computed (Figure 4.1 (b))

$$s = \frac{t_{delay}}{\Delta t} \tag{4.24}$$

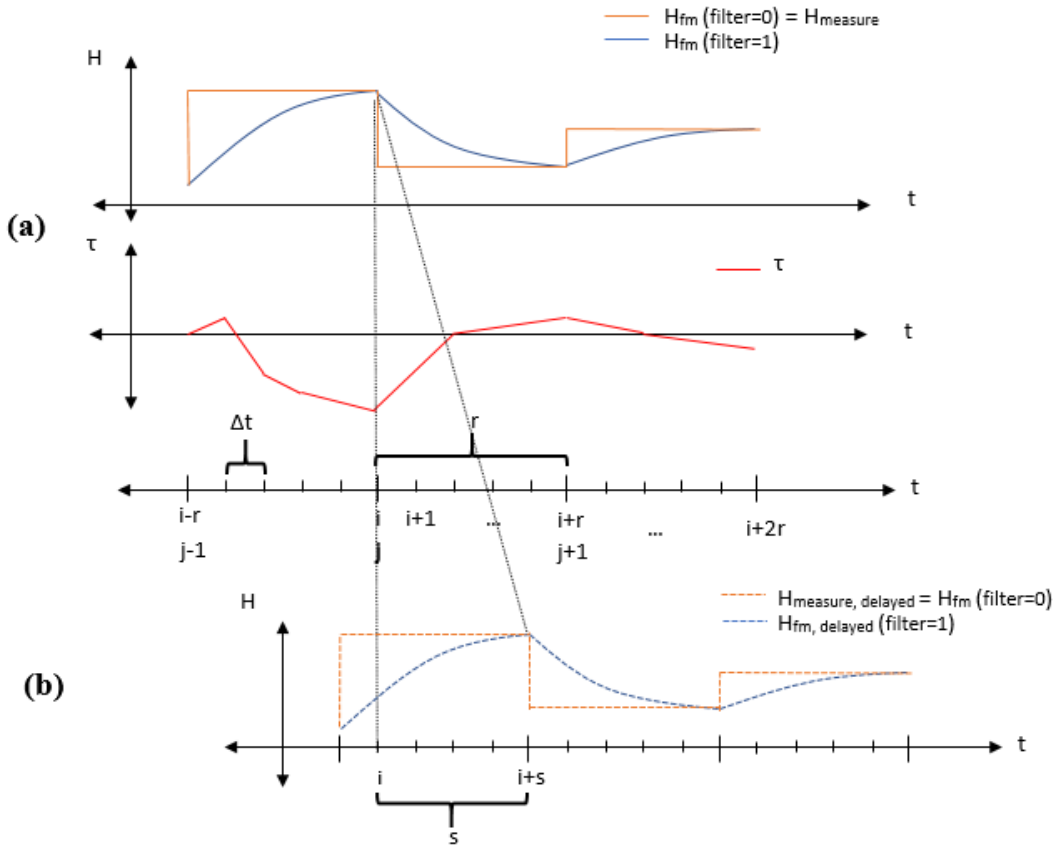

Figure 4.1 – (a) H_f in the finite difference scheme (without delays) – (b) H_f in the finite difference scheme (with delays)

The general equation of the PI Controller with delays and uncertainties included is

$$\Delta\tau^{i} = \left(\left(\frac{H^{i-s}_{fm} - H_{target}}{T_i}\right) + \left(k((H^{i-s}_{fm} - H_{target}) - (H^{i-s-1}_{fm} - H_{target}))\right)\right) * \Delta t \tag{4.25}$$

- If no delays are considered, then s=0
- If no measurement is performed

$$H^{i}_{fm} = H^{i}_{f} \tag{4.26}$$

That is, the level in the forebay is known from the mass balance equation (4.8)

- The usage of filter is considered in equation (4.20)

To account for the effect of the non-instant-valve in the flow control then, equation (3.23) is used in the finite-difference form, the maximum operation $\Delta\tau_{max}$ that can be achieved during time interval Δt is

$$\Delta\tau_{max} = v_{valve,max} \cdot \Delta t \tag{4.27}$$

Therefore, it could be supposed that

$$\Delta\tau_{eff}^{i} = \begin{cases} \Delta\tau^{i}; & |\Delta\tau^{i}| < \Delta\tau_{max} \\ \tau_{max} \cdot sign(\Delta\tau^{i}); & |\Delta\tau^{i}| > \Delta\tau_{max} \end{cases} \tag{4.28}$$

However, this is not the situation. Instead, for the computation of $\Delta\tau_{eff}^{i}$ the following analysis is made: for each time step i the $\Delta\tau_{eff}^{i}$ depends on the consideration of the measurements, the delays and especially on the filter usage. Let us consider a case with no delays and redefine equation (4.25) as

$$\Delta\tau^{i} = \left(\left(\frac{E^{i}}{T_i}\right) + \left(k\, dE^{i}\right)\right) * \Delta t \tag{4.29}$$

where

$$E^{i} = H_{fm}^{i} - H_{target} \tag{4.30}$$

$$dE^{i} = ((H_{fm}^{i} - H_{target}) - (H_{fm}^{i-1} - H_{target})) \tag{4.31}$$

From equations (4.30) and (4.31) and according to equation (4.20), the form of H_{fm} depends on the filter usage and it is possible to say that (Figure 4.2)

$$H_{fm}^{i-1} \neq H_{fm}^{i} \qquad for\ t_j{}^{*} < t_i < t_{j+1}{}^{*};\ \ if\ \ f = 1 \tag{4.32}$$

$$H_{fm}^{i-1} = H_{fm}^{i} \qquad for\ t_j{}^{*} < t_i < t_{j+1}{}^{*};\ \ if\ \ f = 0 \tag{4.33}$$

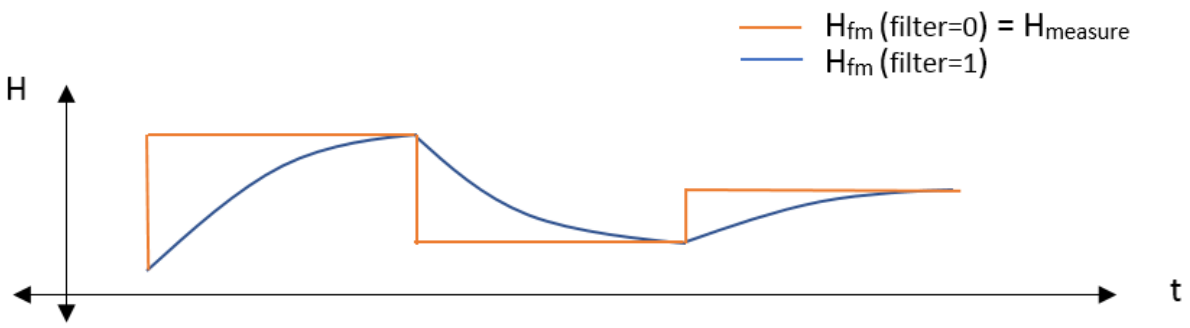

Figure 4.2 – $H_{fm}(t)$ modelled with and without filter

When a filter is used then both E^i and dE^i is considered in the computation of $\Delta\tau^i$ and therefore $\Delta\tau^i$ is in general different to 0. However, as shown in Figure 4.3 when the filter is not considered dE^i is only considered when a new measure is taken [equation (4.18)] because only it this time step that equation

$$H_{fm}^{i-1} \neq H_{fm}^{i} \tag{4.34}$$

for the successive time steps

$$H_{fm}^{i-1} = H_{fm}^{i} = H^j \quad for\ {t_j}^* < t_i < {t_{j+1}}^* \tag{4.35}$$

and therefore

$$dE^i = ((H^j - H_{target}) - (H^j - H_{target})) \tag{4.36}$$

$$dE^i = 0 \tag{4.37}$$

Thus only E^i is used in the computation of $\Delta\tau^i$. In this research it is concerned on the stability of the flow control system and therefore variations of the forebay level are expected to be close to the target value, thus in a range of some centimetres, therefore E^i is often little and has little impact in the computation of $\Delta\tau^i$ compared to that of dE^i. In consequence when no filter is used (Figure 4.3)

$$\Delta\tau^i \neq 0 \quad if\ \ i = n_m r \quad with\ n_m = integer \tag{4.38}$$

$$\Delta\tau^i \approx 0 \quad if\ \ i \neq n_m r \quad with\ n_m = integer \tag{4.39}$$

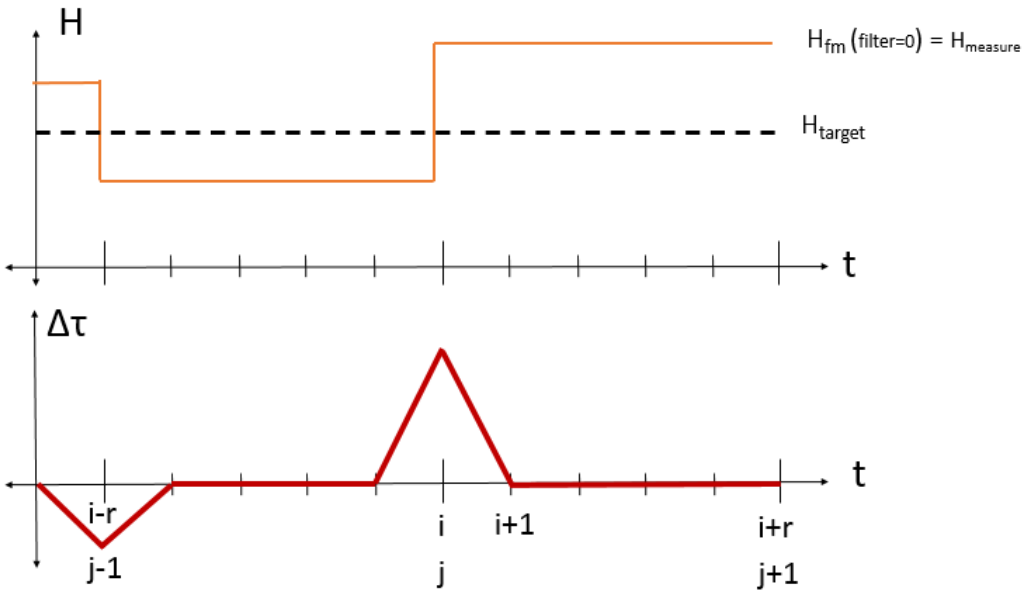

Figure 4.3 – Computation of Δτ when a filter is not used

Now, the consequence of this situation is that if to account for non-instant-valve effects the equation (4.28) was and it happened that

$$\left|\Delta\tau^i\right| > \Delta\tau_{max}$$

when the measure has just been taken then

$$\Delta\tau_{eff}^i = \Delta\tau_{max} \cdot sign(\Delta\tau^i)$$

and then for the other time intervals

$$\Delta\tau_{eff}^i = 0$$

As shown in Figure 4.4

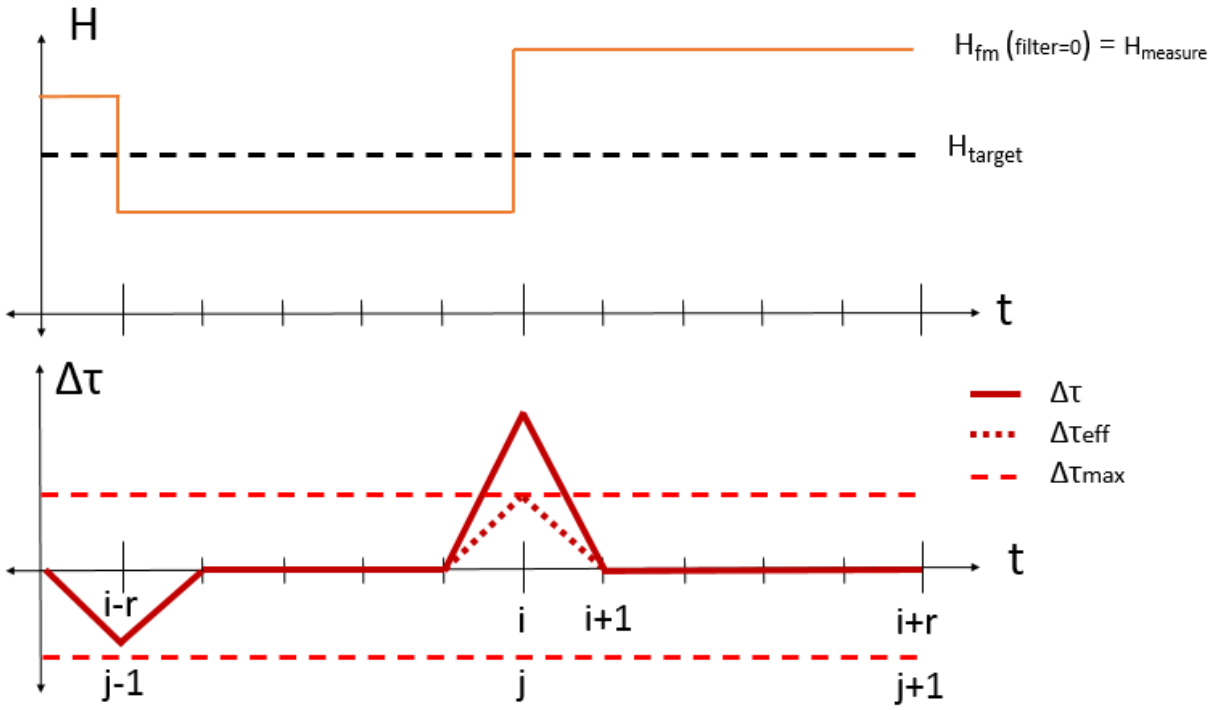

Figure 4.4 – Comparison between the computation of $\Delta\tau$ and $\Delta\tau_{eff}$ when a filter is not used

The consequence is that the valve could not arrange the desired operation when the measure is taken and, in addition, it would not perform any operation until the next measure.

To take advantage that however the level in the forebay is supposed to be constant until the next measure is taken then if filter is not used the $\Delta\tau_{eff}^i$ is determined as follows (Figure 4.5).

If a measure has just been taken that is

$$i = n_m r \quad with\ n_m = integer$$

$$\Delta\tau_{eff}^{i} = \begin{cases} \Delta\tau^{i}; & |\Delta\tau^{i}| < \Delta\tau_{max} \\ \tau_{max} \cdot sign(\Delta\tau^{i}); & |\Delta\tau^{i}| \geq \Delta\tau_{max} \end{cases} \tag{4.40}$$

$$\Delta\tau_{miss}^{i} = \begin{cases} 0; & |\Delta\tau^{i}| < \Delta\tau_{max} \\ |\Delta\tau^{i}| - \Delta\tau_{max}; & |\Delta\tau^{i}| \geq \Delta\tau_{max} \end{cases} \tag{4.41}$$

after the measure, that is

$$i \neq n_m r \quad with\ n_m = integer$$

$$\Delta\tau_{eff}^{i} = \begin{cases} \Delta\tau_{miss}^{i-1} \cdot sign(\Delta\tau_{eff}^{i-1}); & \Delta\tau_{miss}^{i-1} < \Delta\tau_{max} \\ \Delta\tau_{max} \cdot sign(\Delta\tau_{eff}^{i-1}); & \Delta\tau_{miss}^{i-1} \geq \Delta\tau_{max} \end{cases} \tag{4.42}$$

$$\Delta\tau_{miss}^{i} = \begin{cases} 0; & \Delta\tau_{miss}^{i-1} < \Delta\tau_{max} \\ \Delta\tau_{miss}^{i-1} - \Delta\tau_{max}; & \Delta\tau_{miss}^{i-1} \geq \Delta\tau_{max} \end{cases} \tag{4.43}$$

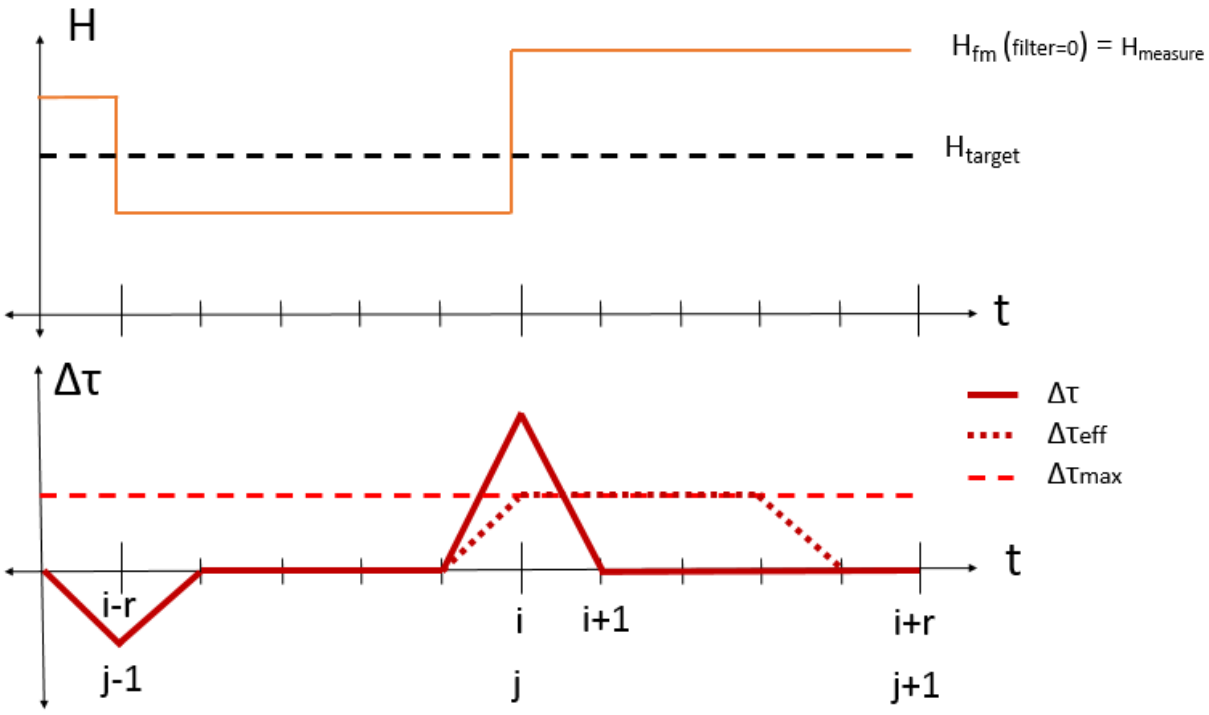

Figure 4.5 – Actual modelled computation of $\Delta\tau_{eff}$ when a filter is not used

If a filter is considered

$$\Delta\tau_{eff}^{i} = \begin{cases} \Delta\tau^{i}; & \left|\Delta\tau^{i}\right| + \Delta\tau_{miss}^{i-1} < \Delta\tau_{max} \\ \Delta\tau_{max} \cdot sign(\Delta\tau^{i}); & \left|\Delta\tau^{i}\right| + \Delta\tau_{miss}^{i-1} \geq \Delta\tau_{max} \end{cases} \tag{4.44}$$

$$\Delta\tau_{miss}^{i} = \begin{cases} 0; & \left|\Delta\tau^{i}\right| + \Delta\tau_{miss}^{i-1} < \Delta\tau_{max} \\ \left|\Delta\tau^{i} - \Delta\tau_{max}\right|; & \Delta\tau_{miss}^{i-1} > \Delta\tau_{max} \end{cases} \tag{4.45}$$

If the non-instant valve effects are not considered

$$\Delta\tau_{eff}^{i} = \Delta\tau^{i} \tag{4.46}$$

To account for the backlash effects, consider that at time *i* the mechanical parts of the valve have a positive gap gap_{pos}, a negative gap gap_{neg} then $\Delta\tau_{real}^{i}$ is given by

If $\Delta\tau_{eff}^{i}$ is positive, i.e. the valve is opened

$$\Delta\tau_{real}^{i} = \begin{cases} 0; & \Delta\tau_{eff}^{i} < gap_{pos}^{i-1} \\ b \cdot \left(\Delta\tau_{eff}^{i} - gap_{pos}^{i-1}\right); & \Delta\tau_{eff}^{i} \geq gap_{pos}^{i-1} \end{cases} \tag{4.47}$$

$$gap_{pos}^{i} = \begin{cases} gap_{pos}^{i-1} - \Delta\tau_{eff}^{i}; & \Delta\tau_{eff}^{i} < gap_{pos}^{i-1} \\ 0; & \Delta\tau_{eff}^{i} \geq gap_{pos}^{i-1} \end{cases} \tag{4.48}$$

$$gap_{neg}^{i} = \begin{cases} -(gap_{total} - gap_{pos}^{i-1}); & \Delta\tau_{eff}^{i} < gap_{pos}^{i} \\ -gap_{total}; & \Delta\tau_{eff}^{i} \geq gap_{pos}^{i} \end{cases} \tag{4.49}$$

If $\Delta\tau_{eff}^{i}$ is negative, i.e. the valve is closed

$$\Delta\tau_{real}^{i} = \begin{cases} b \cdot \left(\Delta\tau_{eff}^{i} - gap_{neg}^{i-1}\right); & \Delta\tau_{eff}^{i} \leq gap_{neg}^{i-1} \\ 0; & \Delta\tau_{eff}^{i} > gap_{neg}^{i} \end{cases} \tag{4.50}$$

$$gap_{neg}^{i} = \begin{cases} 0; & \Delta\tau_{eff}^{i} \leq gap_{neg}^{i-1} \\ gap_{neg}^{i-1} - \Delta\tau_{eff}^{i}; & \Delta\tau_{eff}^{i} > gap_{neg}^{i} \end{cases} \tag{4.51}$$

$$gap_{pos}^{i} = \begin{cases} gap_{total}; & \Delta\tau_{eff}^{i} \leq gap_{neg}^{i-1} \\ -(gap_{total} + gap_{neg}^{i-1}); & \Delta\tau_{eff}^{i} > gap_{neg}^{i} \end{cases} \tag{4.52}$$

Which is the same behaviour described in Figure 3.1. and which in the finitie-difference scheme becomes Figure 4.6 - $\Delta\tau_{real}$ obtained at a given time t as a function of dτ, the gaps and b

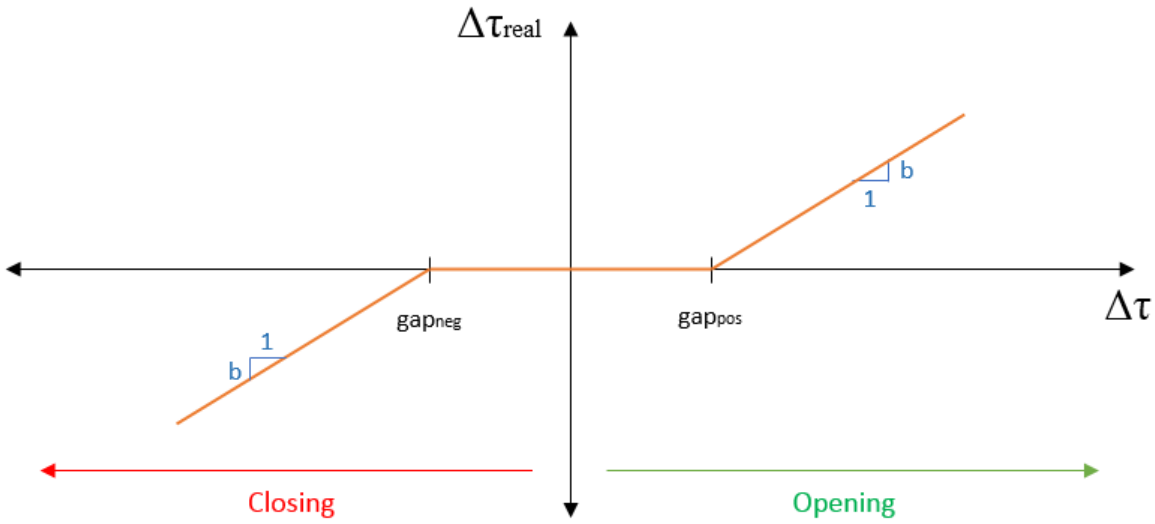

Figure 4.6 - $\Delta\tau_{real}$ obtained at a given time t as a function of dτ, the gaps and b

Once the PI controller has determined the operation to be performed, the τ of the valve at time interval i may be computed as

$$\tau^i = \tau^{i-1} + \Delta\tau^i_{real}; \quad backlash\ considered \tag{4.53}$$

$$\tau^i = \tau^{i-1} + \Delta\tau^i_{eff}; \quad non\ instant\ valve\ considered \tag{4.54}$$

$$\tau^i = \tau^{i-1} + \Delta\tau^i;\ instant\ valve\ and\ no\ backlash\ considered \tag{4.55}$$

Hence the area of the valve at any time interval is

$$A^i_v = \tau^i \cdot A_{vo} \tag{4.56}$$

Once the area of the valve at time step *i* has been determined, the boundary conditions for the downstream valve may be found solving together the equation (3.15) in the finite-difference scheme and equation (4.5)

$$Q^i_{m=2,n=N} = \frac{-\eta^i + \sqrt{(\eta^i)^2 + 4\eta^i C_p}}{2} \tag{4.57}$$

$$H^i_{m=1,n=0} = \frac{C_n - Q^i_{m=2,n=N}}{C_{a,m=2}} \tag{4.58}$$

where

$$\eta^i = \frac{2g(c_v A_v^i)^2}{C_{a,m=2}} \tag{4.59}$$

4.1.3. Initial Conditions

The system of equations that described the steady-state flow described in the Mathematical Model is solved using iterative methods

4.2. Stability function

The variables that make up the stability function were determined analysing the sets defined in Chapter 3.

4.2.1. Set of hydraulic components variables Y_P

Since an existing plant is analysed, all these variables have already been defined, therefore they are not considered in the stability function.

4.2.2. Set of variables related to the flow control system mechanisms effects Y_{FE}

The mechanisms that are considered in the flow control system are:

- Hydraulic transients
- Instrumental uncertainties
- Measuring times
- Delays
- Non-instant valve effects
- Backlash effects

Therefore, the function $Y_{FE,M}$ for each of these mechanisms must be found

Hydraulic Transients

The hydraulic transients are considered in the model itself when the governing equations as functions of time and space were stated, therefore, it will not be considered as a function or as a variable in the stability function.

Instrumental uncertainty function

The instrumental uncertainty function U_e has as Boolean variable U_B = Boolean variable and parameters σ = instrumental uncertainty and f = function. However, considering σ=0 is equivalent to considering the Boolean variables U_B=0 therefore it is convenient not to consider the Boolean variable always on (=1), hence

$$U_e = f(\sigma, f) \tag{4.60}$$

Measuring time function

The measuring time function M_e does not have a Boolean variable to turn it on or off, instead it is considered always on. The only parameter is the time of measuring $t_{measure}$ so

$$M_e = f(t_{measure}) \tag{4.61}$$

Delays function

As well as the measuring time function the delays function has no Boolean variable and is considered always turned on. The only parameter that defines it is the time of delay $t_{dealy,}$ hence

$$D_e = f(t_{delay}) \tag{4.62}$$

Non-instant valve function

The non-instant valve function NIV_e has Boolean variables NIV_B and the parameter $v_{v,max}$=maximum valve velocity. This parameter is considered to be already known so

$$NIV_e = f(NIV_B) \tag{4.63}$$

Backlash function

The backlash effects function BL_e has Boolean variable BL_B=Boolean variable and parameters gap_{pos}, gap_{neg}, fr. The gaps and the friction are constant values (Norconsult SA, 2016), thus

$$BL_e = f(BL_B) \tag{4.64}$$

4.2.3. Set of variables related to the PI Controller

The only parameters that are variable in the PI Controller are α and K_1 therefore

$$PIController_e = f(\alpha, K_1) \tag{4.65}$$

4.2.4. Definitive stability function

Ultimately, combining equations (4.60), (4.61), (4.62), (4.63), (4.64) and (4.65) with equation (3.42), the stability function of this dynamical system is made up by the following variables (Figure 4.7)

$$S = f\left(BL_e(BL_B), NIV_e(NIV_B), U_e(\sigma, f), D_e(t_{delay}), M_e(t_{measure}), \alpha, K_1\right) \quad (4.66)$$

$$S = f\left(BL_B, NIV_B, \sigma, f, t_{delay}, t_{measure}, \alpha, K_1\right) \quad (4.67)$$

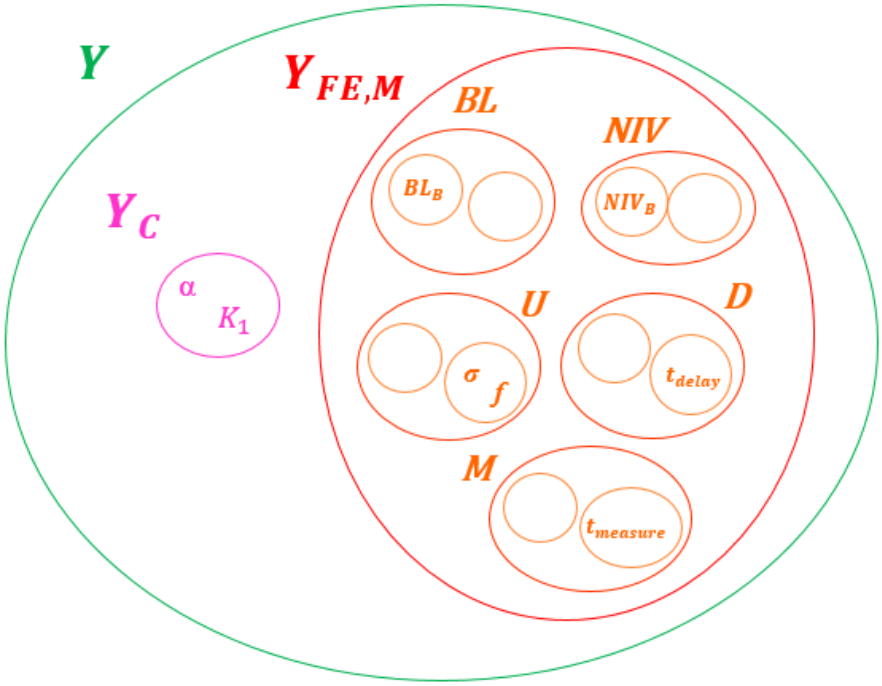

Figure 4.7 – Definite set of variables considered in this study

The empty sets in Figure 4.7. are intended to show the lack of Boolean or other variables in a set.

Let us now define w=generic global case, α_x, a generic α value and $K1_y$, a generic K1 value so that the exponential fit parameter S associated to a *particular case* is called

$$S_{w,\alpha_x,K1_y} = S(w, \alpha_x, K1_y) \quad (4.68)$$

4.3. The Benchmark global case

Let us define as the benchmark case the global case in which none of the exposed mechanisms but the hydraulic transients are considered, therefore a case in which all the variables in the set of Y_{FE} are 0. If the benchmark case is denoted with the subscript BM then stability function of the benchmark case is named as $S_{BM,\alpha_x,K1_y}$ and is defined by

$$S_{BM,\alpha_x,K1_y} = f(BL_B = 0, NIV_B = 0, \sigma = 0, f = 0, D = 0, M = 0, \alpha, K_1) \quad (4.69)$$

4.4. Exponential fit parameter S

To find the parameter S of a particular case $S_{w,\alpha_x,K1_y}$ it was followed this process:

After finding the time series of $H_f(t)$, the new function $H_{f1}(t)$ was computed as

$$H_{f1}(t) = \left|H_f(t) - H_{target}\right| \tag{4.70}$$

As $H_{f1}(t)$ was expected to oscillate around 0, all the peaks were identified and tagged. The peaks were subjected to an exponential fit using a certain fitting method, obtaining the function

$$expfit = ef_{w,\alpha_x,K1_y} = a_{w,\alpha_x,K1_y} \cdot e^{S_{w,\alpha_x,K1_y} \cdot t} \tag{4.71}$$

The values of $a_{w,\alpha_x,K1_y}$ and $S_{w,\alpha_x,K1_y}$ depend on the fitting technique used, in this document the *least squares method* was used.

4.5. Stability limit curves

The *stability limits* were defined in chapter 3 as the surfaces that represent the border between the "stable" and "unstable" cases. The control in this plant is performed by a PI Controller thus the variables Y_C are only α and K_1 therefore the stability limit of a generic global case for this plant is defined as

$$S_w = f(\alpha, K_1) = 0 \tag{4.72}$$

Since it involves only two variables then it is a curve in the α-K_1 plane and is called *stability limit curve* of a certain *global case*. To determine the stability limit curve of a *global case* a finite number of *particular cases* are simulated. Each of the $S_{w,\alpha_x,K1_y}$ are organized in an exponential fit stability matrix $[S_w]$ defined as

$$[S_w] = \begin{bmatrix} S_{w,\alpha_1,K1_1} & \cdots & S_{w,\alpha_1,K1_y} \\ \vdots & \ddots & \vdots \\ S_{w,\alpha_{nx},K1_1} & \cdots & S_{w,\alpha_{nx},K1_{ny}} \end{bmatrix} \tag{4.73}$$

where *nx*=number of α values considered and *ny*=number of K1 values considered. The stability limit curve is obtained interpolating the values of S=0 in the matrix.

4.6. Statistical stability assessment

Since $H_f(t)$ and τ(t) are discrete functions the mean values and the standard deviations of a particular case are described by the discrete form of equations (3.44) to (3.47), hence

$$\overline{H_{f,w,\alpha_x,K1_y}} = \frac{\sum_{i=1}^{n_t} H_{f,w,\alpha_x,K1_y i}}{n_t} \quad (4.74)$$

$$\overline{\tau_{w,\alpha_x,K1_y}} = \frac{\sum_{i=1}^{n_t} \tau_{w,\alpha_x,K1_y i}}{n_t} \quad (4.75)$$

$$s\_H_{f,w,\alpha_x,K1_y} = \sqrt{\frac{\sum_{i=1}^{n_t} \left(H_{f,w,\alpha_x,K1_y} - \overline{H_{f,w,\alpha_x,K1_y}}\right)^2}{n_t - 1}} \quad (4.76)$$

$$s\_\tau_{w,\alpha_x,K1_y} = \sqrt{\frac{\sum_{i=1}^{n_t} \left(\tau_{w,\alpha_x,K1_y\, i} - \overline{\tau_{w,\alpha_x,K1_y}}\right)^2}{n_t - 1}} \quad (4.77)$$

When the oscillations tended very fast to H_{target} the computation of the mean value and the standard deviation was limited to the time intervals before a level $\Delta H_{stability}$ was reached, this means that if for a particular case it existed a time t_s where

$$\left|H_f - H_{target}\right| \leq \Delta H_{stability}; \quad for\ t \geq t_s \quad (4.78)$$

the mean values and the standard deviations were computed for values of $n_t = n_{t,s}$ where $n_{t,stability}$ are the time intervals comprised in $t<t_s$. Here the value $\Delta H_{stability}$ = 1mm was used.

Regarding the mean value, more than the mean value itself it was of interest to analyse how much it deviated from H_{target} therefore the deviations were computed as

$$\overline{\Delta H_{f,w,\alpha_x,K1_y}} = \overline{H_{f,w,\alpha_x,K1_y}} - H_{target} \quad (4.79)$$

$$\overline{\Delta\tau_{w,\alpha_x,K1_y}} = \overline{\tau_{w,\alpha_x,K1_y}} - \tau_{target} \quad (4.80)$$

where τ_{target} is taken as the steady-state value of τ which in this case is τ_{target}=1.

To compare the standard deviation of a particular case of a global case w with the standard deviation of a particular case of the benchmark case the ratios of standard deviations were computed as well as

$$r\_s\_H_{f,w,\alpha_x,K1_y} = \frac{s\_H_{f,w,\alpha_x,K1_y}}{s\_H_{f,BM,\alpha_x,K1_y}} \quad (4.81)$$

$$r\_s\_\tau_{w,\alpha_x,K1_y} = \frac{S\_\tau_{w,\alpha_x,K1_y}}{S\_\tau_{BM,\alpha_x,K1_y}} \quad (4.82)$$

The mean values, the standard deviations and the ratios of standard deviations were organized in matrices called *statistical matrices* and defined as:

Mean deviation matrices

$$\left[\overline{\Delta H_{f,w}}\right] = \begin{bmatrix} \overline{\Delta H_{f,w,\alpha_1,K1_1}} & \cdots & \overline{\Delta H_{f,w,\alpha_1,K1_y}} \\ \vdots & \ddots & \vdots \\ \overline{\Delta H_{f,w,\alpha_{nx},K1_1}} & \cdots & \overline{\Delta H_{f,w,\alpha_{nx},K1_{ny}}} \end{bmatrix} \tag{4.83}$$

$$\left[\overline{\Delta \tau_w}\right] = \begin{bmatrix} \overline{\Delta \tau_{w,\alpha_1,K1_1}} & \cdots & \overline{\Delta \tau_{w,\alpha_1,K1_y}} \\ \vdots & \ddots & \vdots \\ \overline{\Delta \tau_{w,\alpha_{nx},K1_1}} & \cdots & \overline{\Delta \tau_{w,\alpha_{nx},K1_{ny}}} \end{bmatrix} \tag{4.84}$$

Standard deviation matrices

$$\left[s\_H_{f,w}\right] = \begin{bmatrix} s\_H_{f,w,\alpha_1,K1_1} & \cdots & s\_H_{f,w,\alpha_1,K1_y} \\ \vdots & \ddots & \vdots \\ s\_H_{f,w,\alpha_{nx},K1_1} & \cdots & s\_H_{f,w,\alpha_{nx},K1_{ny}} \end{bmatrix} \tag{4.85}$$

$$\left[s\_\tau_w\right] = \begin{bmatrix} s\_\tau_{w,\alpha_1,K1_1} & \cdots & s\_\tau_{w,\alpha_1,K1_y} \\ \vdots & \ddots & \vdots \\ s\_\tau_{w,\alpha_{nx},K1_1} & \cdots & s\_\tau_{w,\alpha_{nx},K1_{ny}} \end{bmatrix} \tag{4.86}$$

Ratio of standard deviation matrices

$$\left[r\_s\_H_{f,w}\right] = \begin{bmatrix} r\_s\_H_{f,w,\alpha_1,K1_1} & \cdots & r\_s\_H_{f,w,\alpha_1,K1_y} \\ \vdots & \ddots & \vdots \\ r\_s\_H_{f,w,\alpha_{nx},K1_1} & \cdots & r\_s\_H_{f,w,\alpha_{nx},K1_{ny}} \end{bmatrix} \tag{4.87}$$

$$\left[r\_s\_\tau_w\right] = \begin{bmatrix} r\_s\_\tau_{w,\alpha_1,K1_1} & \cdots & r\_s\_\tau_{w,\alpha_1,K1_y} \\ \vdots & \ddots & \vdots \\ r\_s\_\tau_{w,\alpha_{nx},K1_1} & \cdots & r\_s\_\tau_{w,\alpha_{nx},K1_{ny}} \end{bmatrix} \tag{4.88}$$

4.7.Comparison between Jimenez's and the present document's approach

Before stepping into the simulation setup and the results it is interesting to make a comparison between the approach proposed by Jimenez and the present document approach to analyse their differences and the consequences of using each one. The comparison is done confronting the characteristics of both methods in two separate columns, being able to compare the characteristics of each method in parallel. At the left side, the Jimenez's approach is presented and at the right side the present document's one.

Sets of variables involved

- Set of variables related to the hydraulic components Y_P
- Set of variables related to the PI Controller Y_C

Control variables

- H_f
- H_s
- τ

Governing equations

- Conduit dynamic equation

$$\frac{L_t}{g\,A_t}\frac{dQ_t}{dt} + C_t|Q_t|Q_t + C_s|Q_s|Q_s = H_f - H_s$$

The equation involves the whole tunnel length, moreover, since the penstock length is much shorter than the tunnel length it is neglected

- Continuity equation for the forebay

$$A_f\frac{dH_f}{dt} = Q_r - Q_w - Q_t$$

- Continuity equation for the surge tank

$$A_s\frac{dH_s}{dt} = Q_s = Q_t - Q_v$$

- Discharge in the downstream valve

$$Q_v = \tau Q_o\sqrt{\frac{H_s + C_s|Q_s|Q_s}{H_o}}$$

- Water-level controller (PI Controller)

$$\frac{d\tau}{dt} = \frac{H_f - H_{ref}}{T_i} + k\frac{d(H_f - H_{ref})}{dt}$$

C_t, C_s= head loss coefficients for the tunnel and the surge tank orifice

Sets of variables involved

- Set of variables related to the hydraulic components Y_P
- Set of variables related to the effects of the mechanisms of the flow control system Y_{FE}
- Set of variables related to the PI Controller Y_C

Control variables

- H_f
- H_s
- τ

Governing equations

- Generic conduit dynamic equation

$$\frac{\partial Q}{\partial t} + gA\frac{\partial H}{\partial x} + \frac{f}{2DA}Q|Q| = 0$$

- Generic conduit continuity equation

$$\frac{a^2}{gA}\frac{\partial Q}{\partial x} + \frac{\partial H}{\partial t} = 0$$

- Continuity equation (mass balance equation in the forebay)

$$A_f\frac{dH_f(t)}{dt} = Q_{in}(t) - Q_t(t, x = 0)$$

- Continuity equation for the surge tank (mas balance equation in the surge tank)

$$A_s\frac{dH_s(t)}{dt} = \left(Q_t(t, x = L_t) - Q_p(t, x = 0)\right)$$

- Discharge in the downstream valve

$$Q_v(t) = A_v(t)c_v\sqrt{2gH_v(t)}$$

Water-level controller (PI Controller)

$$\frac{d\tau}{dt} = \frac{H_f - H_{ref}}{T_i} + k\frac{d(H_f - H_{ref})}{dt}$$

Methods of solution and stability analysis

The aim is to find

- $Q_t(t)$
- $H_f(t)$
- $H_s(t)$
- $\tau(t)$

ODE

Jimenez rewrites the governing equations to obtain a set of dimensionless form and linearized. This allows him to obtain a system of equations written in the matrix form as follows

$$\frac{d\boldsymbol{X}}{dt} = \boldsymbol{AX} + \boldsymbol{B}$$

Where $\boldsymbol{X}$ is the vector of dimensionless variables to be found.

Jimenez determines the stability ***without solving the system of equations*** but by means of the Routh-Hurwitz criterion.

According to the Routh-Hurwitz criterion, ***the system is stable if the real parts of the eigenvalues of the matrix A are negative***.

The stability assessment is performed by ***analytical means***.

Using this criterion, Jimenez determines that the stability of the system is a function of five variables:

n, m, p = variables related to the characteristics of the plant

and

α, K_I = variables related to the PI controller

if the variables n, m and p are known, i.e., the stability analysis is studied over an existing plant, then the stability depends only on the parameters of the PI controller. Since only two variables are left, Jimenez presents his stability analysis on the Rio Macho Hydropower plant using stability curves shown plotted in a α- K_I plane where the points inside the curve represent the stable region.

Methods of solution and stability analysis

The aim is to find

- $Q(x,t)$ in the conduits
- $H(x,t)$ in the conduits
- $H_f(t)$
- $H_s(t)$
- $\tau(t)$

PDE

In opposition to the method exposed by Jimenez, there is no analytical way to assess the stability and, in addition, the set of equations is a set of hyperbolic partial differential equations that has ***no analytical solution, therefore numerical methods need to be used.*** In this context ***the method of the characteristics is used*** to solve the PDE.

Since the equations are functions of the time *t* and the distance *x*, both initial and boundary conditions need to be stated.

In the case of the initial conditions they are found by computing the steady-state flow. In the case of the boundary conditions, special conditions are used in each special node of the system, i.e., the forebay, the surge tank and the control valve. All the new mechanisms are included in the boundary condition for the control valve

Since no analytical solution exists, the behaviour of the system needs to be numerically modelled. The stability of the system is determined after the simulation evaluating if the oscillations in $H_f(t)$ tend to damp in respect to time. To determine if the oscillations dampened the maximum values of the oscillations were subjected to an exponential fit of the form

$$f = a \cdot e^{St}$$

If the coefficient S<0 it meant that the oscillations tended to damp.

Since no analytical way exists to assess stability with this method ***the equations must be solved for different values of variables Y_P and Y_{FE} and then the stability is determined.***

Stability function, Stability criterion

According to the method of solution exposed and the stability analysis done by Jimenez it is possible to say that:

If the assessment is performed over an existing plant, the ***Stability function*** will have the following variables

$$Stability = f(\alpha, K_1)$$

And would be represented by the characteristic polynomial of the Matrix A. It is necessary to highlight the fact that the stability function in this approach is not represented by the parameter S because an exponential fit is no necessary.

In addition, due to the simplifications, the stability is only function of the PI Controller parameters

The ***Stability criterion*** in this approach would be the Routh-Hurwitz criterion, i.e., ***if the real parts of the eigenvalues of the matrix A are negative***.

Stability function, Stability criterion

The ***Stability function*** is

$$S = f\left(BL_B, NIV_B, \sigma, f, t_{delay}, t_{measure}, \alpha, K_1\right)$$

Where S is the parameter of the exponential fit and whose form depend on the fitting technique.

Since the new mechanisms are considered, the stability function depends not only on the PI Controller parameters but on the variables of the different mechanisms.

The ***Stability criterion*** used was:

a dynamic system is stable if

$$S < 0$$

4.8.Simulation setup

Numerical simulations were performed to systematically assess the stability of the flow control system.

The followed process was:

1. Set hydropower plant characteristics
- Hydraulic conditions
- Geometry
- Steady-state conditions
- Simulation parameters
    - Total time of simulations
    - Δt
    - Δx
2. Fix a *global case*, i.e., define the Y_{FE} variables
3. Fix a *particular case*, i.e., define α and K_1.
4. Perform numerical simulation using the Method of the Characteristics for the given case
5. Obtain time-series of $H_f(t)$ and $\tau(t)$
6. Determine stability using the exponential fit and the stability criterion
7. Determine the mean values and the standard deviations of $H_f(t)$ and $\tau(t)$

The steps 2-7 were performed in a loop varying all the variables to finally

8. Obtain the exponential fit matrices [S]
9. Obtain the stability limit curves in the α-K_1 plane.
10. Obtain the mean values, standard deviations, and ratio of standard deviations matrices [H] [τ] [s_H] [s_τ] [r_s_H] [r_s_τ]

Regarding the stability function the Boolean variables considered were those considered in Table 4.1.

Table 4.1 – Boolean variables considered

Boolean variable	Symbol	Range
Non-instant valve	NIV_B	0, 1
Backlash	BL_B	0, 1

The rest of the variables were considered in ranges reported in Table 4.2

Table 4.2 – Values and ranges of the non-Boolean variables

Variable	Symbol	Unit	Range
Instrumental uncertainty	σ	m	0, 0.01, 0.05, 0.1
Filter	*f*	(-)	0, 1
Delay time	t_{delay}	s	0, 0.1, 0.5, 1
Measuring time	$t_{measure}$	s	0, 1
PI Controller parameter 1	α	(-)	5, 10, 15, 20, 25, 30, 35, 40, 45, 50, 55, 60, 65, 70, 75, 80, 85, 90
PI Controller parameter 2	K_1	(-)	0.5, 1.0, 1.5, 2.0, 2.5, 3.0, 3.5, 4.0, 4.5, 5.0, 5.5, 6.0, 6.5 7.0, 7.5, 8.0, 8.5, 9.0

Any combination of these parameters was tested and the only restrictions that were added were

- If $\sigma \neq 0$ then $t_{measure}=1$
- If $\sigma = 0$ then $f=0$

These combinations can be organized in a tree diagram from Figure 4.8. In the figure the delays t_{delay} and the measuring time $t_{measure}$ are represented by the variables D and M, respectively. The most relevant constant parameters that describe the plant and each of the mechanisms are shown in Table 4.3

Table 4.3 –Most relevant constant parameters used in the simulations

Variable	Symbol	Unit	Value
	Forebay		
Incoming river flow	Q_{in}	m^3/s	36.1
Surface area of the forebay	A_f	m^2	1297.3
Head target value	H_{target}	m	112
	Tunnel		
Tunnel Length	L_t	m	4005.00
Cross-sectional area of the tunnel	A_t	m^2	8.04
D-W Friction factor	f_t	(-)	0.009
Tunnel wave speed	a_t	m/s	1365.1
	Penstock		
Penstock Length	L_p	m	276
Cross-sectional area of the penstock	A_p	m^2	8.04
D-W Friction factor	f_p	(-)	0.01
Penstock wave speed	a_p	m/s	683.5
	Surge tank		
Surface area of the surge tank	A_s	m^2	61.20
	Non-instant valve		
Maximum valve velocity	$v_{v,max}$	%/s	2.5
	Backlash		
Positive gap	gap_{pos}	%	0.15
Negative gap	gap_{neg}	%	-0.15
Backlash friction	fr	%	0.5

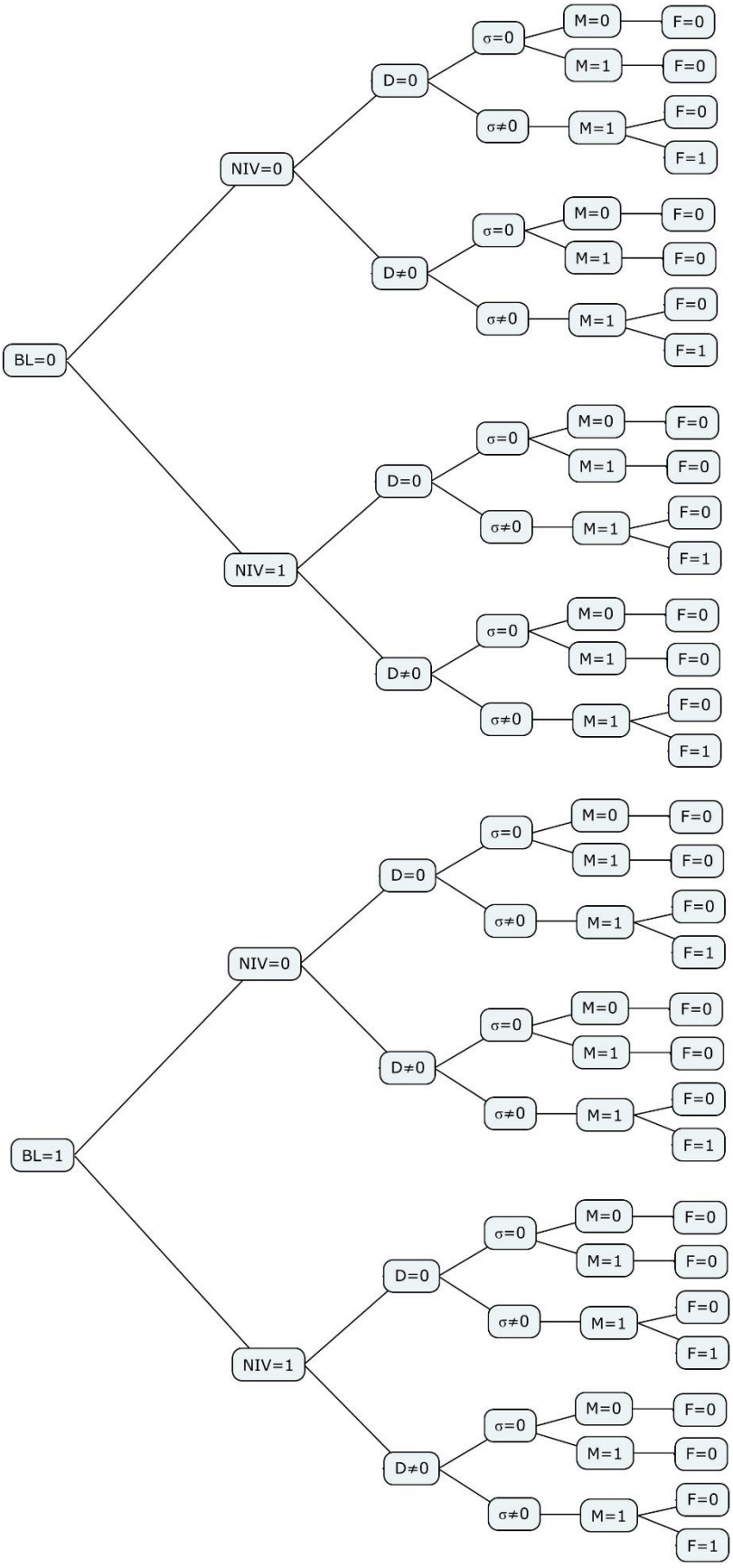

Figure 4.8 – Tree diagram of the possible combinations of global cases

The *particular* and *global cases* shown in Table 4.4 and Table 4.5 respectively are considered to show typical results.

Table 4.4 – Particular cases shown in typical results

Variable	Symbol	Unit	Particular Case A (BM)	Particular Case B	Particular Case C	Particular Case D
Non-instant valve	NIV_B	(-)	0	0	1	0
Backlash	BL_B	(-)	0	0	0	1
Instrumental uncertainty	σ	m	0	0.1	0	0
Filter	f	(-)	0	1	0	0
Delay time	t_{delay}	s	0	0.5	0.1	1
Measuring time	$t_{measure}$	s	0	1	0	1
PI Controller parameter 1	α	(-)	65	45	25	50
PI Controller parameter 2	K_1	(-)	2.5	5.5	3.5	5

Table 4.5 – Global Cases shown in typical results

			Exponential Fit			Statistical Analysis		
Variable	**Symbol**	**Unit**	**Set of Global Cases A**	**Set of Global Cases B**	**Set of Global Cases C**	**Global Case D**	**Global Case E**	**Global Case F**
Non-instant valve	NIV_B	(-)	0	1	0	0	1	1
Backlash	BL_B	(-)	0	0	0	1	0	1
Instrumental uncertainty	σ	m	0	0	0.05	0	0.05	0.1
Filter	f	(-)	0	0	0	0	0	1
Delay time	t_{delay}	s	0, 1	0, 1	0, 1	1	1	1
Measuring time	$t_{measure}$	s	0	0	1	0	1	1

The simulations were performed for the values shown in Table 4.6.

Table 4.6 – Values used for the simulation

Variable	Symbol	Unit	Value
Tunnel space discretization	Δx_t	m	58.44
Penstock space discretization	Δx_p	m	29.26
Time discretization	Δt	s	0.04
Total simulation time	t_{total}	s	10^4
Number of time intervals	n_t	(-)	2.5×10^5

5. RESULTS

5.1.Typical Results of a Particular Case

Typical results of a particular case after one simulation consisted of: time-series of the level in the forebay $H_f(t)$, the valve opening $\tau(t)$ and the valve opening derivative $\Delta\tau(t)$, namely, the variable that is modified by the PI Controller; Exponential fit of the peaks of the oscillations of $H_f(t)$ around H_{target} and computations of the mean, the standard deviation and the ratio of standard deviation of $H_f(t)$ and $\tau(t)$. The results from the particular cases exposed in Table 4.4 are shown in Figure 5.1 and Figure 5.2

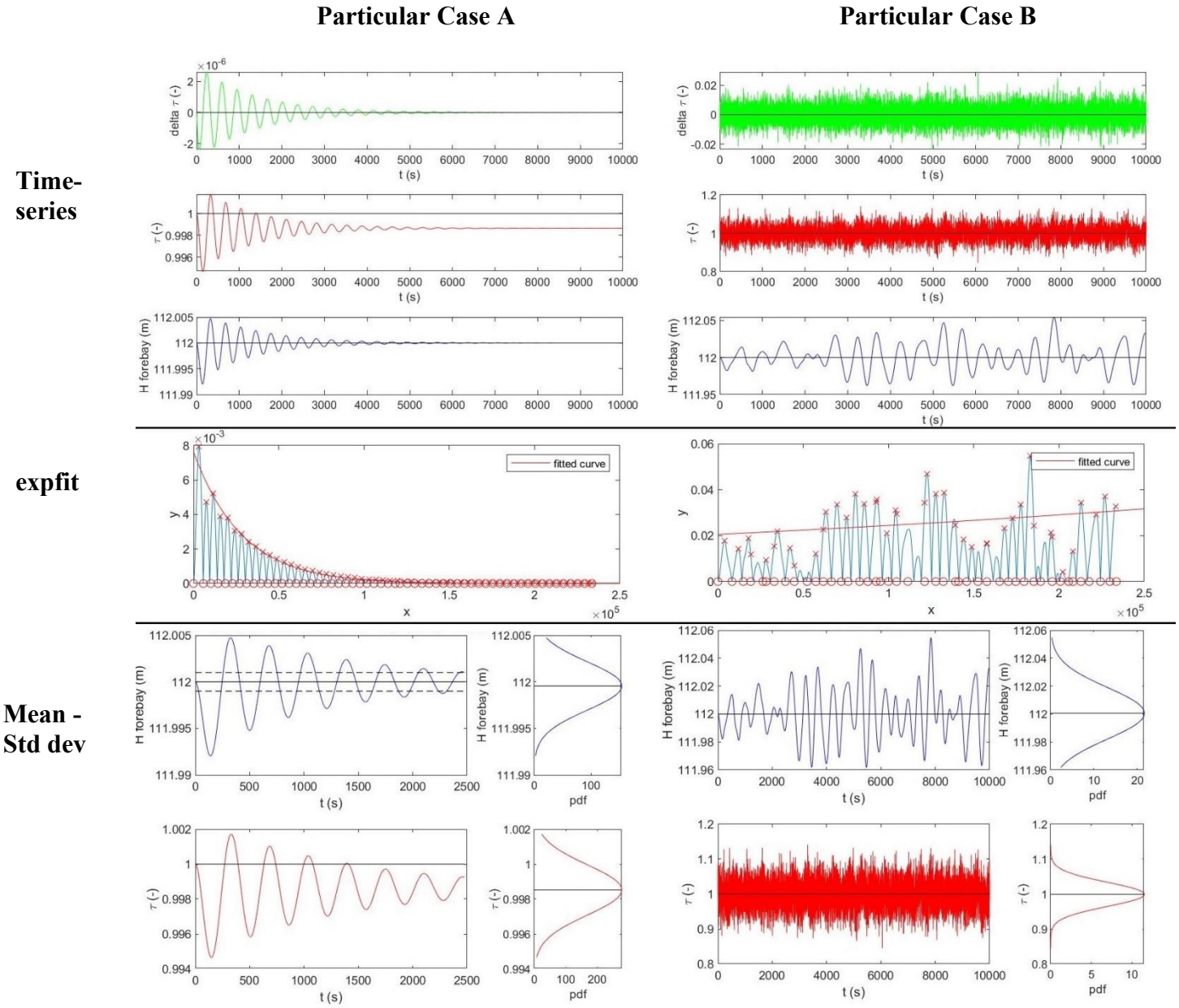

Figure 5.1 – Results of the Particular Cases A and B from Table 4.4

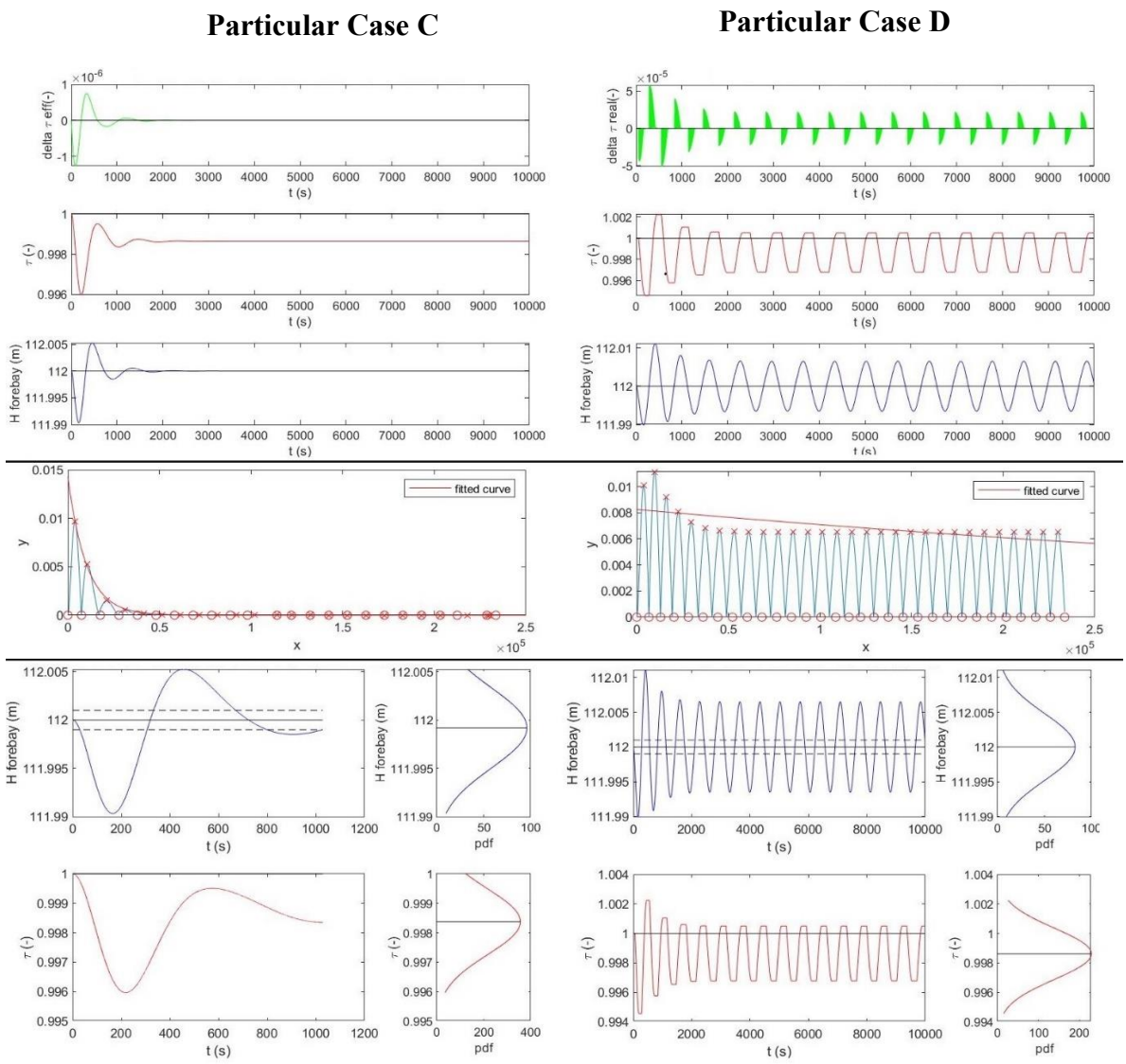

Figure 5.2 - Results of the Particular Cases C and D from Table 4.4

The time-series are graphs showing the simulation time t and the variables $\Delta\tau(t)$, $\tau(t)$ and $H_f(t)$ as a function of time. The straight black lines in the time-series graphs represent the reference values, thus, in the case of the level in the forebay $H_f(t)$ and the valve opening $\tau(t)$ these lines represent H_{target} and τ_{target}, and in the case of the valve opening derivative $\Delta\tau(t)$, this black line represent the zero-value which is arranged when $H_f(t)$ has converged to H_{target}. The exponential fit part of the figures shows a variable *y* which is the same variable described by equation (4.70), namely $y=H_{f1}(t)$ and the peaks and exponential fit curves in red colour. Finally, the part of the statistical values shows the time series of $H_f(t)$ and $\tau(t)$ at left and at right the obtained probability density function (pdf) of the corresponding variables. The dashed lines indicate the interval

$$\left|H_f - H_{target}\right| \leq \Delta H_{stability}$$

Described in section 4.6. The results obtained from the particular cases in Table 4.4 are shown in Table 5.1.

Table 5.1 – Computed typical results for the particular cases

Variable	Symbol	Unit	Particular case A (BM)	Particular case B	Particular case C	Particular case D
Parameter S of the expfit	$S_{w,\alpha x,K1y}$	(-)	-3.52E-05	1.73E-06	-9.88E-05	-1.52E-06
$H_f(t)$ mean value	$H_{f,w,\alpha x,K1y}$	m	111.99	112.00	111.99	112.00
$\tau(t)$ mean value	$\tau_{w,\alpha x,K1y}$	(-)	0.9985	0.9992	0.9984	0.9986
$H_f(t)$ mean deviation value	$\Delta H_{f,w,\alpha x,K1y}$	cm	-4.47E-02	5.56E-02	-8.21E-02	1.16E-03
$\tau(t)$ mean deviation value	$\Delta\tau_{w,\alpha x,K1y}$	(-)	-0.0015	-8.43E-04	-0.0016	-0.0014
$H_f(t)$ standard deviation	$s\_H_{f,w,\alpha x,K1y}$	cm	0.26	1.85	0.42	0.48
$\tau(t)$ standard deviation	$s\_\tau_{w,\alpha x,K1y}$	(-)	0.0014	0.0346	0.0011	0.0017
$H_f(t)$ ratio of standard deviation	$r\_s\_H_{f,w,\alpha x,K1y}$	(-)	1	5.02	1.0009	1.42
$\tau(t)$ ratio of standard deviation	$r\_s\_\tau_{w,\alpha x,K1y}$	(-)	1	21.71	1.0011	1.12

5.2.Typical Results for Global Cases

Typical results of a global case were obtained after the simulation of all the particular cases and consisted on the stability limit curve obtained from the exponential fit matrix, mean deviation, standard deviation, and ratio of standard deviation matrices of $H_{f,w}$ and τ_w (Figures Figure 5.3 to Figure 5.6). The results are shown in graphs instead of numerical. On the first hand, the exponential fit the stability limit curve was obtained interpolating the 0-value across the exponential fit matrix and is plotted in the α-K_1 plane in red colour. On the other hand, the mean, standard deviation and ratio of standard deviation matrices are shown in form of graphs with scaled colors using the values shown in Table 5.2. This means that for the computed value of each pair (α_x, K_{1y}) (e.g. $s\_H_{f,w,\alpha x,K1y}$), a color was assigned, so that the computed values could be compared easily knowing that the scaled colours go from the lightest colour (lower numerical value) to the darkest colour (greater numerical value). In Figure 5.3, in black colour, it was also plotted the analytical stability limit curve obtained by Jimenez & Chaudhry (1992), This is done to compare the effect the variables on the stability of the system. In each of the graphs of Figure 5.4 and Figure 5.5, the analytical stability limit curve obtained by Jimenez & Chaudhry (1992) is also shown together with the stability limit curve obtained from the global benchmark case. This is done to show only results of the statistical values under these curves because there was no concern of studying the statistical parameters on presumably unstable pairs of (α, K_1).

Table 5.2 – Values and units of the colorbars

Variable	Symbol	Colorbar range	Unit
H_f mean deviation matrix graph	$[H_{f,w}]$	0 - 0.5	m
τ mean deviation matrix graph	$[\Delta\tau_w]$	0 - 0.01	(-)
H_f standard deviation matrix graph	$[s\_H_{f,w}]$	0 - 1.5	m
τ standard deviation matrix graph	$[s\_\tau_w]$	0 - 0.25	(-)
H_f ratio of standard deviation matrix graph	$[r\_s\_H_{f,w}]$	0 - 400	(-)
τ ratio of standard deviation matrix graph	$[r\_s\_\tau_w]$	0 - 250	(-)

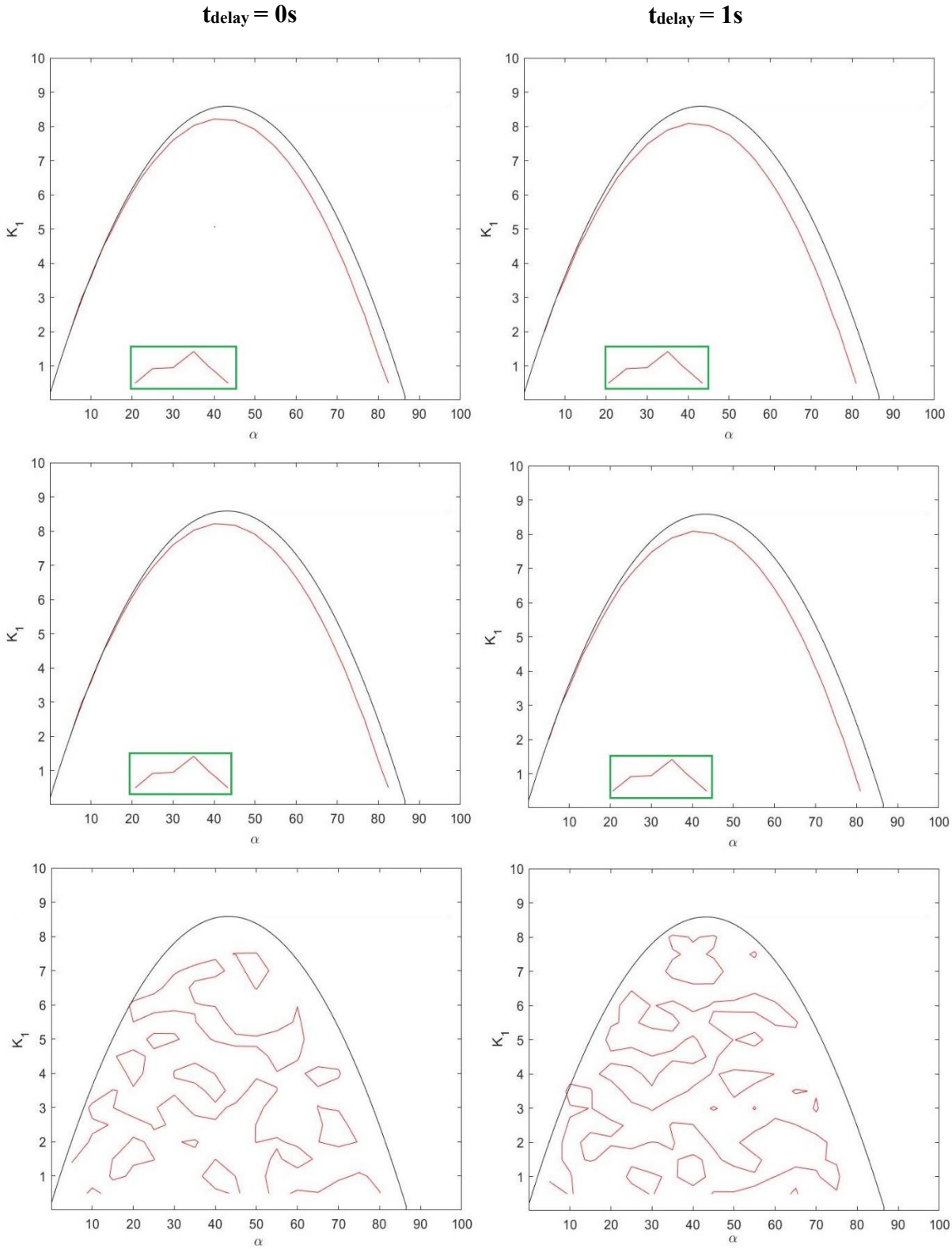

Figure 5.3 – Stability limit curves for the set of global cases A, B and C from Table 4.5

Global Case D

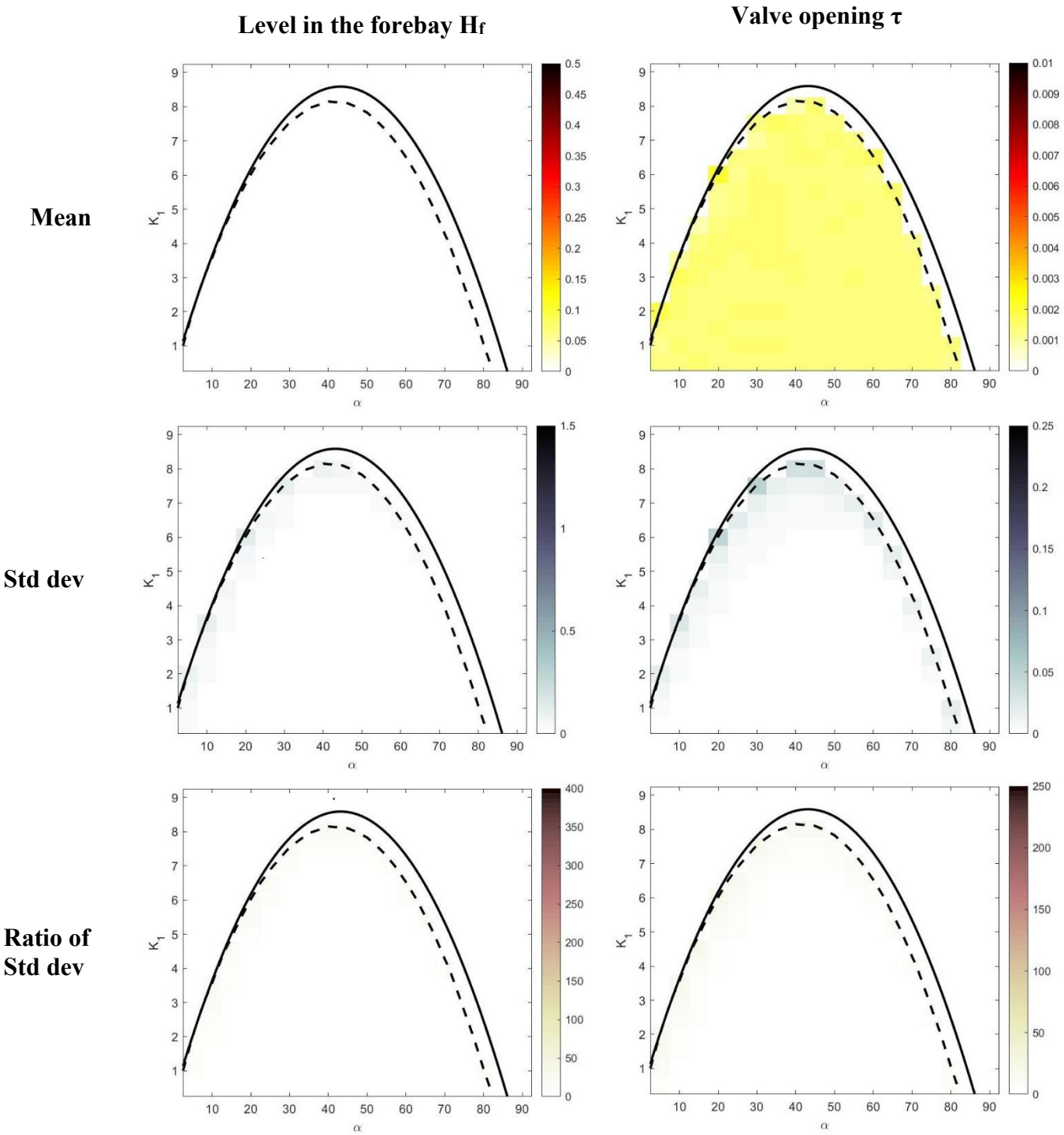

Figure 5.4 – Computed statistical matrices from the Global Case D from Table 4.5 shown in scaled color graphs

Global Case E

Level in the forebay H_f | **Valve opening τ**

Mean

Std dev

Ratio of Std dev

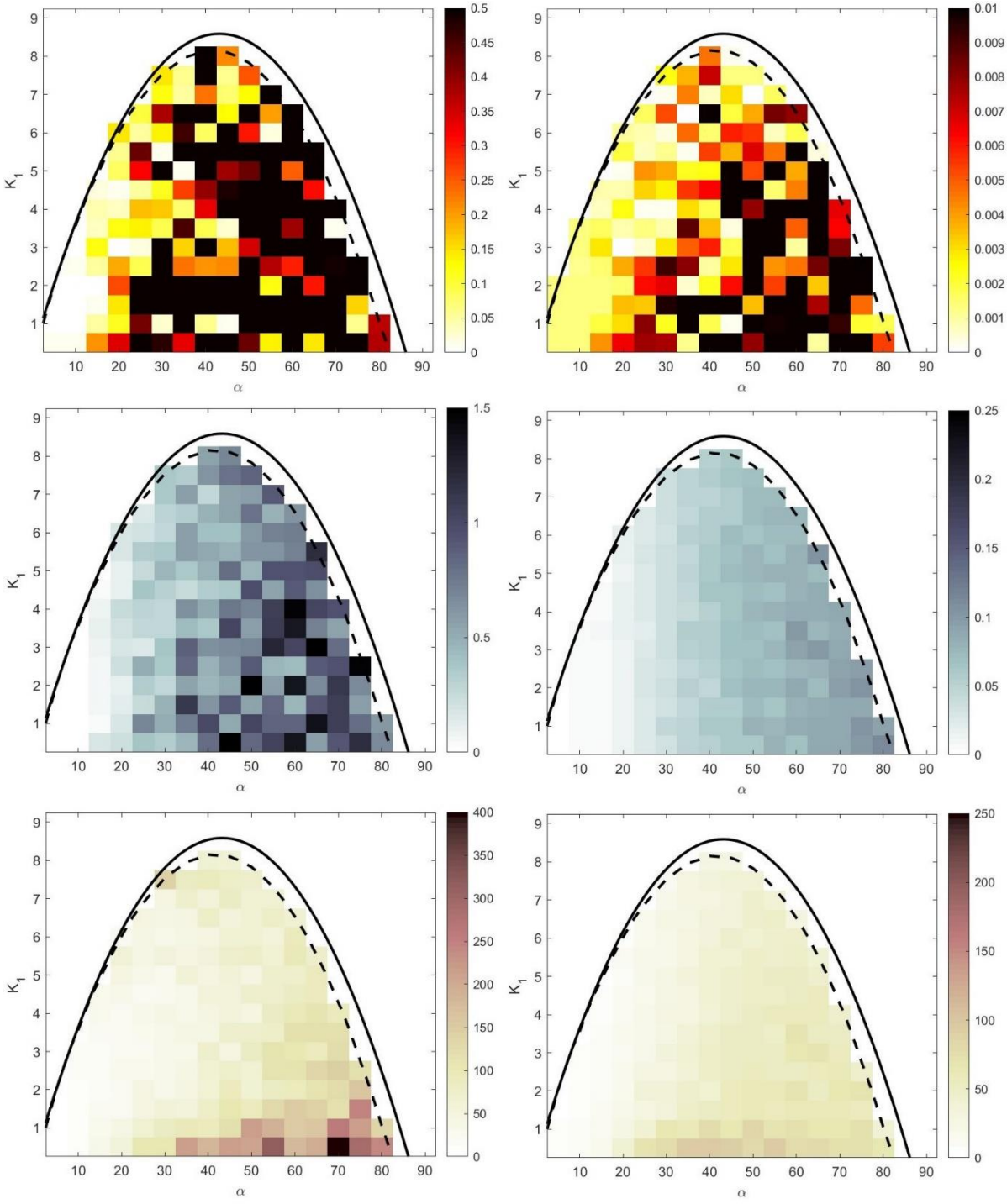

Figure 5.5 - Computed statistical matrices from the Global Case E from Table 4.5 shown in scaled color graphs

Global Case F

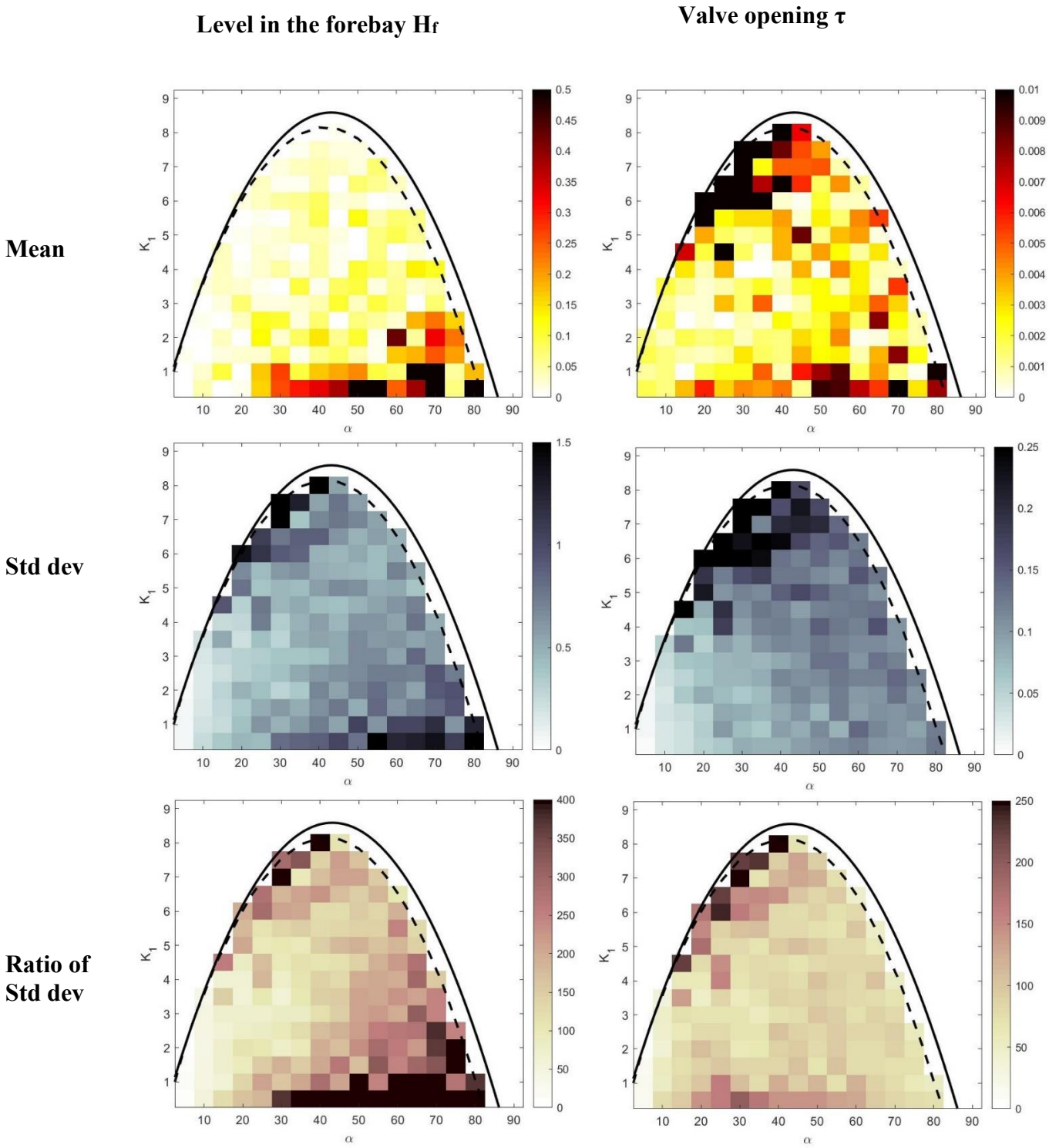

Figure 5.6 - Computed statistical matrices from the Global Case F from Table 4.5 shown in scaled color graphs

5.3. Results discussion

The analysis of the results may be divided in two: first, it is discussed the effect of each variable (mechanism) alone on the stability and then, some remarkable combinations of variables are analysed. In the second place the exponential fit technique as stability criterion is studied with the statistical matrices.

5.3.1. Effect of each variable maintaining the rest off(=0)

It is now possible to expose the effect of each of the mechanisms involved. They are shown first as isolated cases, that is, the effect of them alone maintaining the other variables off (=0) and then some of their combinations are shown in more detail due to their impact

Transients

The only transients' particular cases have a stability function of the form

$$S = f\left(BL_B = 0, NIV_B = 0, \sigma = 0, f = 0, t_{delay} = 0, t_{measure} = 0, \alpha, K_1\right)$$

and make up the benchmark global case. Considering the transients in the conduits alone (while keeping the other variables off), as in the Particular Case A of Figure 5.1, showed to have negligible impact on the stability of the flow control system. In fact, the stability limit curve of the Global Cases A in Figure 5.3 with t_{delay}=0s, here amplified (Figure 5.7), corresponds to the benchmark case and as observed the curve has just slightly shrunk in respect to the analytical curve.

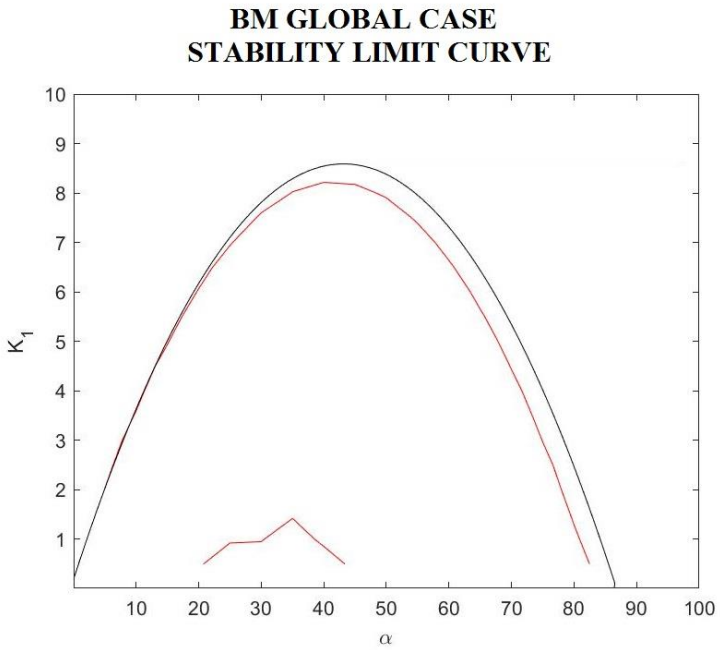

Figure 5.7 – BM Global Case stability limit curve

Delays

With stability function of the form

$$S = f\left(BL_B = 0, NIV_B = 0, \sigma = 0, f = 0, t_{delay} \neq 0, t_{measure} = 0, \alpha, K_1\right)$$

the delays in the control system did not show to have an important impact on the stability of the controller. In the particular cases the behaviours of $H_f(t)$ and $\tau(t)$ were similar to that of the only transients case and in the global cases the impact in the stability curve is very similar to the only transients case as well, as may be seen in the set of Global Cases A of Figure 5.3 with t_{delay}=1s. In fact, if a delay were applied to the Particular Case A of Table 4.4, almost identical time-series would be obtained as shown in Figure 5.8.

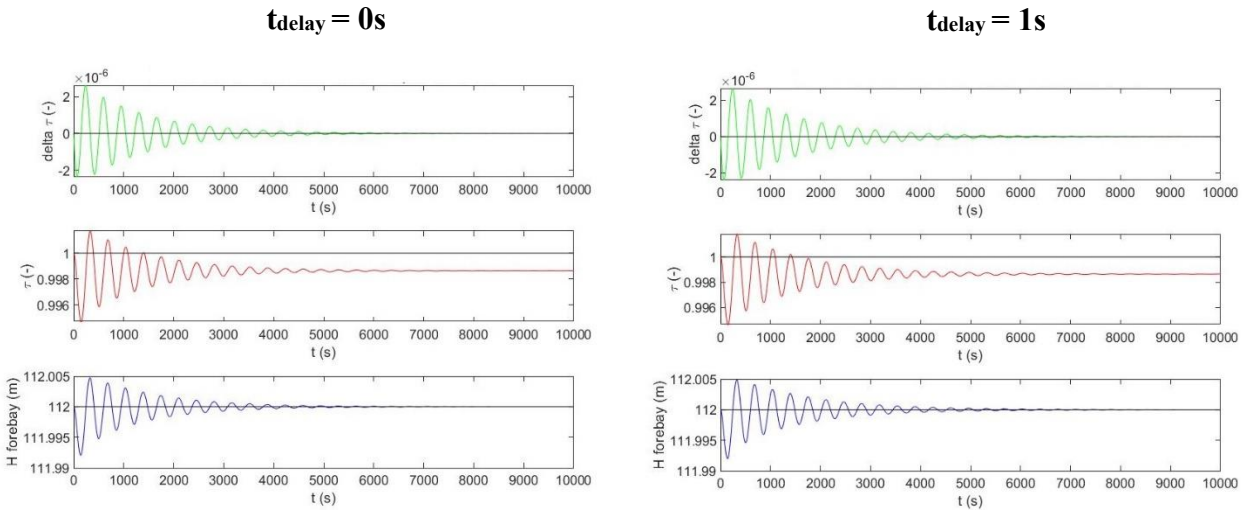

Figure 5.8 – Comparison of the time-series of Particular Case A from Table 4.4 for delay times of 0s and 1s

For the delays to be an important issue in the flow control system, the t_{delay} must be of around 30 seconds or more, which is not verified in these systems. The time-series of the Particular Case A from Table 4.4 are shown with a time of delay of 30 and 45 seconds in Figure 5.9 to evidence how the flow control system starts to lose control with the delay of 30s and how it becomes absolutely instable for a delay of 45s.

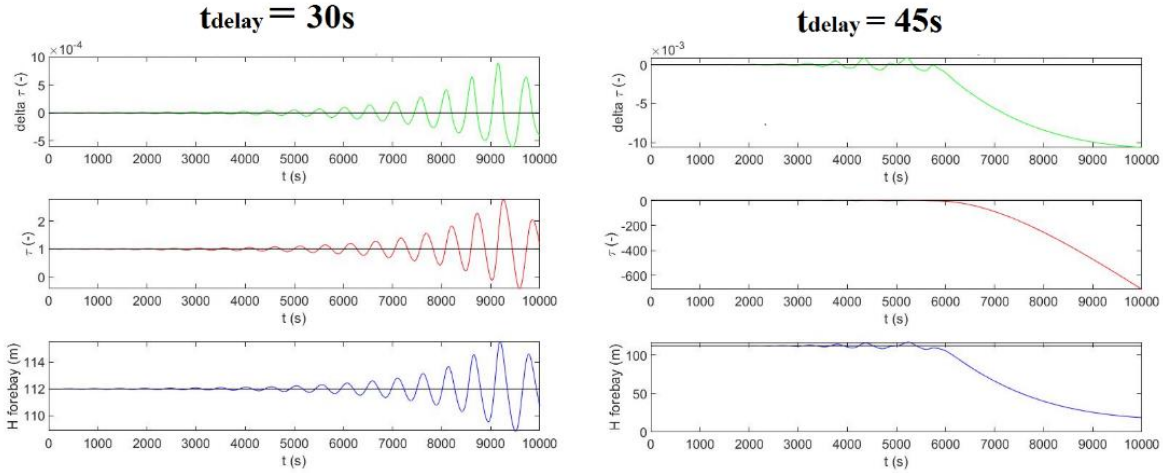

Figure 5.9 – Particular Case A from Table 4.4 with time of delay of 30 and 45 seconds

Non-instantaneous valve

With stability function of the form

$$S = f\left(BL_B = 0, NIV_B = 1, \sigma = 0, f = 0, t_{delay} = 0, t_{measure} = 0, \alpha, K_1\right)$$

the non-instantaneous valve alone did not affect the stability of the controller, in fact, the cases with NIV_B=1 while maintaining the other variables off(=0) showed to have the same behaviour of the BM case. However, this behaviour may be explained analysing that in the BM case the $\Delta\tau(t)$ kept always under $\Delta\tau_{max}$ hence $\Delta\tau_{eff}(t)=\Delta\tau(t)$. As a matter of fact, the stability limit curves from the set of global cases B (Figure 5.3) shows that the non-instantaneous valve alone is equivalent to have the BM case.

Measuring time

The measuring time alone is described by a stability function of the form

$$S = f\left(BL_B = 0, NIV_B = 0, \sigma = 0, f = 0, t_{delay} = 0, t_{measure} = 1, \alpha, K_1\right)$$

To analyse the physical effect of this variable let us inspect Figure 5.10 in which a measuring time has been added to the particular case A from Table 4.4.

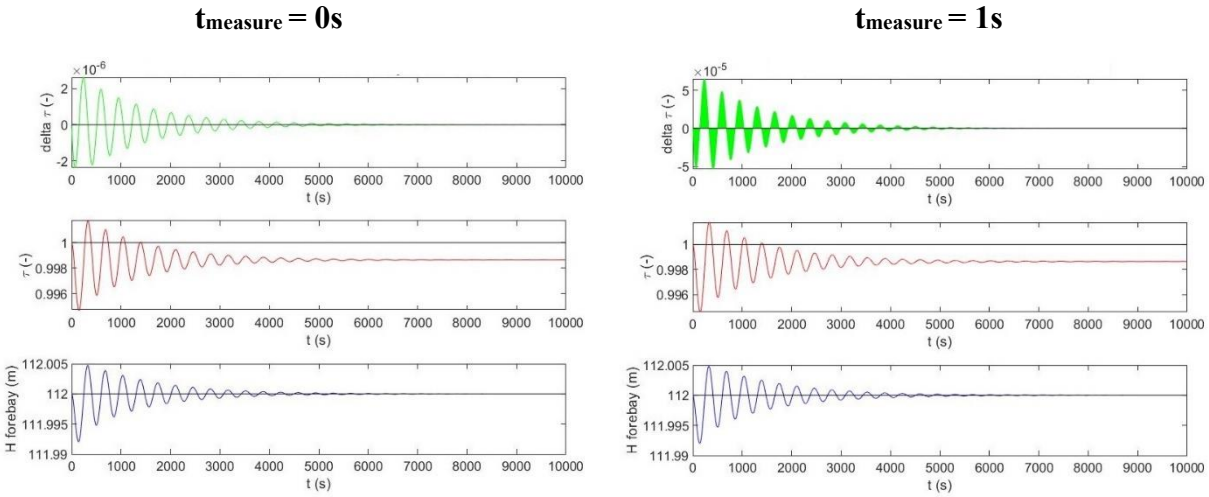

Figure 5.10 - Comparison of the time-series of Particular Case A from Table 4.4 for measuring times of 0s and 1s

As may be observed, the main difference is present in the form of the function $\Delta\tau(t)$ in which, when the measuring time is not considered, the function is continuous whereas when the measuring time is considered it appears to have a strange form giving the sense like if an integral were being computed. However if a little interval of $\Delta\tau(t)$ with measuring time is amplified, as in Figure 5.11, it will show that in fact what happens is that the function is discontinuous but when shown in a bigger interval seems to have that form of "integral" and, in addition, it has

non-zero values only for integer values of time every second. This situation arises from the fact that, in reality, the measuring time has been set as 1s and additionally, when this measuring time is set up, it considers the level in the forebay to be constant during the measuring time interval (except for the case of uncertainties with filter whose case is analysed later) and therefore it is only at this time interval that the controller performs an operation. This situation was already described in section 4.1.2 where the details of the flow control were given.

In spite of this difference in the form of $\Delta\tau(t)$, the time-series $H_f(t)$ and $\tau(t)$ seem to be almost identical. The comparison of the BM global case with the global case

$$S = f\left(BL_B = 0, NIV_B = 0, \sigma = 0, f = 0, t_{delay} = 0, t_{measure} = 1\right)$$

as shown in Figure 5.12 shows us that the stability limit curves are almost identical, therefore, it could be said that the measuring time alone has negligible impact on the stability of the system.

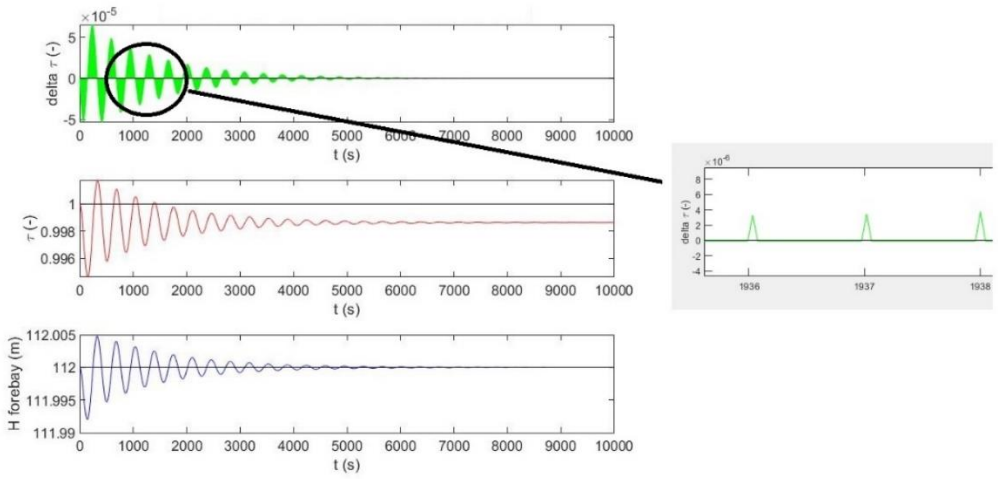

Figure 5.11 – Time- series of a particular case with measuring time considered and amplification of a little interval of Δτ(t)

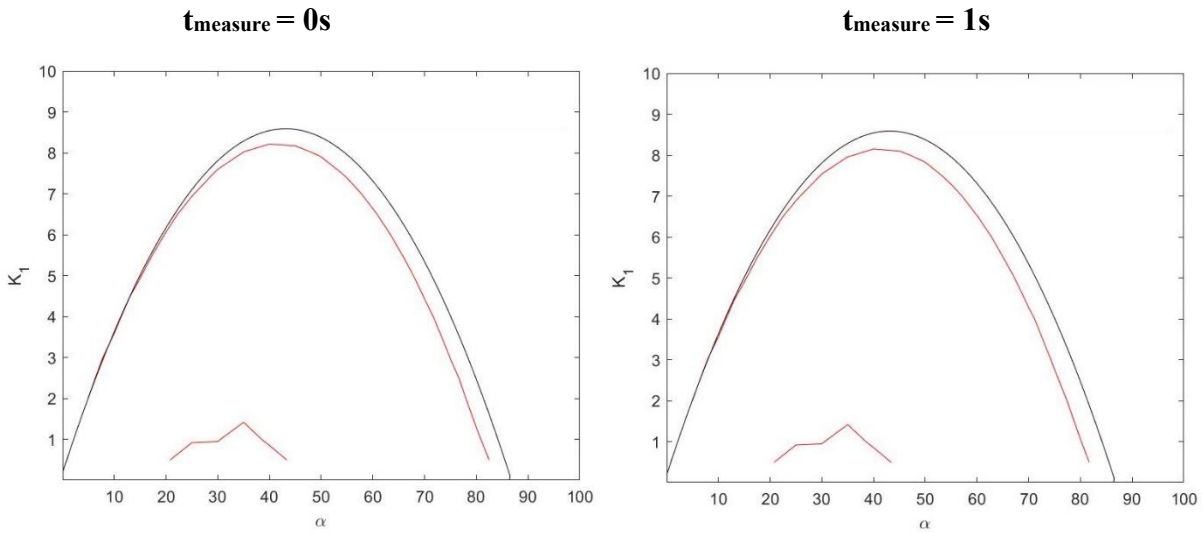

Figure 5.12 – Comparison of the stability limit curves of the BM case and the global case with only measuring time considered

Uncertainties

Considering the case of uncertainties alone, i.e., having stability function with the form of

$$S = f\left(BL_B = 0, NIV_B = 0, \sigma \neq 0, f = 0, t_{delay} = 0, t_{measure} = 0, \alpha, K_1\right)$$

showed to significantly affect the behaviour of the flow control system. From the Particular Case B in Figure 5.1 it can be seen that with the uncertainties, $H_f(t)$ oscillates around H_{target} but does not converge to it throughout time, meaning that asymptotic stability is not verified with this mechanism. This situation however, may can be explained studying equations (4.16) and (4.20) to (4.23)

$$\Delta\tau^i = \left(\left(\frac{H_{fm}^i - H_{target}}{T_i}\right) + \left(k((H_{fm}^i - H_{target}) - (H_{fm}^{i-1} - H_{target}))\right)\right) * \Delta t \quad (4.16)$$

$$H_{fm}^i = H_{measure}^{j-1} + \Delta H * \left(1 - f \cdot e^{-\left(\frac{t_i - t^*_j}{T_f}\right)}\right) \; for \; {t_j}^* < t_i < {t_{j+1}}^* \quad (4.20)$$

$$\Delta H = H_{measure}^j - H_{measure}^{j-1} \quad (4.21)$$

$$H_{measure}^j = H_f^i + (\sigma * rand) \quad (4.23)$$

Let us suppose that for given values of α and K_1 the PI Controller could in fact make H_f converge to H_{target}, in this case if H_{target} is subtracted from equation (4.23) and the limit is taken then

$$(H_{measure}^j - H_{target}) = (H_f^i - H_{target}) + (\sigma * rand) \quad (5.1)$$

$$\lim_{t \to t_t}(H_{measure}^j - H_{target}) = \lim_{t \to t_t}(H_f^i - H_{target}) + \lim_{t \to t_t}(\sigma * rand) \quad (5.2)$$

$$\lim_{t \to t_t}(H_{measure}^j - H_{target}) = \lim_{t \to t_t}(\sigma * rand) \quad (5.3)$$

Since the limit has no fixed value and does not converge to 0 because the combination *(σ+rand)* always gives a casual number, then in general from equations (4.20) and (4.21)

$$H_{measure}^j \neq H_{measure}^{j-1} \quad (5.4)$$

$$\Delta H \neq 0 \quad (5.5)$$

$$H_{fm}^i \neq H_{target} \quad (5.6)$$

And therefore, from equation (4.16)

$$\Delta\tau^i \neq 0 \quad (5.7)$$

In addition to the non-convergence (non-asymptotical stability) of the uncertainties case, another important effect that this variable has on the dynamic system is the magnitude of the amplitude of the oscillations. As may be seen in Figure 5.13 where the time-series of the Particular Case B from Table 4.4 are compared to the time-series of the same case but with σ=0m, the maximum amplitude of the uncertainties case is around six times bigger than the BM particular case. This situation may be observed in a more general way in Figure 5.14 where the standard deviation and the ratio of standard deviation matrices of the level in the forebay are shown. The oscillations may be up to 10 times greater but are kept in a smaller range for pairs (α, K_1) away from the stability limit curve. Though the amplitude of the alone uncertainties cases is in general bigger than the BM cases, they do not have the biggest amplitudes, instead the biggest amplitudes are found in a combination of uncertainties with other variables which is detailed in section 5.3.2.

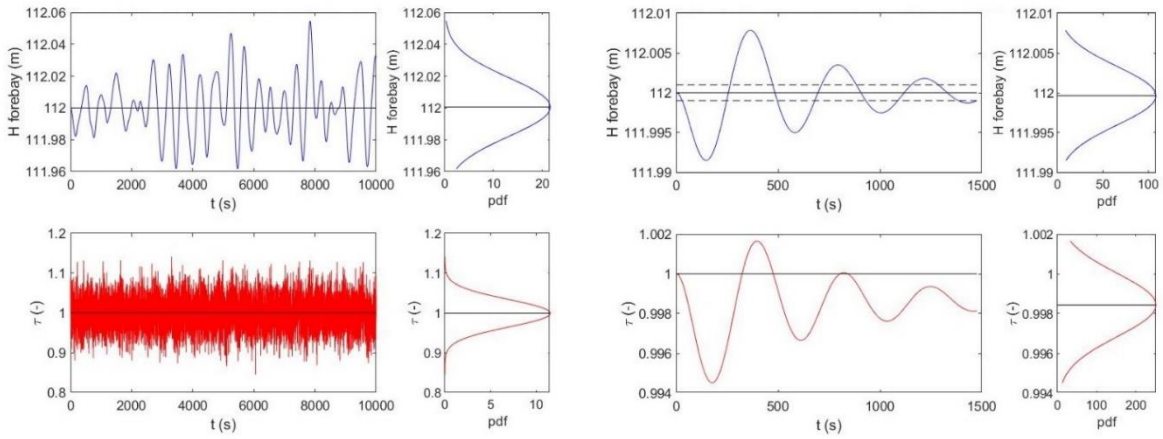

Figure 5.13 - Comparison of the time-series of Particular Case B from Table 4.4 for instrumental uncertainty of 0m and 0.1m

Std dev **Ratio of Std dev**

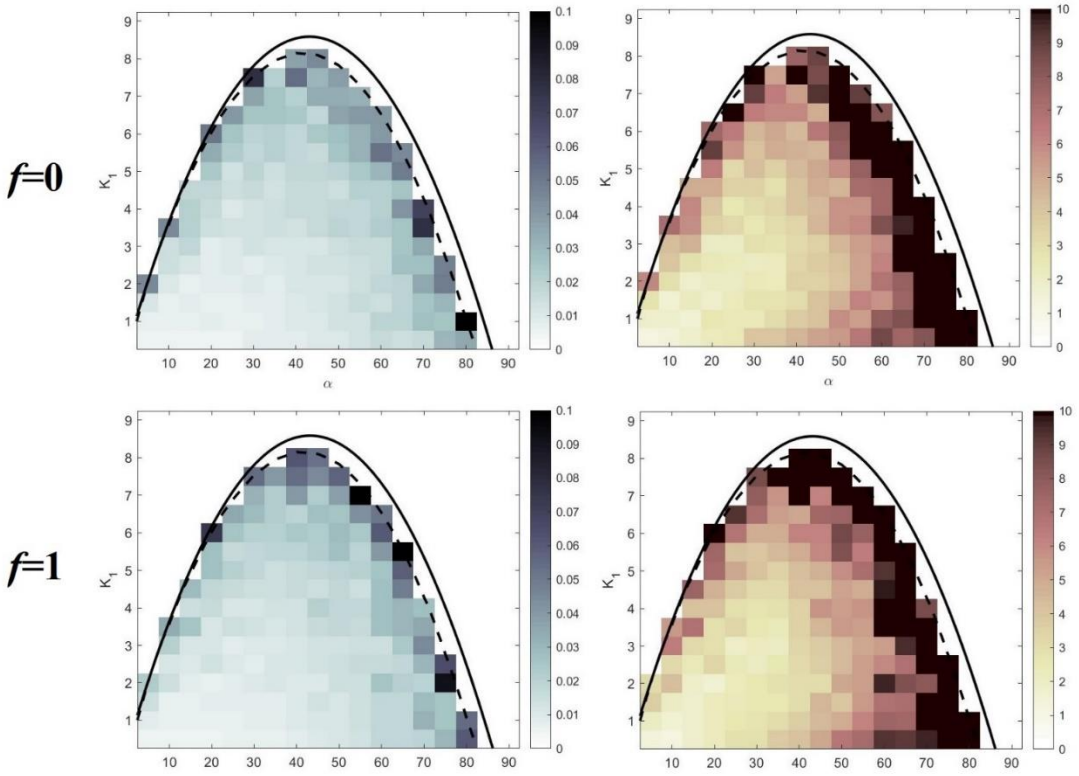

Figure 5.14 – Standard deviation and Ratio of standard deviation matrices for a global case considering only uncertainties with σ=0.1 with and without filter

Backlash

With stability function of the form

$$S = f\left(BL_B = 1, NIV_B = 0, \sigma = 0, f = 0, t_{delay} = 0, t_{measure} = 0, \alpha, K_1\right)$$

Backlash is a mechanism that showed to have a significant impact on the stability of the flow control system. Just as what happened to the instrumental uncertainty and as can be observed in the particular case D of Figure 5.2, H_f oscillates around H_{target} without converging to it, i.e., there is no asymptotic stability. This behaviour may be explained inspecting equations (4.16), (4.47) and (4.50) and Figure 4.6 supposing $NIV_B=0$ ($\Delta\tau_{eff}=\Delta\tau$).

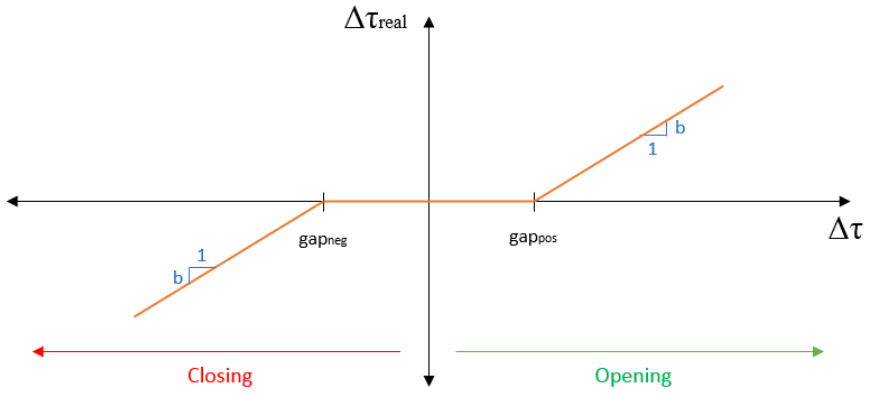

Figure 4.6. (repeated) - $\Delta\tau_{real}$ obtained at a given time t as a function of dτ, the gaps and b

The valve opening is given by

$$\Delta\tau^i = \left(\left(\frac{H_{fm}^i - H_{target}}{T_i}\right) + \left(k((H_{fm}^i - H_{target}) - (H_{fm}^{i-1} - H_{target}))\right)\right) * \Delta t \quad (4.16)$$

If $\Delta\tau^i$ is positive, i.e. the valve is opened

$$\Delta\tau_{real}^i = \begin{cases} 0; & \Delta\tau^i < gap_{pos}^{i-1} \\ b \cdot (\Delta\tau^i - gap_{pos}^{i-1}); & \Delta\tau^i \geq gap_{pos}^{i-1} \end{cases} \quad (4.47)$$

If $\Delta\tau_{eff}^i$ is negative, i.e. the valve is closed

$$\Delta\tau_{real}^i = \begin{cases} b \cdot (\Delta\tau^i - gap_{neg}^{i-1}); & \Delta\tau^i \leq gap_{neg}^{i-1} \\ 0; & \Delta\tau^i > gap_{neg}^i \end{cases} \quad (4.50)$$

Let us analyse an interval of time from the particular case D

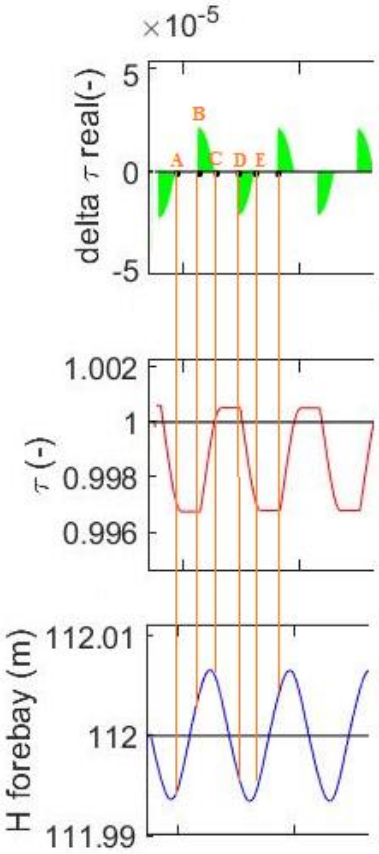

Figure 5.15 – Sample interval from the time-series of the particular case D

From points A to B, H_f is close enough to H_{target} and therefore

$$gap_{neg}^{i-1} < \Delta\tau^i < gap_{pos}^{i-1}$$

So

$$\Delta\tau_{real}^i = 0$$

The level in the forebay will keep rising because no operation has been performed due to backlash effects. Then at point B the gap is overpassed, and the valve starts to change its τ, so from points B to C the flow control is going to have nonzero $\Delta\tau_{real}$

$$gap_{neg}^{i-1} > \Delta\tau^i \quad or \quad \Delta\tau^i > gap_{pos}^{i-1}$$

$$\Delta\tau_{real}^i \neq 0$$

As H_f approaches again H_{target} in the C-D interval, the Δτ decreases and enters again in the zone where

$$gap_{neg}^{i-1} < \Delta\tau^i < gap_{pos}^{i-1}$$

And will have zero $\Delta\tau_{real}$ until the backlash effects will be again overpassed at interval D-E. This situation occurs in loops throughout time and that is why asymptotic stability is never verified.

Though the backlash cases are not asymptotically stable, in contrast to the uncertainties case, the amplitudes of the oscillations are not a big issue as may be seen in Figure 5.16 where the time-series of the Particular Case D from Table 4.4 are shown with and without backlash. As observed, the amplitude of the oscillations is kept under similar values which, in this case, is around 0.1m.

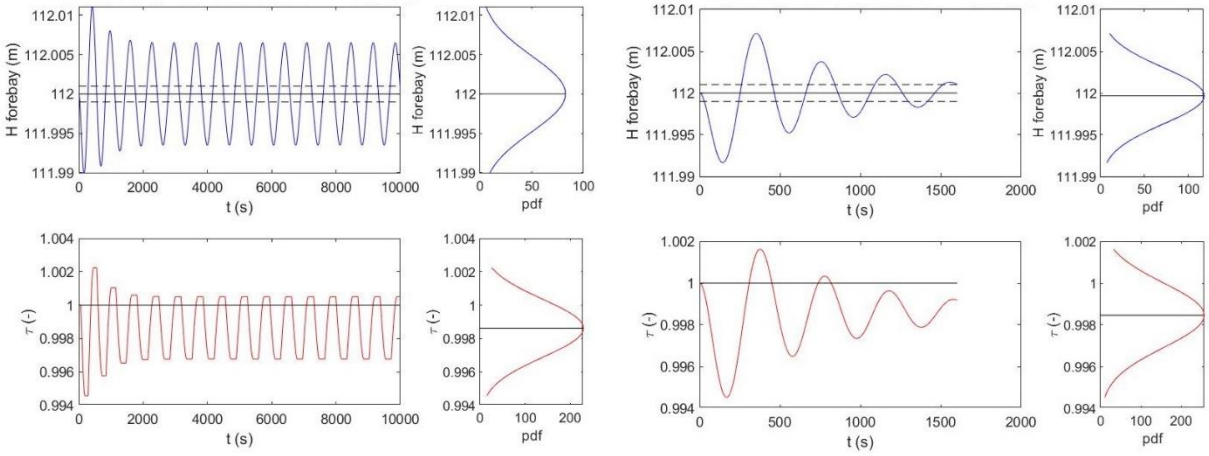

Figure 5.16 - Comparison of the time-series of Particular Case D from Table 4.4 with and without backlash

Evaluating the standard deviation and the ratio of standard deviation matrices of $H_f(t)$ of the only-backlash global case (Figure 5.17) (using a different scale colour than the one from Table 5.2) it may also be seen that the standard deviations are, in general, kept within a small range of 0.05m

and the ratios of standard deviation exceed the value of 5 only for cases near the BM stability limit curve.

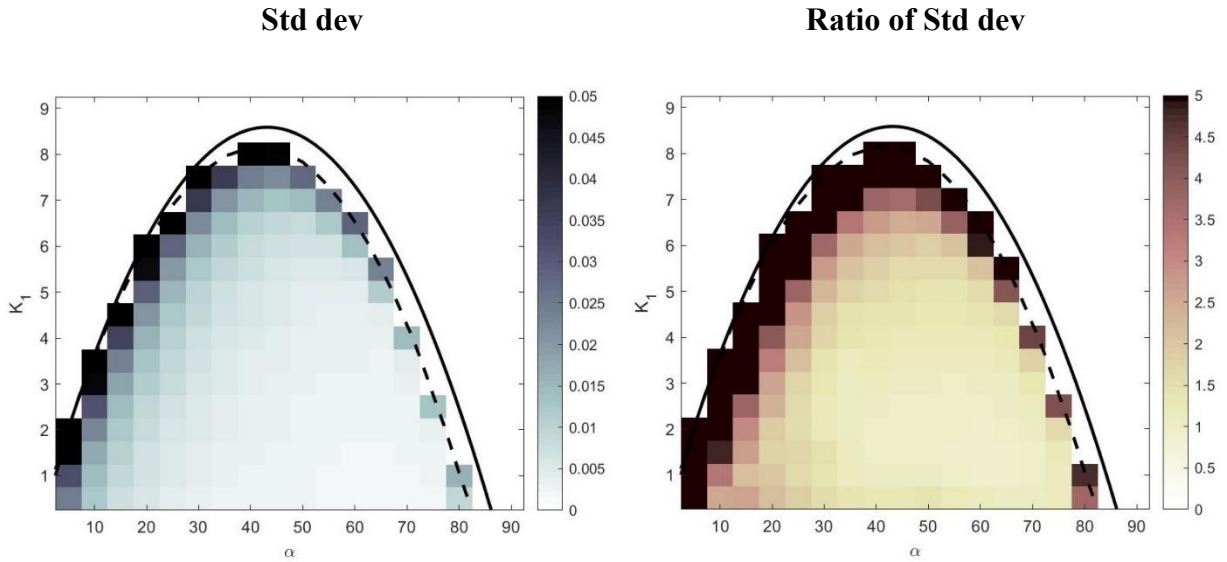

Figure 5.17 – Standard deviation and ratio of standard deviation matrices of the only backlash global case

5.3.2. Remarkable combinations of variables

The effects of the mechanisms in the last section were exposed for those mechanisms maintaining the rest of the variables off(=0), however, there are some remarkable combinations of variables that need special attention and that represent the key derivations from the stability assessment.

Delays or measuring time + any other mechanism

The delays and measuring time with any other mechanism are represented by the stability functions of the form

$$S = f\left(BL_B, NIV_B, \sigma, f, t_{delay} \neq 0, t_{measure} \neq 0, \alpha, K_1\right)$$

Their combination with any other variable has shown to have no significant impact in the stability of the controller. Table 5.3 shows three particular that were evaluated in Figure 5.18 (a)-(c) with and without the effect of the delays.

Table 5.3 – Particular Cases used to show the negligible effect of the delays and the measuring times

	Variable	Symbol	Unit	Particular cases D-M-1		Particular cases D-M-2		Particular cases D-M-3	
Global Cases	Non-instant valve	NIV_B	(-)	0	0	0	0	0	0
	Backlash	BL_B	(-)	0	0	0	0	1	1
	Instrumental uncertainty	σ	m	0	0	0.1	0.1	0	0
	Filter	f	(-)	0	0	1	1	0	0
	Delay time	t_{delay}	s	0	1	0	1	0	1
	Measuring time	$t_{measure}$	s	0	1	1	1	0	1
	PI Controller parameter 1	α	(-)	35	35	50	50	25	25
	PI Controller parameter 2	K_1	(-)	3	3	2	2	1	1

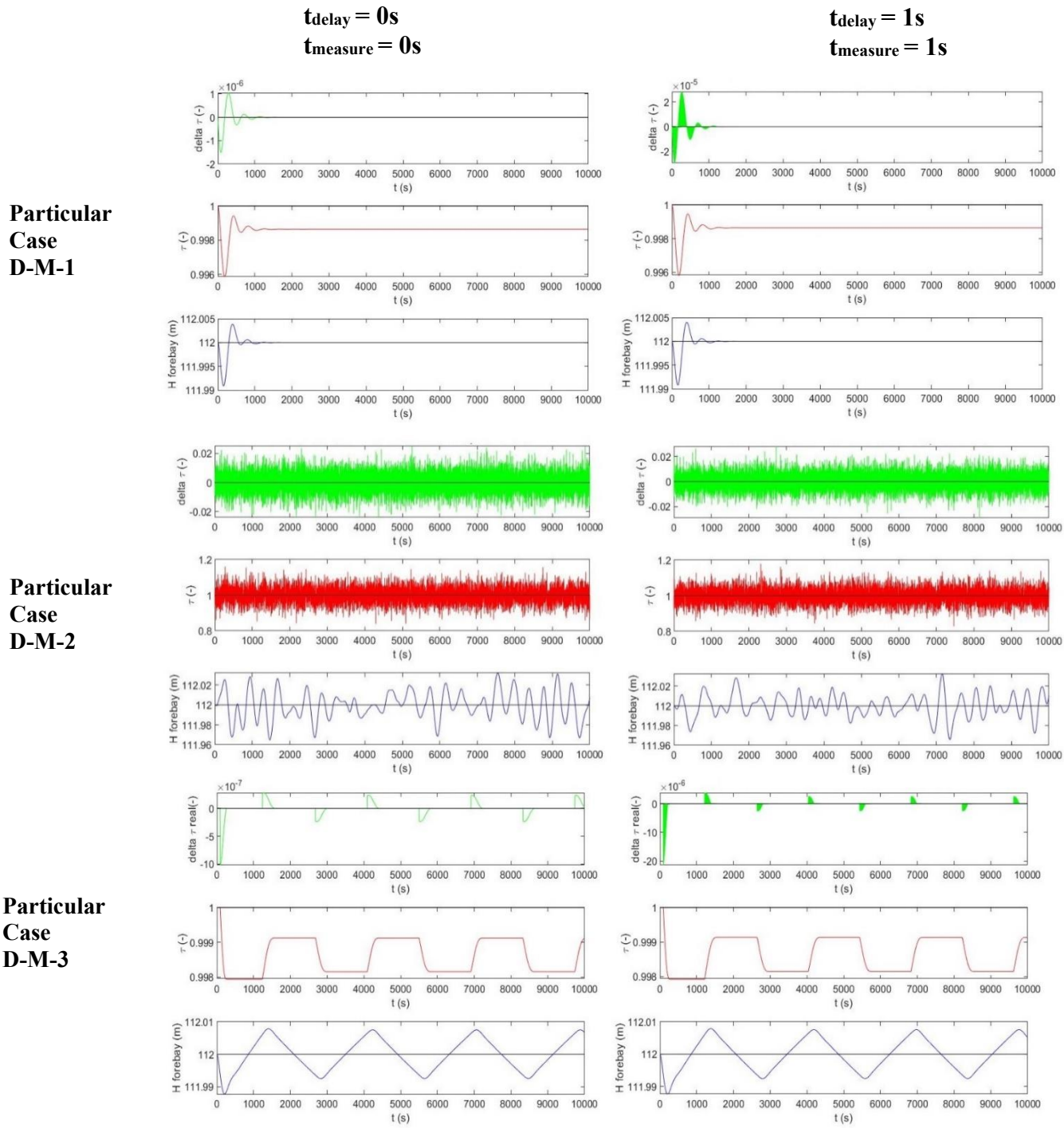

Figure 5.18 – Time-series of the Particular cases from Table 5.3

As shown in the figures the consideration of these mechanisms has no relevant impact on the stability and therefore may be neglected. However, the measuring time must be always considered when combined with uncertainties because it has no sense to have an instantaneous measuring instrument.

Backlash + Non-instant valve without Uncertainties

The combination of the backlash and non-instant variables without uncertainties is represented by a stability function of the form

$$S = f\left(BL_B = 1, NIV_B = 1, \sigma = 0, f, t_{delay}, t_{measure}, \alpha, K_1\right)$$

Such a combination results to have little impact on the stability of the system as shown in figures This occurs because though backlash does not have asymptotic stability, its amplitudes are very narrow, thus $\Delta\tau$ is in general kept under $\Delta\tau_{max}$ and therefore $\Delta\tau_{eff} = \Delta\tau$. Figure 5.19 shows the Particular Case C from Table 4.4 for only backlash, only non-instant valve and the combination of both and, as may be seen, when backlash is combined with non-instant valve without uncertainties, the backlash predominates over non-instant valve effects.

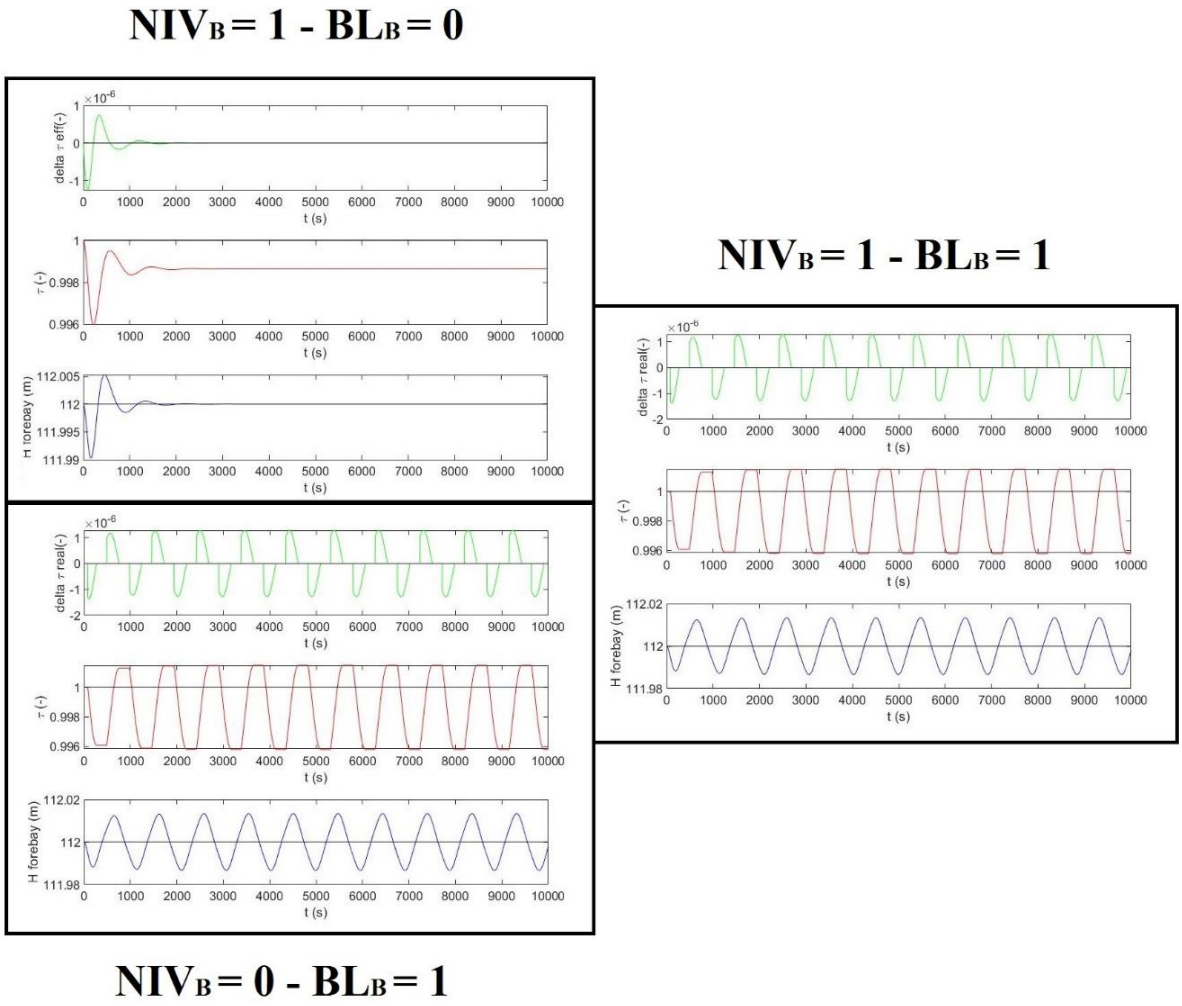

Figure 5.19 - Comparison of the time-series of Particular Case C from Table 4.4 for only backlash, only non-instant valve and the combination of both

Uncertainties + Backlash

In both uncertainties and backlash consideration there was no asymptotic stability in the dynamic system, and they were the most relevant cases when the other variables are not considered, however, when both mechanisms are combined, namely

$$S = f\left(BL_B = 1, NIV_B, \sigma \neq 0, f, t_{delay}, t_{measure}, \alpha, K_1\right)$$

the backlash effects vanish because due to the uncertainties in general

$$gap_{neg}^{i-1} > \Delta\tau^i \quad or \quad \Delta\tau^i > gap_{pos}^{i-1}$$

$$\Delta\tau_{real}^i \neq 0$$

Therefore, when they are combined the uncertainties effects have more weight and backlash effects become negligible, as shown in Figure 5.20 where the Particular Case B from Table 4.4Figure 4.4 has been evaluated also for only backlash and for the combination of backlash and uncertainties.

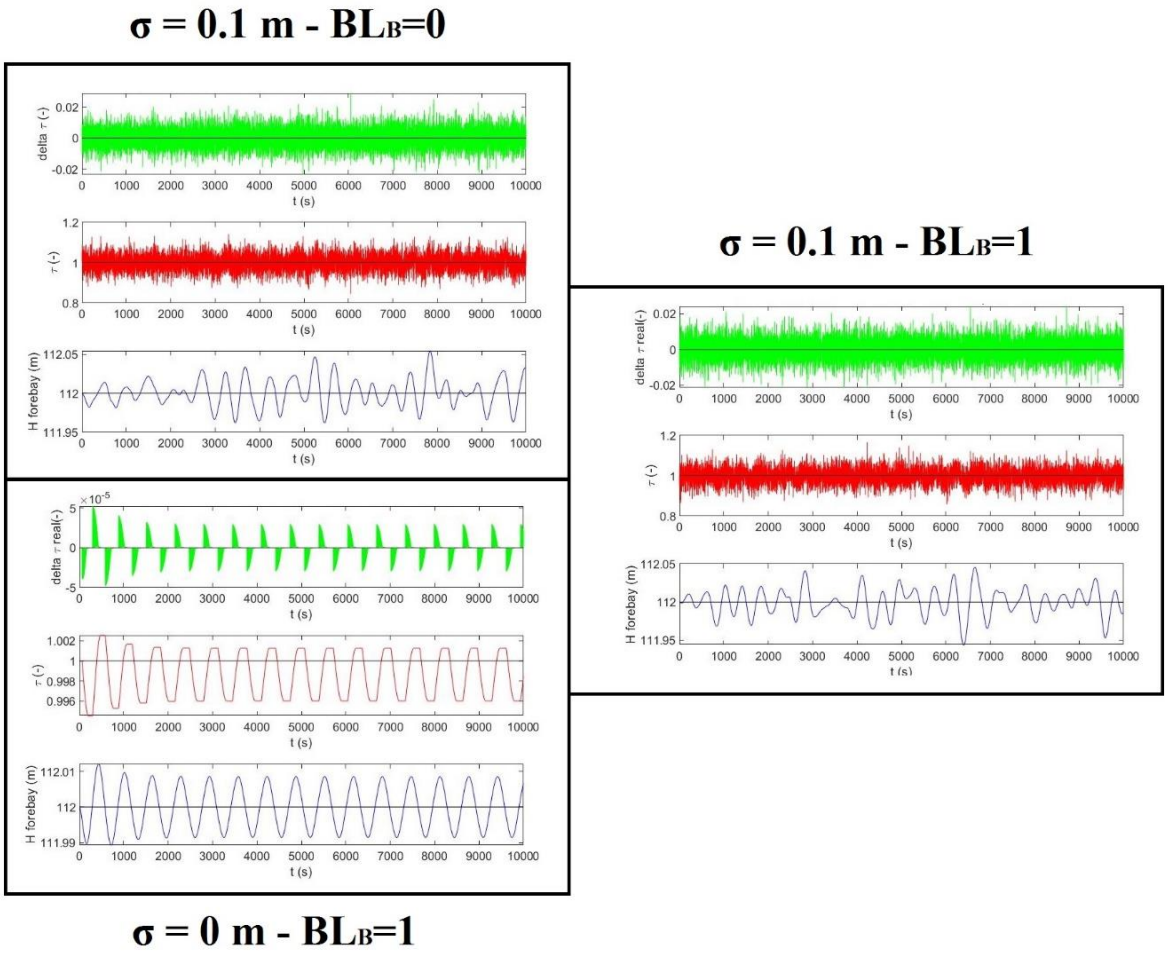

Figure 5.20 - Comparison of the time-series of Particular Case B from Table 4.4 for only uncertainties, only backlash and the combination of both

Non-instantaneous valve + Uncertainties

Although the non-instantaneous valve has shown to have no impact in the stability while keeping the other variables off, it takes a key role when it is combined with the instrumental uncertainties, i.e.,

$$S = f\left(BL_B, NIV_B = 1, \sigma \neq 0, f, t_{delay}, t_{measure}, \alpha, K_1\right)$$

This situation occurs because it is when uncertainties are considered that significant values of $\Delta\tau$ take place, causing the available $\Delta\tau_{eff}$ to have an important effect and making it not certain whether the desired operations will be actually achieved. To examine this situation in a more detailed way, let us analyse the Particular Case B from Table 4.4 including this time the non-instant valve and evaluated with and without filter.

When the filter is considered (Figure 5.21)

$$S = f\left(BL_B, NIV_B = 1, \sigma \neq 0, f = 1, t_{delay}, t_{measure}, \alpha, K_1\right)$$

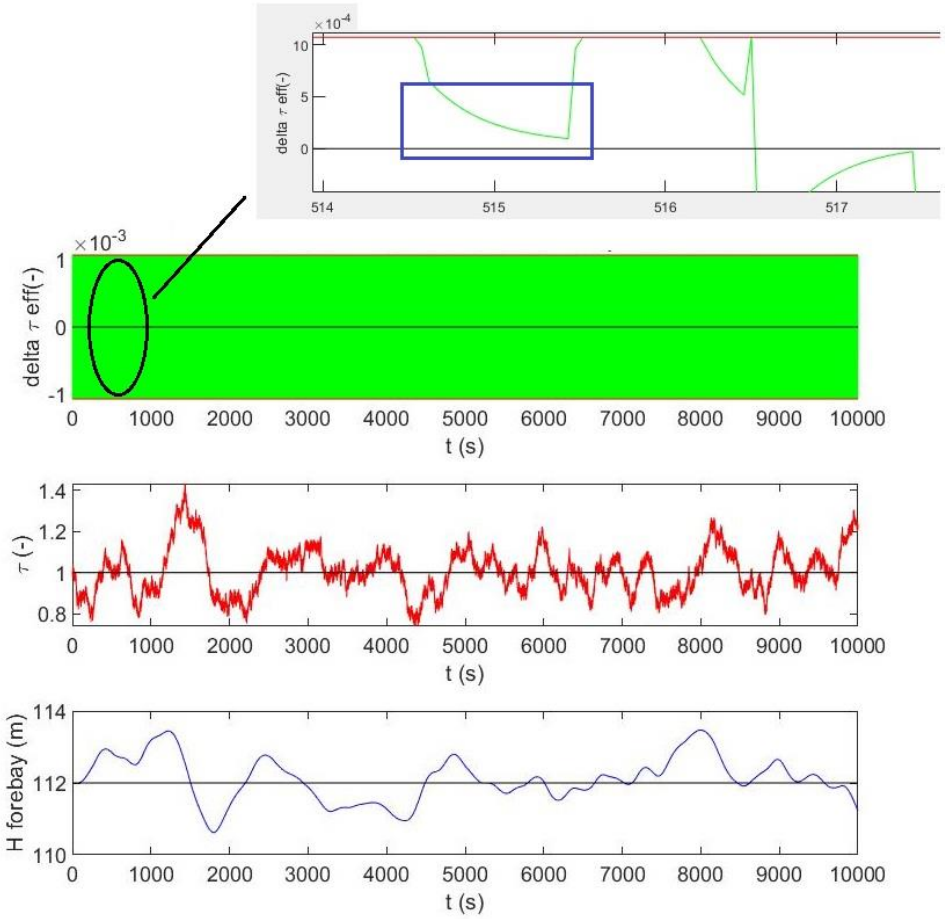

Figure 5.21 – Time-series of the Particular Case B from Table 4.4 with filter and non-instant valve

the effects of the non-instant valve are important but less harmful for the stability because the filter gives the opportunity to perform gradual opening/closing operations in the valve. This situation has been depicted in Figure 5.21 amplifying a little interval of time and enclosing with a blue square a portion of the function $\Delta\tau_{eff}$, where a gradual change could be performed due to the filter effects.

In contrast when a filter is not considered (Figure 5.22)

$$S = f\left(BL_B, NIV_B = 1, \sigma \neq 0, f = 0, t_{delay}, t_{measure}, \alpha, K_1\right)$$

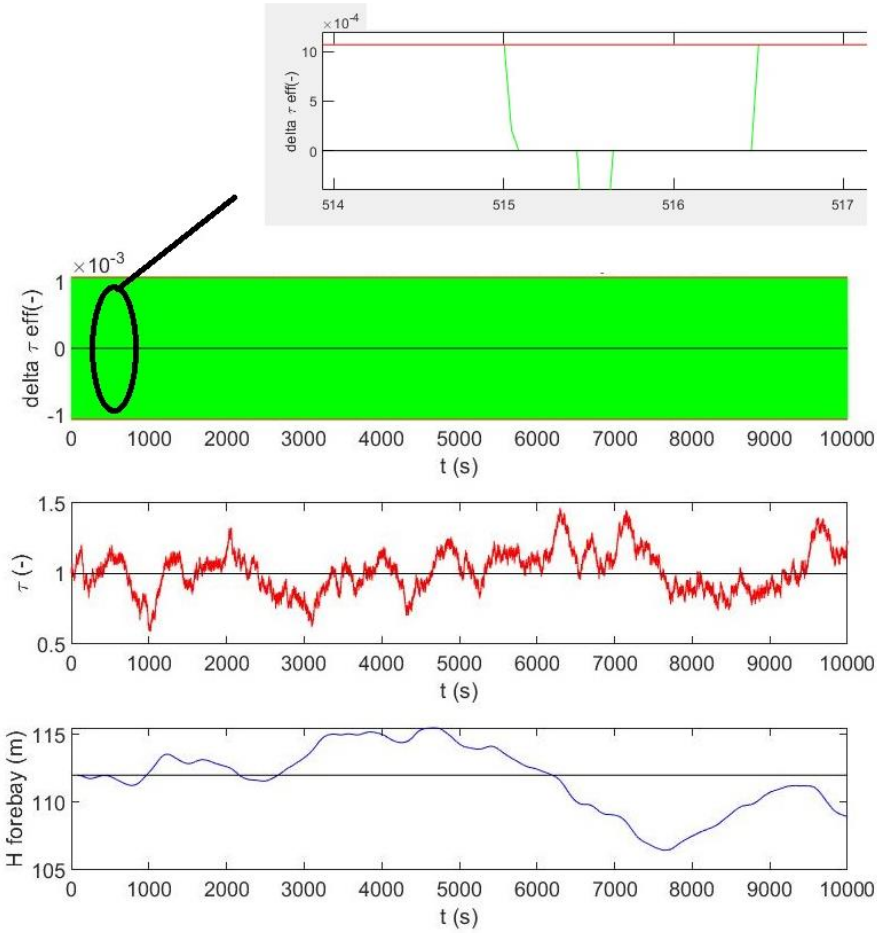

Figure 5.22 - Time-series of the Particular Case B from Table 4.4 without filter and non-instant valve

The non-instantaneous valve becomes a big problem in the stability assessment, because without a filter and with big instrumental uncertainty, the values of $\Delta\tau$ become significantly high respect to the other cases. Although the model was programmed to adjust the equations when filter was not considered (as shown in Figure 4.5 and equations (4.40) to (4.43)) the differences in the amplitude of the oscillations considering filtering or not showed to be very high. To illustrate this situation, Figure 5.23 and Figure 5.24 show the standard deviations $s\_H_{f,w}$ of the set global cases from Table 5.4. Both sets of global cases include non-instant valve and uncertainties with and without filter.

Table 5.4 – Set of Global Cases used to show the effect of the combination of the uncertainties and non-instant valve

Variable	Symbol	Unit	Set of Global Cases G	Set of Global Cases H
Non-instant valve	NIV_B	(-)	1	1
Backlash	BL_B	(-)	0	0
Instrumental uncertainty	σ	m	0.05	0.1
Filter	*f*	(-)	0, 1	0, 1
Delay time	t_{delay}	s	1	1
Measuring time	$t_{measure}$	s	1	1

f=0 ***f=1***

σ = 0.05m

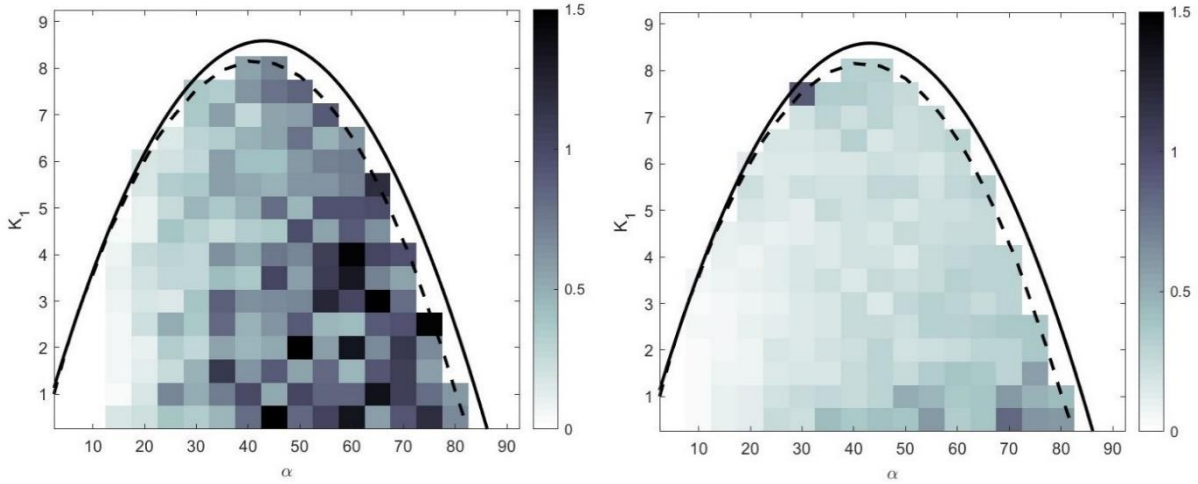

Figure 5.23 – Standard deviation matrices of the forebay level of the set of Global Cases G from Table 5.4

f=0 ***f=1***

σ = 0.1m

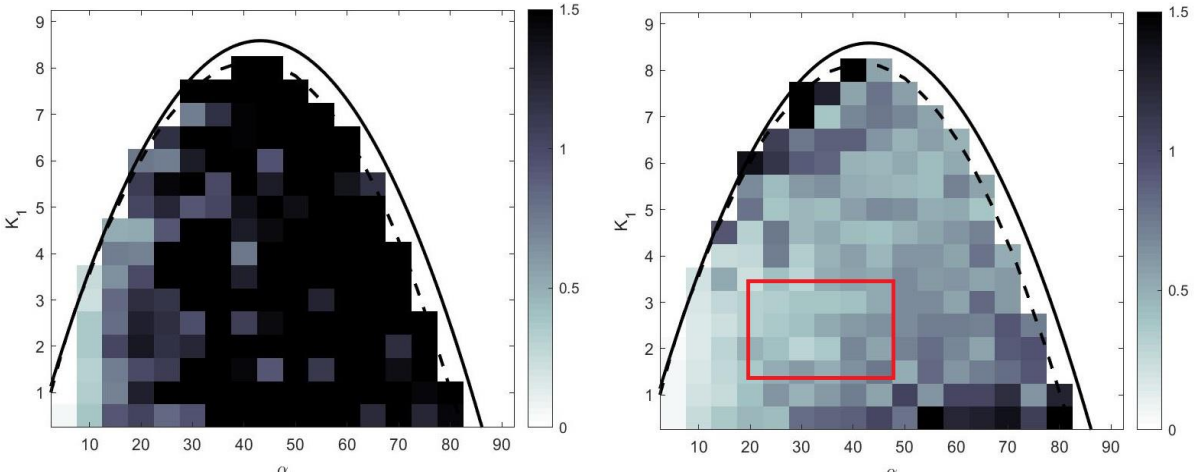

Figure 5.24 - Standard deviation matrices of the forebay level of the set of Global Cases H from Table 5.4

As observed from Figure 5.23 and Figure 5.24, the usage of a filter can reduce the standard deviation significantly. In the worst case scenario, which corresponds to σ=0.1m, the usage of filter may keep the standard deviation even under a meter and for pairs (α, K_1) well inside the curve, enclosed with a red square (approximately in the range of (20≤α≤50, 1≤K_1≤3.5)) the standard deviation may be kept even around 0.5m whereas when a filter is not used, for either σ=0.05m or σ=0.1m, the standard deviation is in general equal or greater than 1.5m.

In general, such combination of non-instantaneous valve with uncertainties and no filter showed to change absolutely the behaviour. Figure 5.5 shows the Global Case E where this combination was used and inspecting the mean values it could be thought that the cases are in general unstable, however, when a particular case of this global case is analysed, using values of α=55 and K_1=4, the situation depicted in Figure 5.25 is observed. The Mean value of $H_f(t)$ is evidently away from H_{target} but the particular case does not seem to have a strong instability, meaning that nor remarked filling or emptying of the forebay nor unreasonable values of τ (e.g. negative values) are observed. A similar situation was found for pairs (α, K_1) out of the BM stability limit curve as shown in Figure 5.25, where the same global case with α=20 and K_1=7.5, showed not to be strongly unstable.

When the combination of non-instant valve with uncertainties and no filter is thus used, it is obtained: deviated mean and wide oscillations but no strong instability for the whole α - K_1. The incompatibility of these results suggests that the non-instant valve effects should not be considered as in equations (4.40) to (4.43) but should be implemented in the tuning of the PI Controller itself rather than from this numerical approach.

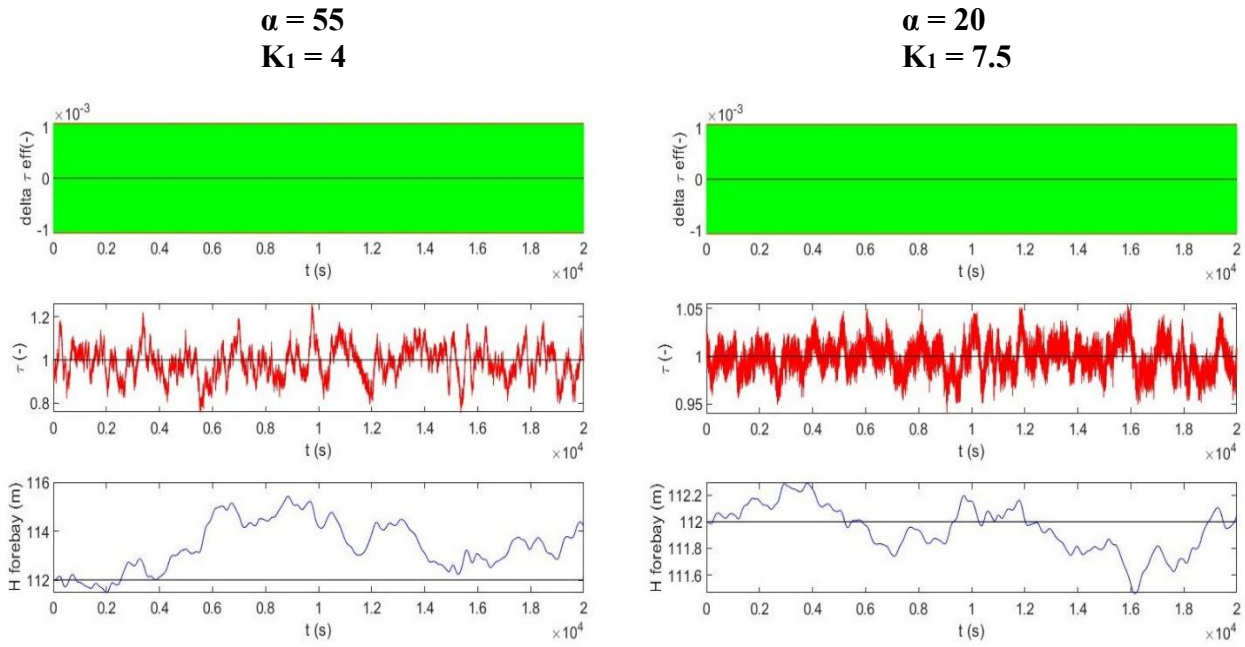

Figure 5.25 – Time-series of two particular cases, one with (α=55, K_1=4) and the other one with (α=20, K_1=7.5)), of the Global Case E from Table 4.5

5.3.3. Exponential fit as a stability criterion

Up to this point a lot has been said about the effect of the mechanisms on H_f or τ themselves but none has been said about the stability criterion to define mathematically if they were stable or not. The exponential fit technique showed to be an effective stability criterion when the oscillations of H_f showed an asymptotic stability as was observed in any case where uncertainties or backlash were not considered, that is where

$$S = f\left(BL_B = 0, NIV_B, \sigma = 0, f = 1, t_{delay}, t_{measure}\right)$$

In such cases the 0-values can be easily interpolated in the exponential fit matrix $[S_w]$ because they show a clear monotonical decay until some (α, K_1) pairs and then amplify. In addition, for such cases, a small zone shown in green colour is enclosed (Figure 5.3) representing a zone defined as *very stable zone* where H_f did not even oscillated around H_{target} but converged immediately as can be observed in Figure 5.26 where the following particular case was simulated

$$S = f\left(BL_B = 0, NIV_B = 0, \sigma = 0, f = 0, t_{delay} = 0, t_{measure} = 0, \alpha = 35, K_1 = 0.5\right)$$

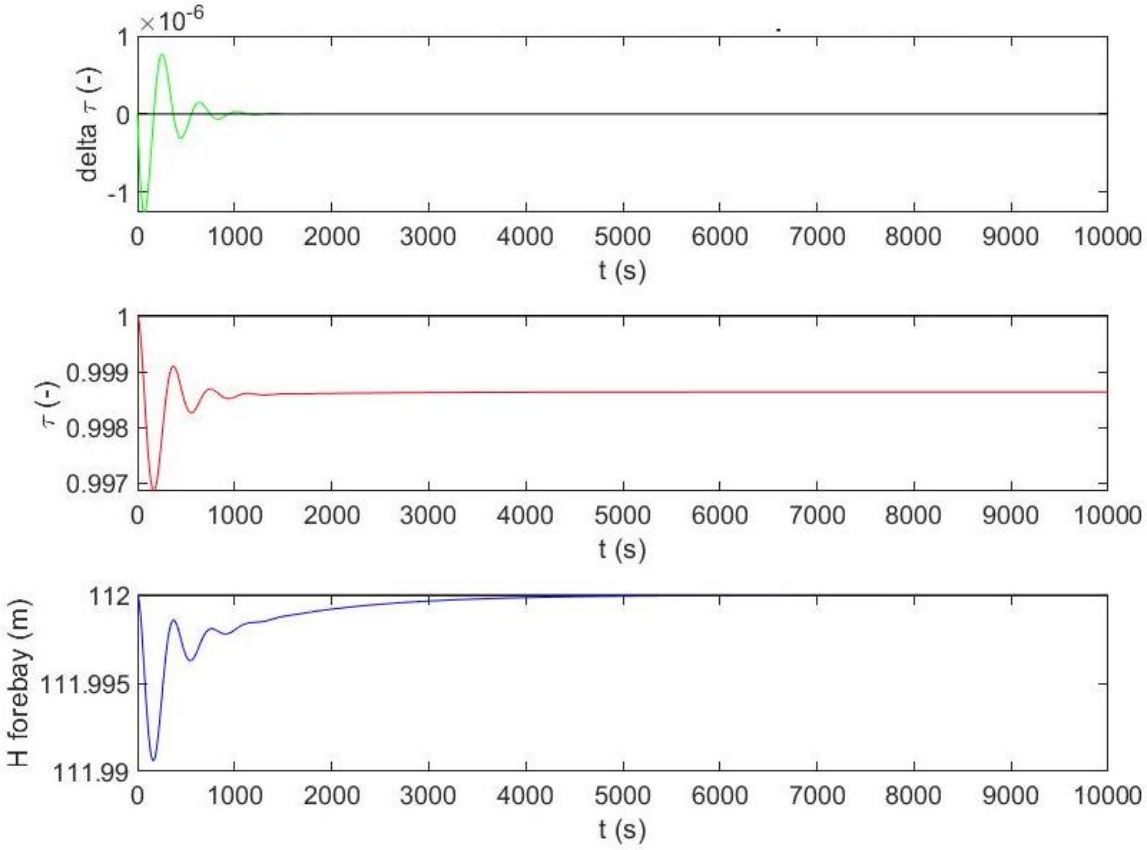

Figure 5.26 – Time-series for a particular case in the very stable zone

The nearby points to this zone are also very stable cases as they show very fast convergence to H_{target} or small oscillations around it, so it is convenient to defined as *optimum stability zone* the pairs (α, K_1) contained in the following domain (Figure 5.27)

$$20 \leq \alpha \leq 50$$

$$0 < K_1 \leq 2$$

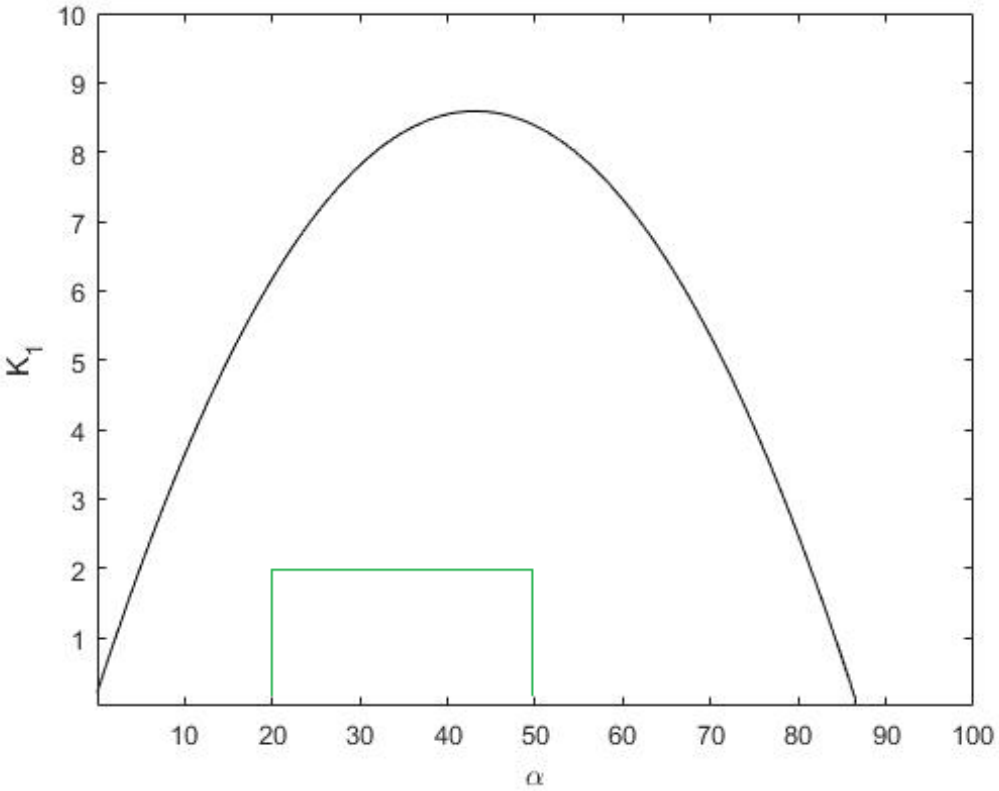

Figure 5.27 – optimum stability zone on the α - K_1 plane

When the uncertainties or the backlashes are considered, the peaks oscillations of H_f around H_{target} do not have a monotonical decay but have a random behaviour as may be seen in Figure 5.28 which show the particular cases B and D from Table 4.4.

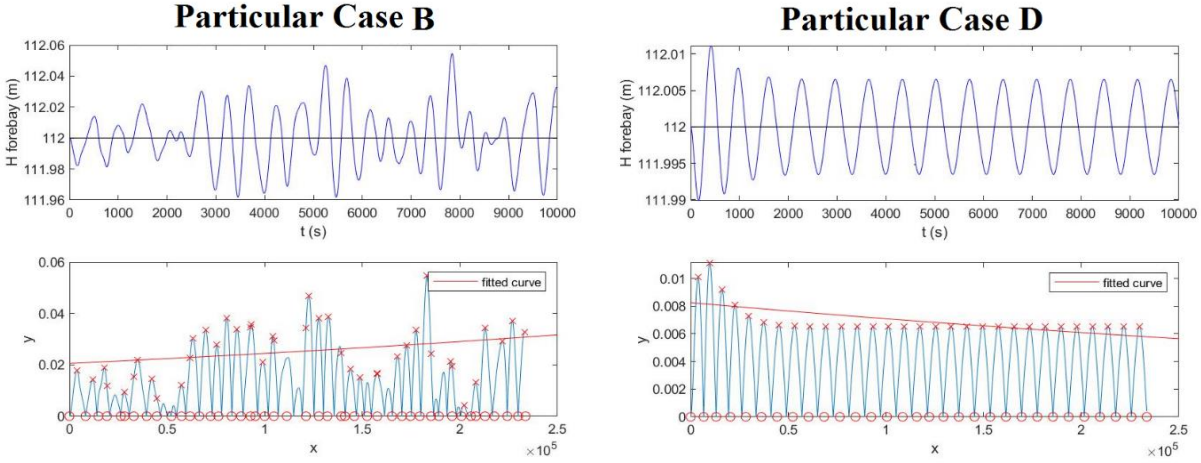

Figure 5.28 – Exponential fit applied on the Particular cases B and D

Because of this randomness, when the exponential fit is applied, the fitting parameter $S_{w,\alpha_x,K1_y}$ may take any value and as a consequence, the interpolation of the 0-values in the exponential fit matrix [S_w] does not enclose a defined stability limit curve as shown in Figure 5.3 for the set of global cases C which has been amplified in Figure 5.29

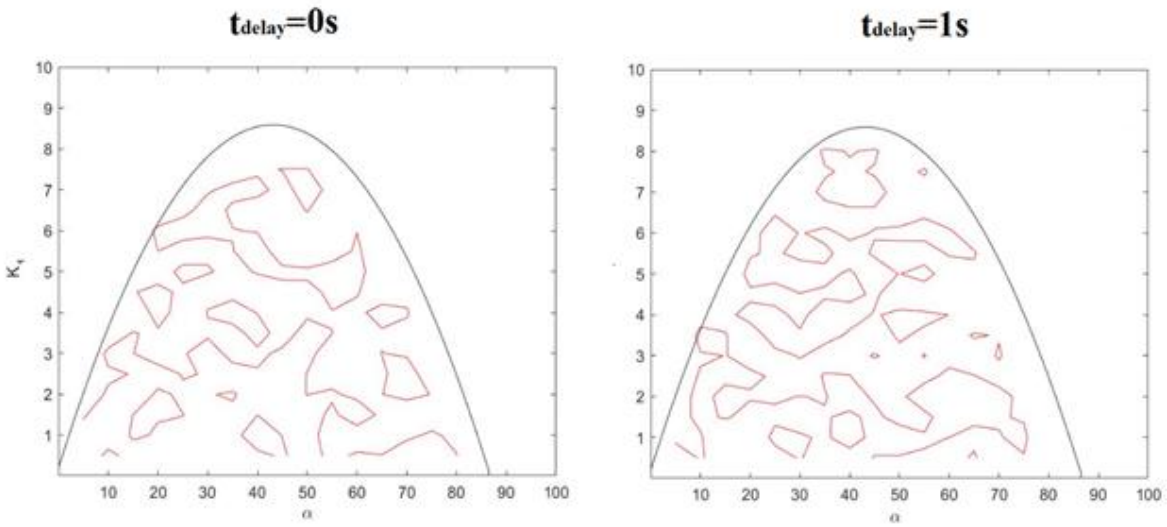

Figure 5.29 – Exponential fit for the set of global cases C

5.3.4. Mean deviation, Standard deviation, and ratio of standard deviation matrices

The mean deviation, standard deviation and the ratio of standard deviation matrices graphs show information about the centre and the amplitude of the oscillations. From the obtained matrices it is possible to say that

- The mean deviation is not affected by any global cases and thus the centre of the oscillations remains very close to $H_{target.}$
- The amplitude of the oscillations is very narrow where there is asymptotic stability and do not represent a problem for the dynamic system, but for the cases in which there are uncertainties this becomes an important issue. In the graphs, many of the uncertainties' cases show standard deviations of 1m or more, therefore, attention must be paid to the maximum amplitude and safety zones where the H_f may be allowed to oscillate.
- It is important to notice the amplitude differences of using or not filtering, because as shown in the graphs a difference between their standard deviations may have values up to 50cm. Nevertheless, as has been said before the combination of non-instantaneous valve with no filtering should not be analysed because of the incompatibility of the results

5.3.5. Results summing-up

To end the discussion, Table 5.5 summarized the effect of the variables and their combinations as well as the effect of the stability criterion and the statistical analysis.

Table 5.5 – Results summary

Variable	Method of analysis		Effect of the variable alone	Remarkable combination	Final observations
	Expfit	Statistical			
Transients	✓	✓	Negligible	-	-
Non-instant valve	✓	✓	Negligible	Very harmful when combined with uncertainties	Should be implemented in the PI Controller tuning
Backlash	✗	✓	No asymptotic stability but small amplitude of oscillations	When combined with uncertainties it is negligible	Backlash may increase in time due to wear of mechanical parts
Instrumental uncertainty	✗	✓	No asymptotic stability but considerable amplitude of oscillations	Very harmful when combined with non-instant valve effects	Consider implementation in PI controller tuning
Delay time	✓	✓	Negligible for the considered values of t_{delay}	Negligible for any combination	-
Measuring time	✓	✓	Negligible for the considered values of $t_{measure}$	Negligible for any combination	-

5.3.6. Redefining stability and new stability criteria

Until now and based on the stability criterion of the exponential fit only for the global cases without uncertainties or backlash a defined stability limit curve has been obtained and only for their particular cases the dynamic systems have been classified as “stable” or “unstable”. The results obtained from the exponential fit showed not to be suitable for any global case having uncertainties or backlashes because the time-series of their particular cases did not expose monotonic decay or asymptotic stability. However, for such cases, although the oscillations of $H_f(t)$ did not damp or converge to H_{target}, as long as the (α, K_1) pairs remained under the BM stability curve, the oscillations of $H_f(t)$ did not amplify, giving a new sense of stability. This suggests that stability may be also assessed for these cases if the concepts of “stability” in a mathematical way and the stability criterion are changed.

In this sense, let us redefine stability and divide it in two types, the first being the already defined asymptotic stability based upon convergence of $H_f(t)$ to H_{target} throughout time using the exponential fit criterion, hence using the same equations from chapter 3 for a particular case

$$as_{w,\alpha_x,K1_y} = \begin{cases} 1; S_{w,\alpha_x,K1_y} < 0 \\ 0; S_{w,\alpha_x,K1_y} \geq 0 \end{cases} \quad (5.8)$$

Where S is the exponential fit parameter from equation (4.71). The stability limit curve is found afterwards using the interpolation of S=0 along the exponential fit matrix.

Now, let us define a second type of stability called *pseudo-stability*

$$ps_{w,\alpha_x,K1_y} = \begin{cases} 1; \ ps1_{w,\alpha_x,K1_y} = 1 \ and \ ps2_{w,\alpha_x,K1_y} = 1 \\ 0; else \ case \end{cases} \quad (5.9)$$

Where

$$ps1_{w,\alpha_x,K1_y} = \begin{cases} 1; \left|\overline{\Delta H_{f,w,\alpha_x,K1_y}}\right| \leq \Delta H_{lim} \\ 0; \left|\overline{\Delta H_{f,w,\alpha_x,K1_y}}\right| > \Delta H_{lim} \end{cases} \quad (5.10)$$

$$ps2_{w,\alpha_x,K1_y} = \begin{cases} 1; \ \ s\_H_{f,w,\alpha_x,K1_y} \leq s\_H_{lim} \\ 0; \ \ s\_H_{f,w,\alpha_x,K1_y} > s\_H_{lim} \end{cases} \quad (5.11)$$

$\Delta H_{f,w,\alpha_x,K1_y}$ and $s\_H_{f,w,\alpha_x,K1_y}$ are the mean deviation and the standard deviation defined in equations (4.79) and (4.76)

This means that a new type of stability has been created based upon the fact that $H_f(t)$ of a particular case may oscillate around H_{target} without converging to it but without amplifying its oscillations. The pseudo-stability type I (ps1) refers to the centre of the oscillations and limits the mean deviation and the pseudo-stability type II (ps2) refers to the amplitude of the oscillations and limits their width. The values of ΔH_{lim} and s_H_{lim} are not fixed and depend on the particular case considered, because every plant has its own restrictions and the designer shall have knowledge of the restrictive value that keeps the oscillations harmless to the conditions of the plant.

The stability limit curves based on pseudo stability may be found inspecting the limit values of the both types of pseudo-stability or shall be omitted simply performing the stability assessment for pairs of (α, K_1) under the BM case stability curve.

5.3.7. Recommendations in the design and the running on the plant

After deriving the consequences of considering each of the mechanisms, some recommendations in the design or the running phases may be proposed:

1. Considering the transients in the flow may be negligible because their effect made the stability limit curve to shrink slightly compared to Jimenez's model
2. The values of delays and measuring times should be kept as little as possible. It has been proven that when the values remain in the ranges used in this document, they can be neglected.
3. When considering backlash effects, though the dynamic system does not show asymptotic stability, there is no significant impact on the oscillations as they remain very narrow. However, it should be highlighted that the backlash effects were considered constant in time but they may change after some months or years of operation due to wear of the mechanical parts and therefore changing their impact on the flow control system
4. Since the instrumental uncertainties are the most significant mechanism considered, special attention should be paid to them and the precision of the instrument should be kept in ranges less than 0.05m. It was proved that keeping the uncertainties under this value allows to have very narrow oscillations.
5. The non-instantaneous valve should be only used with filtering when considered with the uncertainties case. However, in general, to the author's opinion, the non-instant valve effects should be included in the PI Control tuning rather than in the numerical simulations.

6. APPLICATION (STUDY CASE)

To validate the information extracted from the simulations applied on the Palomo Hydroelectric Project in Costa Rica, a set of simulations were also applied in the Bajo Tuluá ROR hydropower plant in Colombia. This plant, unlike the Palomo one, had a different hydraulic scheme because the surge tank was not directly linked to the tunnel but was connected with a standpipe, as shown in Figure 6.1.

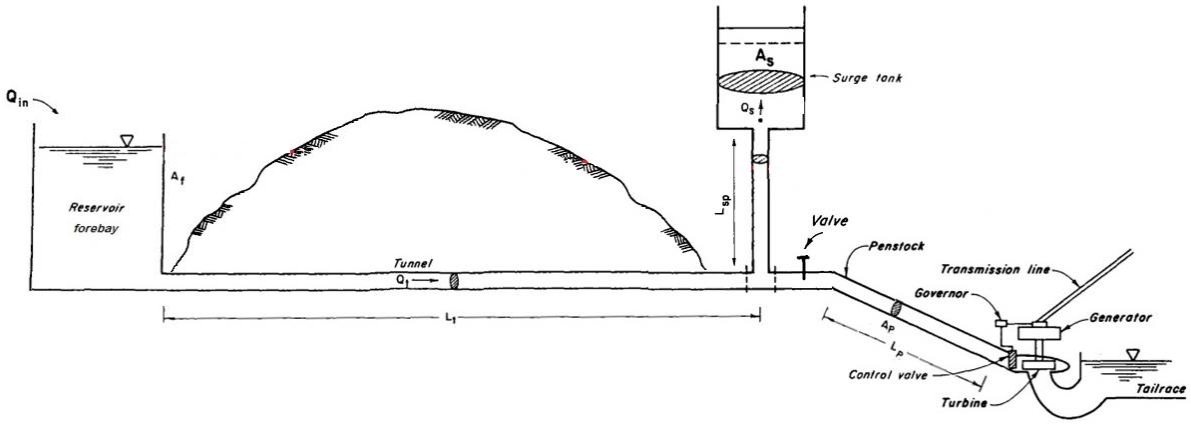

Figure 6.1 – Bajo Tuluá ROR Hydropower plant scheme adapted from Chaudhry (1979)

The Bajo Tuluá ROR hydropower plant has two Francis turbines and the characteristics shown in Table 6.1

Table 6.1 – Characteristics of the Bajo Tuluá ROR Hydropower plant

Variable	**Symbol**	**Unit**	**Value**
Incoming river flow	Q_{in}	m^3/s	12
Surface area of the forebay	A_f	m^2	810.98
Surface area of the surge tank	A_s	m^2	102.07
Tunnel Length	L_t	m	5735.04
Penstock length	L_p	m	398.03
Standpipe length	L_{sp}	m	106.73

The behaviour of the plant was simulated for the same particular cases from Table 4.4 and the results are shown in Figure 6.2

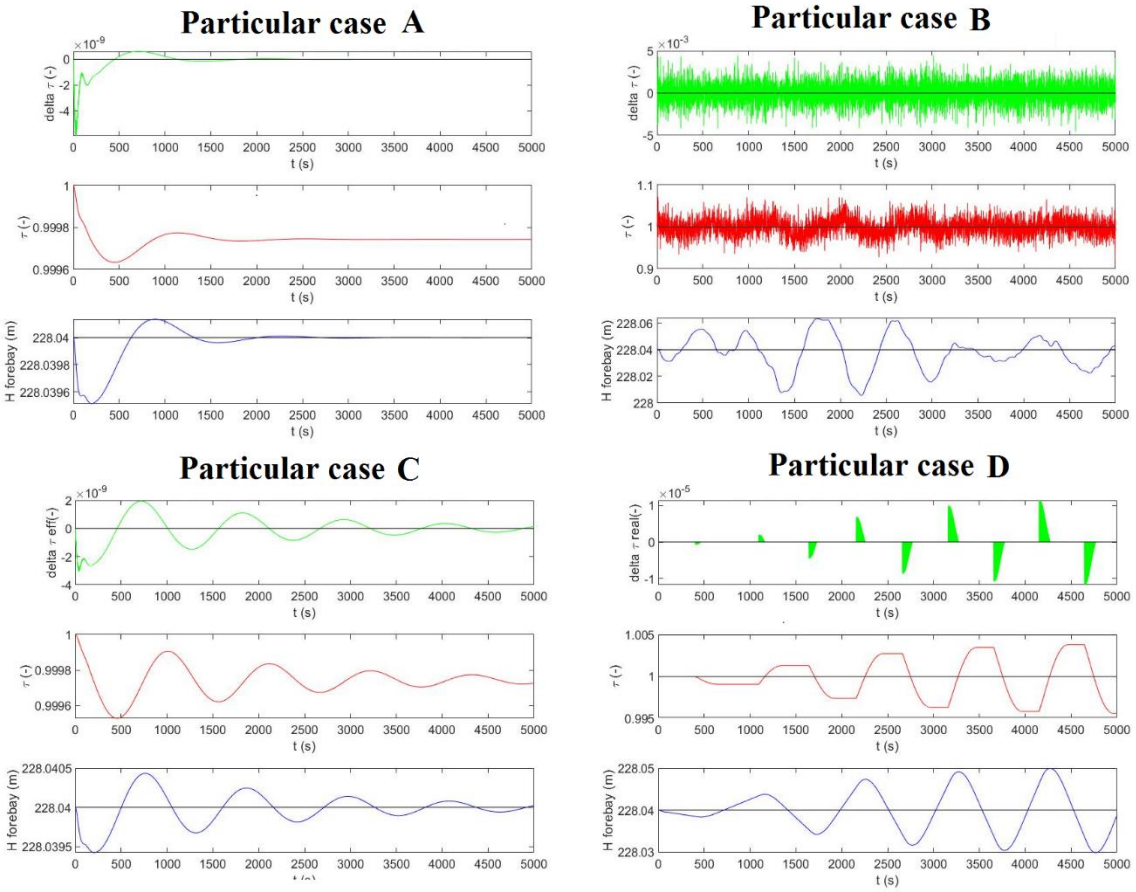

Figure 6.2 – Results of the particular cases A, B, C and D for the Bajo Tuluá ROR Hydropower plant

The results show to be compatible with those obtained in Chapter 5 and therefore the model shows to be applicable.

REFERENCES

Chaudhry, M. H. (1979). *Applied Hydraulic Transients.* New York: Van Nostrand Reinhold.

Devore, J. L. (2012). *Probability & Statistics for Engineering and the Sciences.* Boston: Cengage.

Farris, A., & Helston, C. (2017, February). *Run of River Power*. Retrieved from EnergyBC: http://www.energybc.ca/runofriver.html

Freedman, R. A., & Young, H. D. (2012). *University Physics.* San Francisco: Pearson.

international hydropower association [iha]. (2019, June 18). *Hydropower facts*. Retrieved from international hydropower association Web site: https://www.hydropower.org/a-brief-history-of-hydropower

international hydropower association [iha]. (2019, June 18). *Hydropower facts*. Retrieved from international hydropower association Web site: https://www.hydropower.org/types-of-hydropower

Jiménez, O. F., & Chaudhry, M. H. (1992). Water-Level Control in Hydropower Plants. *Journal of Energy Engineering*, *118*(3), 180–193. https://doi.org/10.1061/(ASCE)0733-9402(1992)118:3(180)

Liu, F., Jiang, H., Zhang, L., & Chen, L. (2017). Analysis of vibration characteristic for helical gear under hydrodynamic conditions. *Advances in Mechanical Engineering*, *9*(1), 1–9. https://doi.org/10.1177/1687814016687962

Norconsult SA. (2016, 03 07). *Svenska kraftnät.* Retrieved from Svenska kraftnät SA: https://www.svk.se/en/press-och-nyheter/news/news/nordic-common-project-for-review-of-primary-reserve-requirements--finalized-phase-1/

Nunez, C. (2019, May 13). *Hydropower, explained*. Retrieved from National Geographic Web site: https://www.nationalgeographic.com/environment/global-warming/hydropower/

Vesipa, R., & Fellini, S. (2019). Instability of the Tank-Level Control System of Water Mains in Mountainous Environments. *Journal of Hydraulic Engineering*, *145*(7), 04019025. https://doi.org/10.1061/(ASCE)HY.1943-7900.0001609

Wang, B., Liu, J., & Wang, C. (2019). Measurement and analysis of backlash on harmonic drive. *{IOP} Conference Series: Materials Science and Engineering*, *542*, 12005. https://doi.org/10.1088/1757-899x/542/1/012005

White, F. M. (2011). *Fluid Mechanics.* New York: McGraw-Hill.

Wylie, E. B., & Streeter, V. L. (1978). *Fluid Transients.* McGraw-Hill.